Carbon starvation in the filamentous fungus Aspergillus niger

Nitsche, B.M.

Benjamin M. Nitsche

Carbon starvation in the filamentous fungus *Aspergillus niger*

Carbon starvation in the filamentous fungus *Aspergillus niger*

Proefschrift

ter verkrijging van
de graad van Doctor aan de Universiteit Leiden,
op gezag van Rector Magnificus Prof. Mr. P.F. van der Heijden,
volgens besluit van het College voor Promoties
te verdedigen op dinsdag 23 oktober 2012
klokke 15:00 uur

door

Benjamin Manuel Nitsche
geboren te Berlijn, Duitsland
in 1979

Promotie commissie

Promoter:	Prof. Dr. C.A.M.J.J. van den Hondel
Co-promoter:	Dr. A.F.J. Ram
Overige leden:	Prof. Dr. M.J.E.C. van der Maarel (Universiteit Groningen)
	Prof. Dr. V. Meyer (Technische Universität Berlin)
	Prof. Dr. H.P. Spaink (Universiteit Leiden)
	Prof. Dr. G.P. van Wezel (Universiteit Leiden)
	Dr. J.R. Wortman (Broad Institute)
	Prof. Dr. H.A.B. Wösten (Universiteit Utrecht)

Cover:	Artwork made from binarized microscopic pictures of exponentially growing (green) and carbon-starved (red) hyphae using the the "worm drawings algorithm" as implemented by Francis Shanahan (http://francisshanahan.com/demos/worms/test.html)
Printed by:	CPI Germany
ISBN:	978-94-6203-054-1

Für meine Familie
gratias vobis ago

Contents

List of Figures

List of Tables

Chapter 1

General introduction

The impact of filamentous fungi

Fungi are amongst the most simple eukaryotic organisms. Similar to other microorganisms, they play essential roles in decomposition of organic matter and nutrient cycling in nature. According to Whittakers early four-kingdom system (Whittaker, 1959; Hagen, 2012), they constitute their own taxonomic kingdom, the Mycetae, which is a very diverse group of microorganisms comprising generally known species including yeast, molds and mushroom forming fungi such as *Agaricus bisporus*, also called the champignon mushroom. In contrast to the majority of yeasts which are unicellular and grow by budding (e.g. *Saccharomyces cerevisiae* also known as baker's yeast) or fission (e.g. *Schizosaccharomyces pompe*), molds grow in a polar manner forming hyphae which are long tubular tip-growing cells. Due to this key morphological characteristic, molds are (more) frequently referred to as filamentous fungi.

Filamentous fungi have an immense impact on human society. *Penicillium camenberti* and *Aspergillus oryzae* have for example long been used for the production of camembert cheese and Japanese soy sauce (*shōyu*), respectively. According to legend, the production of the latter dates back to 1254 (Murooka *et al.*, 2008) and Japanese cuisine cannot be imagined without it. β-lactam antibiotics are another famous example for the significant impact of filamentous fungi on human society. In 1928 the physician Alexander Fleming, who worked with *Staphylococus* bacteria, accidently discovered that a mold contaminating his culture plates secreted an agent with antibacterial activity. The mold was identified as *Penicillium notatum* and the antibacterial compound was named Penicillin (Kardos *et al.*, 2011). Driven by increasing demands for anti-infective drugs during World War II, the development of industrial production technology, process and strain improvements are outstanding examples of industrial fungal biotechnology. In 1945, the annual world production of penicillin G amounted to 5 tons, this had increased to more than 12,000 tons in 1982 and reached 33,000 tons by 1995 (Beek *et al.*, 1984; Elander, 2003). However, industrial fungal biotechnology is not limited to pharmaceuticals. Most filamentous fungi used in industrial biotechnology are efficient saprophytes (e.g. *Trichoderma reesei* or *Aspergillus niger*) meaning that they naturally have high secretion capacities for various hydrolytic enzymes required to extracellularly decompose dead organic matter. These high secretion capacities together with their versatile primary and secondary metabolisms make filamentous fungi outstanding production hosts for a variety of commercial products including primary metabolites (e.g. organic acids and vitamins), secondary metabo-

lites (e.g. antibiotics and bioactive compounds such as alkaloids), natural secreted hydrolases (e.g. cellulases, pectinases and proteases) and, since the development of efficient molecular genetic tools for filamentous fungi, heterologous proteins (e.g. Interleukin 6 and manganese peroxidase) (Punt *et al.*, 2002). Thus, industrial sectors applying products from filamentous fungal biotechnology are as diverse as the products themselves and include amongst others, health, food, beverages and feed.

Industrial biotechnology is continually increasing its effort to establish economic and sustainable production processes which can compete with alternative processes from the chemical industry. Of great importance are second generation feedstocks (substrates) such as lignocellulosic biomass waste products (e.g. sugar cane bagasse or wheat straw) that can be used as substrates in bioprocesses after hydrolytic pretreatments. Second generation feedstocks are cheaper than traditional first generation feedstocks (e.g. sugar canes or corn) and do not compete with food or feed supply. However, as lignocellulosic biomass hydrolyzates contain complex mixtures of sugars and inhibitory compounds, there can be considerable differences in the performance of industrial microorganisms. Very promising results were recently shown for *A. niger* (Rumbold *et al.*, 2009; Rumbold *et al.*, 2010), thus further emphasizing the importance of this filamentous fungus as a versatile industrial cell factory.

Apart from the above-mentioned positive aspects, there is also a downside to filamentous fungi as many species can negatively impact health and the economy. These include, for example, field infection with phytopathogenic species (e.g. rice blast fungus *Magnaporthe oryzae*) and post-harvest contamination of food and feedstocks with mycotoxin-producing fungi such as *Aspergillus flavus* (carcinogenic aflatoxins) which can result in substantial economic losses in the agricultural industry. Airborne fungal spores are ubiquitous and can be found both indoors and outdoors where they often exceed pollen concentrations by up to 1,000-fold and are considered important perpetrators of respiratory allergies and asthma. Most allergenic filamentous fungal species are asexual Ascomycetes as, for example, *Alternaria alternata* and *Aspergillus fumigatus* (Horner *et al.*, 1995). For the latter, it has been estimated that humans inhale several hundred conidia per day (Latge, 1999). These conidia are a life-threatening danger for immunocompromised patients (e.g. cancer, organ transplantation and HIV), as they can cause invasive pulmonary aspergillosis with mortality rates up to 50%, even when treated with antifungals (Fedorova *et al.*, 2008).

The black mold *Aspergillus niger* is a ubiquitous saprophytic filamentous fungus belonging to the *Aspergillus* section *Nigri*, which together with the section *Flavi*, accounts for the most common mycotoxigenic fungi contaminating agricultural goods including, amongst others, corn, peanuts, raisins and onions (Mogensen *et al.*, 2010). Nevertheless, *A. niger* is one of the major hosts in industrial biotechnology for the production of food ingredients (e.g. cit-

ric acid/E330 or gluconic acid/E574) (Ruijter *et al.*, 2002) and industrial enzymes (e.g. Lipases, pectinases and catalases) (Fogarty, 1994). *A. niger* has a long history of safe use and many of its products have acquired GRAS status, meaning that they are generally recognized as safe food ingredients by the American Food and Drug Administration (FDA) (Schuster *et al.*, 2002). Industrial-scale production of citric acid with *A. niger* dates back to 1923. Nowadays, citric acid is a bulk product which, due to its flavor, acidity and chelating property, is a common ingredient in food, beverages, cosmetics and pharmaceuticals with an annual world production of 900,000 tons in the year 2000 (Ruijter *et al.*, 2002).

Carbon starvation: Dynamics of the fungal mycelium

In contrast to most laboratory growth conditions, microorganisms experience dramatic changes and fluctuations of environmental factors in their natural habitats, including light conditions, temperature, moisture, pH, osmolarity, nutrient availability and competitors. Depending on the niche, diverse stress responses have evolved which are dedicated to survival and propagation. The favored commercial production process in fungal biotechnology is submerged cultivation in stirred tank reactors which can reach volumes of up to 300,000 liters (Elander, 2003). Many of these processes are operated as fed-batch cultures (Zustiak *et al.*, 2008) preventing catabolite repression by ensuring a nutrient-limited growth regime. However, substrate limitation towards the end of production processes in particular, can cause severe stress to the production host which subsequently can translate into reduced yields. The focus in the following will be on carbon starvation during submerged cultivation. Various aspects related to the complex physiological and morphological consequences for the fungus will be briefly introduced.

The fungal mycelium; a network of hyphal cells

The formation of a mold colony from a single spore is initiated by germination, which involves isotropic growth (swelling) and the establishment of polarity in the form of a germ tube. Apical elongation and branching of the germ tube leads to the formation of individual substrate exploring hyphae. As a result of further apical extension of hyphae, branching and hyphal fusion (anastomosis) an interconnected hyphal network evolves which is referred to as "fungal mycelium" (see Figure 1.1).

Hyphae of higher fungi (e.g. Ascomycetes and Basidiomycetes) are multicellular and multinucleated. They consist of several compartments (see Figure 1.2). These compartments are separated from each other by a so-called septum, a structure consisting of cell wall material (mainly polysaccharides) that is continuous with the lateral cell wall of the fungus. Com-

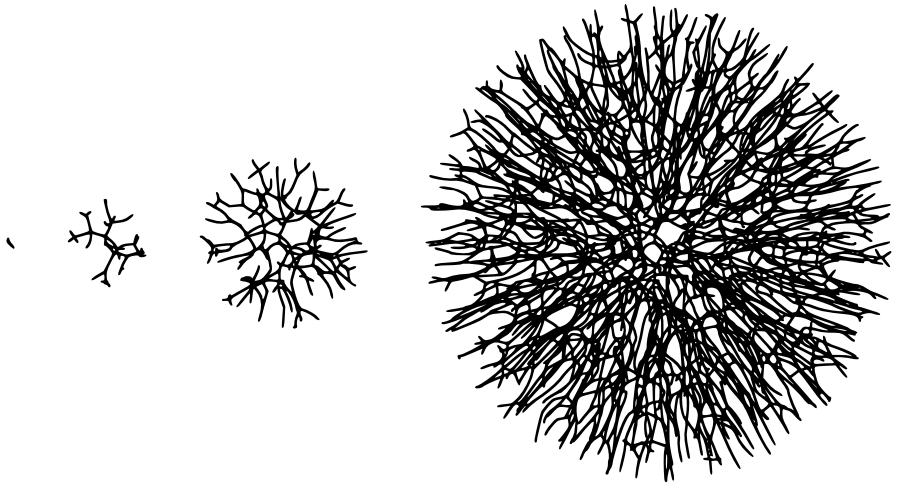

Figure 1.1 — Development of a filamentous fungal colony
Neighbor-Sensing model simulating colonial growth of a filamentous fungus on an isotropic substrate (Meškauskas *et al.,* 2004). A young germling undergoes branching forming a low density mycelial layer. Further branching and hyphal fusion (anastomosis) lead to the formation of a denser radially growing mycelial mat which forms a mycelial entity.

partments can communicate with each other via a septal pore. This pore in the septum is large enough to allow organelles (e.g. nuclei and mitochondria) and protein complexes (ribosomes) or proteins and metabolites to be transported from one compartment to the other. When required e.g. in response to hyphal damage of the tip cell or environmental conditions (*Schizophyllum commune*) (Peer *et al.*, 2009), filamentous fungi can close the septal pore by plugging it with a specialized organelle, which, in case of Ascomycetes, is called the Woronin body (Markham *et al.*, 1987). A recent study for *A. oryzae* (Bleichrodt, 2012) reported that 60% of the first three septa in substrate exploring hyphae were closed, independent of environmental conditions and the state of the other two septa. It was assumed that septal pore plugging in *A. oryzae* is a stochastic process, which consequently impedes cytoplasmic continuity and thus promotes hyphal heterogeneity. Indeed, monitoring glucoamylase gene expression, the authors demonstrated that hyphal heterogeneity was abolished in the Δ*hex*1 mutant, which does not form Woronin bodies and as a consequence cannot plug septal pores.

Autophagy

During surface growth on an isotropic substrate (e.g. agar plate cultures, a typical laboratory growth condition), colonies of filamentous fungi expand radially (see Figure 1.1). Hyphae at the periphery of the colony experience nutrient rich conditions, whereas the nutrient avail-

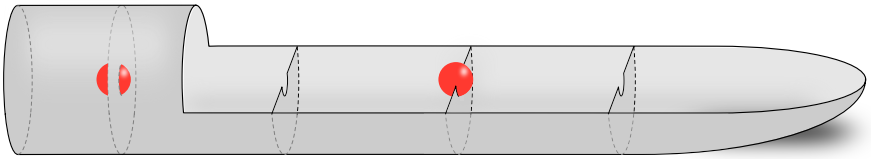

Figure 1.2 – Septated hypha
Schematic representation of the cell wall skeleton of a septated hypha. Hyphae are compartmentalized by septa, while compartments are connected via septal pores which allow intercompartmental trafficking of organelles, protein complexes, proteins and metabolites. Septal pores can be reversibly plugged to protect from cytoplasmic bleeding upon damage or to allow specification of compartments (e.g. commitment to conidiation.).

ability decreases towards the center of the colony, where nutrients eventually become depleted. Unlike colonies of unicellular microorganisms that form and expand by the production of daughter cells, colonies of filamentous fungi are able to grow beyond a nutrient depleted region, as for example, on a non-isotropic natural substrate, by providing hyphae at the periphery of the colony with resources from basal hyphal compartments. Interconnectivity of the mycelial network is essential for this foraging strategy and is a key-advantage of the filamentous lifestyle over unicellular microbes (Richie *et al.*, 2007).

Autophagy is a process that has been shown to be important for the maintenance of foraging hyphae in *A. fumigatus* (Richie *et al.*, 2007). Autophagy is a well conserved catabolic process constitutively active in eukaryotic cells. Together with proteasome-mediated degradation, autophagy is the major pathway for protein and organelle turnover being important for cellular homeostasis and maintenance (Reggiori *et al.*, 2002). A fine-tuned balance of biosynthetic (anabolic) and degradative (catabolic) pathways is essential to maintain cellular activity and allow adaptation to changing environmental conditions. There are two distinct mechanisms of autophagy, micro- and macroautophagy (Klionsky *et al.*, 1999). The first describes the invagination of cytoplasmic constituents directly at the vacuolar membrane, whereas the latter (from now on simply referred to as autophagy) involves engulfing cytoplasmic content in double-membrane vesicle cargos that finally fuse to the vacuole and become degraded (see Figure 1.3). Both non-specific bulk turnover of cytoplasm and organelle-specific forms of autophagy exist including pexophagy (degradation of peroxisomes), ribophagy (degradation of ribosomes), ERphagy (degradation of the endoplasmic riticulum) and mitophagy (degradation mitochondria) (Bernales *et al.*, 2007; Mao *et al.*, 2011). Although autophagy is known to be induced by nutrient starvation (carbon and nitrogen) and leads to recycling of building blocks from degraded cytoplasmic constituents, autophagy is not simply a recycling pathway as it is also clearly associated with cell death. Interestingly, autophagy has been shown to be both protective against and causative of cell death. It has been demonstrated in filamentous fungi,

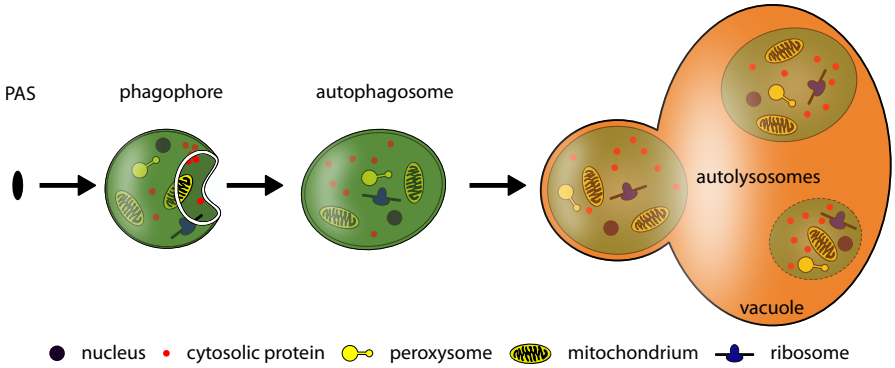

Figure 1.3 – Macroautophagy
Schematic representation of non-specific bulk macroautophagy. Macroautophagy is initiated by the formation of a pre-autophagosomal structure (PAS). Subsequently bulk cytoplasm becomes engulfed in double-membrane cargos that fuse to the vacuoles were they are finally degraded and building blocks are recycled.

for example, that autophagy protects against cell death during the heterokaryon incompatibility reaction (a mechanism of non-self recognition) in *Podospora anserina* (Pinan-Lucarré *et al.*, 2005) or during carbon starvation in *Ustilago maydes* (Nadal *et al.*, 2010). Contrary to this, autophagy induced cell death has been reported to be required for rice plant infection by *Magnaporthe grisea* (Veneault-Fourrey *et al.*, 2006). Shoji *et al.* (2011) suggest that autophagy in filamentous fungi might represent a final effort to endogenously recycle and translocate cytoplasmic resources to adjacent compartments prior to cell death. Shoji *et al.* (2010) even demonstrated autophagic degradation of whole nuclei for *A. oryzae* and suggested that nuclei might serve as storage for phosphorus and nitrogen in multinucleate organisms.

Programmed cell death

There is an immense body of literature on cell death but terms are frequently confused or inappropriately used (Lockshin *et al.*, 2004; Kroemer *et al.*, 2008). The increasing attention being paid to the field of cell death is explained by the fact that cell death plays a fundamental role in development, aging and serious human pathologies such as cancer and neurodegenerative disorders including Alzheimer's, Parkinson's and Huntington's diseases. A brief, general introduction on programmed cell death (PCD) and a summary of a few important historic milestones followed by a more specific overview of fungal PCD are provided below.

The classical concept of PCD relates to the observation that fetal and larval structures regress during ontogenetic development of higher eukaryotes, a phenomenon that was possibly already known to Aristotle (384 BC – 322 BC) (Clarke *et al.*, 1996). However, it was not until the mid 19th century, when advancements in microscopy and histology allowed the observa-

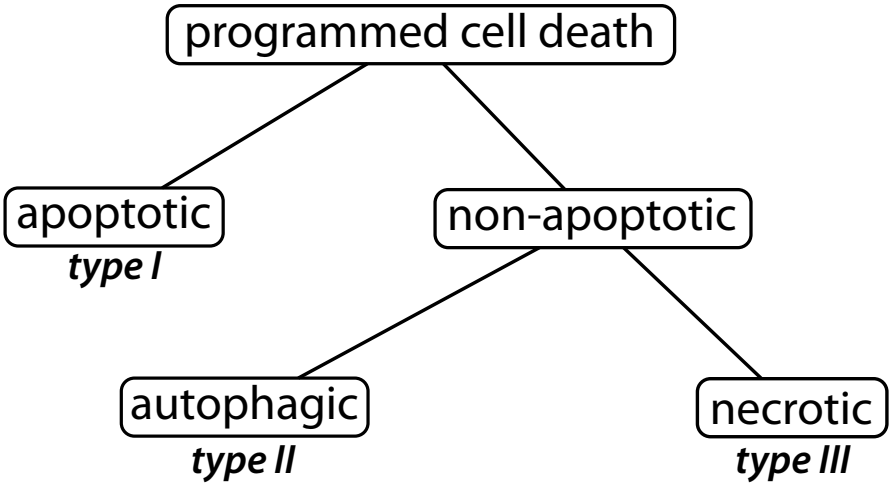

Figure 1.4 — Programmed cell death
Simplified flowchart showing the relationship of the three types of PCD: Type I (apoptosis), type II (autophagy) and type III (programmed necrosis or necroptosis).

tion of cells and the establishment of the cell theory by Schwann (1839) and Schleiden (1842), that cell death was first described and the concept of developmental cell death was initiated by Carl Vogt (Clarke *et al.*, 1996). In 1885, Walther Flemming was the first to suggest that cell death is caused rather by chemical changes within the cell than by mechanical disturbance. 80 years later, Lockshin *et al.* (1964) coined the term "programmed cell death" emphasizing the existence of a cell-intrinsic and genetically programmed developmental cell death. Around the same time, John Kerr histologically described a distinctive form of active necrosis, which he initially referred to as "shrinkage necrosis" and later coined it "apoptosis", a word that originates from the Greek word describing the falling-off of leaves (ἀπόπτωσισ) (Kerr *et al.*, 1972; Diamantis *et al.*, 2008).

In contrast to the traditional view which claims the existence of two principally distinct forms of cell death in higher eukaryotes, namely apoptosis as a programmed, cell-intrinsic suicide mechanism and necrosis as an unorganized, passive form of cell death, it has been suggested that cell death is generally organized and three types of PCD have been delineated (see Figure 1.4). Type I PCD refers to apoptosis, the traditional PCD, type II and type III PCD describe the non-apoptotic forms that are autophagy and programmed necrosis (also referred to as necroptosis (Galluzzi *et al.*, 2008)), respectively (Lockshin *et al.*, 2004). Subsequently, this clearly implies that the terms "apoptosis" and "programmed cell death" are not considered as synonyms (Kroemer *et al.*, 2008). It has to be noticed that in contrast to type I and type III PCD, which are clear cell death mechanisms, autophagy, as mentioned earlier, is also a normal

cell physiological process important for cellular homeostasis and maintenance. These different types of PCD can be distinguished by the presence or absence of certain sets of morphological and biochemical hallmarks which will not be outlined here. The interested reader is referred to a publication on cell death classification by Kroemer *et al.* (2008). Importantly, the authors emphasize that it is inappropriate to use specific biochemical assays as an exclusive means to define apoptosis, as this specific form of PCD can also occur without certain hallmarks such as internucleosomal DNA fragmentation. Interestingly Kroemer *et al.* (2008) say the following on autophagic cell death: "Although the expression 'autophagic cell death' is a linguistic invitation to believe that cell death is executed by autophagy, the term simply describes cell death with autophagy", thereby emphasizing that autophagy is simply associated with cell death. Indeed, depending on what is studied, autophagy has been demonstrated to be both causative of and protective against cell death.

Before proceeding with the description of PCD in fungi, it is worth noting that cell death in microbial and higher eukaryotes has substantially different consequences. For higher eukaryotes, ontogenetic, pathological or physiological cell death preserves the individual as an entity, whereas microbial cell death, especially in the case of unicellular eukaryotes such as *Saccharomyces cerevisiae*, has severe consequences, namely death of the individual organism. Although, of course, microbes act as communities and death of individuals does not lead to death of a microbial population. In multicellular filamentous fungi in particular, it is an interesting hypothesis that certain hyphal compartments undergo cell death for the benefit of the mycelial entity e.g. when confronted with life-threatening starvation conditions.

The best described form of PCD in fungi is type II. Interestingly, after the initial description of autophagy in mammalian cells in the 1960s, it was yeast as a genetically tractable model organism that considerably contributed to the understanding of the molecular mechanisms of autophagy in the 1990s (Yang *et al.*, 2010). The autophagic core machinery is highly conserved from yeast to man and more than 30 autophagy (*atg*) genes have been identified for *S. cerevisiae* and other fungi to date (Kanki *et al.*, 2011; Xie *et al.*, 2007; Meijer *et al.*, 2007). In contrast, only an ancestral core apoptotic machinery has been identified in fungi for type I PCD (Fedorova *et al.*, 2005) and the term apoptosis should be interpreted in a broader sense (Hamann *et al.*, 2008). For example, no orthologs of caspases, cystein-dependent aspartate-directed proteases, that play essential roles in mammalian apoptosis as initiator and effector enzymes, have been identified in fungi. Instead, it has been suggested that metacaspases are functional homologues of caspases in fungi (protozoa and plants). Metacaspases are cystein proteases that probably share the same ancestor as caspases (Hamann *et al.*, 2008). Similarly, orthologs of BCL-2-like proteins, which have pro- or anti-apoptotic properties, have not been identified in fungi, but their heterologous expression has been shown to affect apoptosis-like processes in yeast and

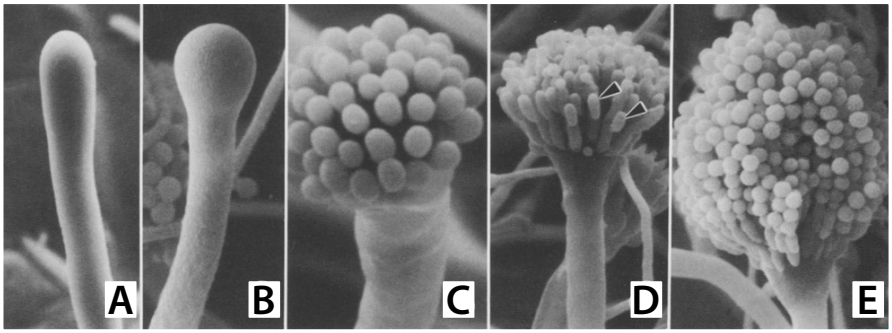

Figure 1.5 – Conidiophore development
Scanning electron micrographs showing different morphological stages of conidiophore development in *A. nidulans*: (A) Conidiophore stalk, (B) vesicle, (C) metulae, (D) phialides and (E) mature conidiophore with conidial chains. Adapted from Mims *et al.* (1988).

Colletotrichum gloeosporioides (Barhoom *et al.*, 2007; Owsianowski *et al.*, 2008). Cell death has been studied in fungi as valuable model organisms and in a variety of contexts of fungal biology including host defense mechanisms (e.g. oxidative burst and α-tomatin), sexual and asexual development, nutritional starvation, putative antagonistic mediators (e.g. antifungal proteins and farnesol), aging and heterokaryon incompatibility.

Carbon starvation, conidiation and autolysis in submerged cultures

A. niger belongs to the fungi imperfecti (Deuteromycota) as a sexual life cycle has never been observed for this species. Consequently, the only (known) reproductive mode is conidiation, the formation of asexual spores, so called conidia (see Figure 1.5E). Those conidia are airborne, highly melanized (dark pigmentation) and hydrophobic haploid cells which are more resistant to harsh conditions than vegetative cells and thereby improve the chance of successful proliferation of the fungus. Once a conidium meets the right conditions it can germinate and form a new mycelium, completing the life cycle (see Figure 1.1).

Asexual differentiation and the underlying spatio-temporal regulatory mechanisms leading to the formation of conidiophores, spore bearing structures consisting of multiple cell types (see Figure 1.5), were studied in detail in the model fungus *A. nidulans* (Adams *et al.*, 1998). Core genes involved in signal transduction and asexual development (see Figure 1.6) have also been identified in *A. niger* (Pel *et al.*, 2007), suggesting that the regulation of asexual development is conserved.

In the review by Adams *et al.* (1998) a model has been established describing the interactivity of important developmental regulators controlling vegetative growth and development in *A. nidulans* (see Figure 1.6). A central and early developmental regulator for asexual devel-

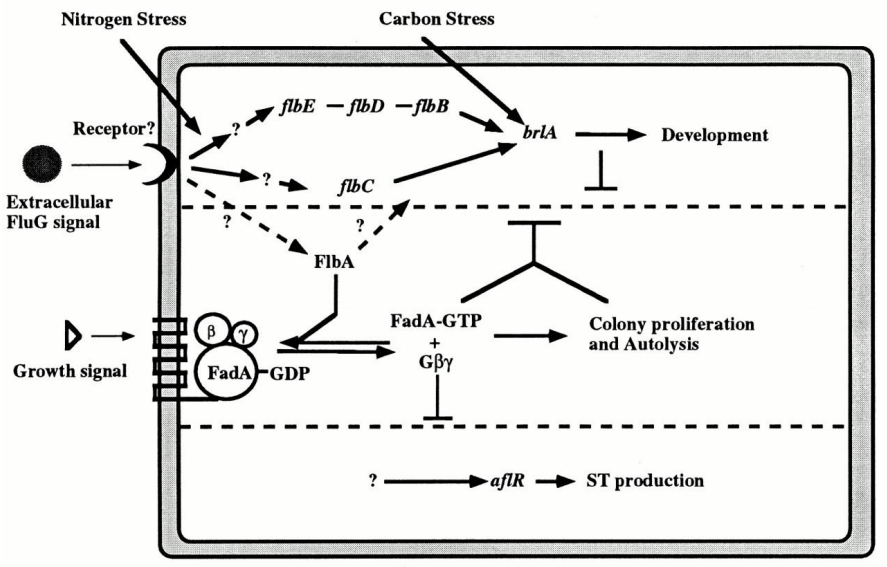

Figure 1.6 — Regulation of asexual development
Two antagonistic pathways were supposed to promote either vegetative growth or asexual development and secondary metabolism in *A. nidulans*. In its GTP-bound form, the Gα subunit FadA promotes vegetative growth and inhibits asexual development as well as secondary metabolism. Early developmental signals lead to the activation of FlbA, a regulator of G-protein signaling, which in turn enhances the FadA intrinsic GTPase activity and consequently leads to growth arrest, initiation of asexual development and activation secondary metabolism. Adapted from Adams *et al.* (1998)

opment is the transcriptional activator BrlA (bristle A), which acts downstream of the regulatory circuit consisting of five proteins FlbA-FlbE encoded by the so called fluffy genes *flbA* to *flbE*. BrlA induces its own transcription and that of downstream regulators including AbaA and WetA. Due to its autoregulation, BrlA mRNAs accumulate strongly during conidiation. Deletion of *brlA* completely blocks asexual differentiation at the stage after the formation of conidiophore stalks (see Figure 1.5A), giving mutant colonies a bristle-like appearance.

The transition from vegetative growth to asexual development is regulated by a heterotrimeric G-protein consisting of Gα, Gβ and Gγ subunits. In its active GTP-bound form, the Gα subunit FadA dissociates from Gβγ promoting colony proliferation and blocking asexual differentiation. FlbA, a regulator of G-protein signaling, is thought to enhance the intrinsic GTPase activity of FadA, whereby FadA becomes converted into its inactive GDP-bound form which associates with Gβγ forming the heterotrimeric Gαβγ complex. Consequently, vegetative growth is blocked and asexual development is initiated. Depending on upstream signals, FlbA is thus required for the initiation of conidiation by the inactivation of FadA. Similar to colonies of other mutants of the fluffy genes, FlbA mutant colonies have a fluffy a-conidial

appearance. However, in contrast to other fluffy mutants, the colony centers of FlbA mutants begin to disintegrate after about three days of growth resulting in collapsing of aerial hyphae and autolysis.

Although development and differentiation have mostly been studied at a substrate/air interphase, these processes also take place in submerged cultures under carbon or nitrogen starvation. Submerged cultivation of filamentous fungi can be accomplished by shaking liquid cultures or by cultivation in bioreactors. Aside from the industrial applicability, the latter has several advantages including high reproducibility, monitoring and controlling of physiological parameters. A number of recent studies for *A. niger* (Jørgensen *et al.*, 2009; Jørgensen *et al.*, 2010; Jørgensen *et al.*, 2011) have demonstrated the potential of bioreactor cultivation to dissect fungal physiology and development.

As described above, nutrient starvation in submerged cultures of filamentous fungi induces asexual development. In addition, complex physiological and morphological changes occur, leading to disintegration of the fungal biomass. These self-degradative processes are generally referred to as fungal autolysis and hallmarks are described to include biomass decline, hyphal fragmentation, emergence of empty hyphae, increase of extracellular hydrolase (proteases and glycosyl hydrolases) activities and extracellular ammonium (White *et al.*, 2002). Subsequently, cytological heterogeneity increases and it has been suggested that recycled resources fuel the maintenance of surviving compartments, conidiation and cryptic growth, a term used to describe re-growth under starvation conditions (Trinci *et al.*, 1969; Bainbridge *et al.*, 1971; McNeil *et al.*, 1998). As a consequence, yields of bioprocesses can be negatively affected e.g. by hydrolytic degradation of products, decreasing active biomass fractions or even problems during filtration (filter plugging by hyphal fragments) in downstream processing (White *et al.*, 2002; McNeil *et al.*, 1998). However, in some cases autolysis might even be desirable for the recovery of intracellular products.

Depending on the study, hydrolytic weakening of the fungal cell wall in aging nutrient deprived cultures of filamentous fungi has been reported to be either a key-characteristic or not evident. Excessive hyphal fragmentation has been reported, for example, for cultures of *P. chrysogenum* (McNeil *et al.*, 1998) and *A. nidulans* (Emri *et al.*, 2004), whereas another investigation with *A. nidulans* (Bainbridge *et al.*, 1971) stated that there were no cytological indications for lysis of cell walls. Studies with *Neurospora crassa* (Martinez *et al.*, 1969) and *A. niger* (Lahoz *et al.*, 1986) even assert that the stability of fungal cell walls in cultivations lasts up to 60 days.

The fungal cell wall is an essential component that determines the shape of the fungus, prevents it from lysis and protects it from the environment. It is rigid but dynamic and adapts its composition and molecular structure during spore germination, growth, development and in

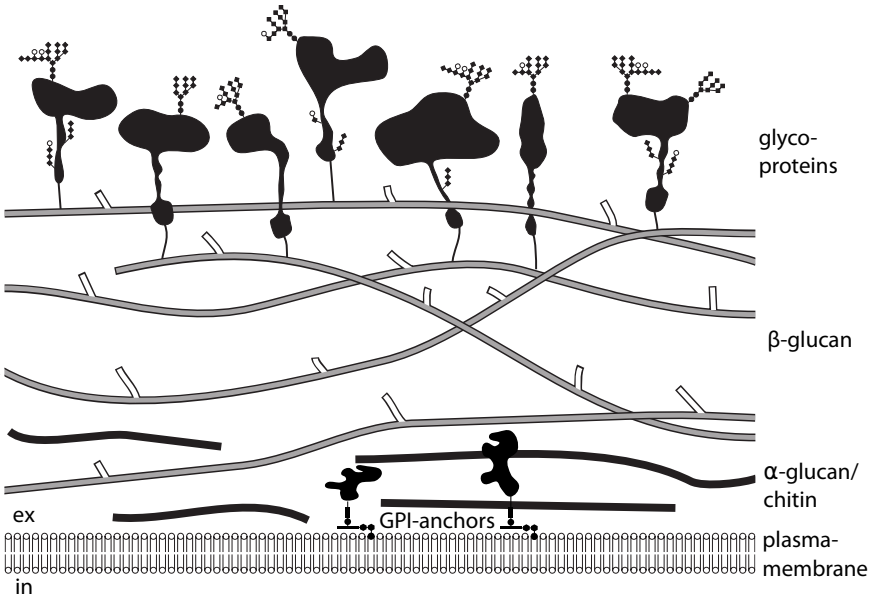

Figure 1.7 – The fungal cell wall
Schematic representation showing the organization of the different cell wall components: α-glucans, β-glucans, chitin and glycoproteins. Adapted from Grün (2003).

response to stress. The three major components of fungal cell walls are glycoproteins, glucan (mainly 1,3-β-glucan) and chitin (1,4-β-N-acetylglucosamine) polymers (see Figure 1.7). In general, there are considerable differences in the cell wall compositions between filamentous fungi and yeasts such as *S. cerevisiae* (Nobel *et al.*, 2000). Glucans and glycoproteins are the two major components of yeast cell walls, respectively, with 35-60% and 30-50% of the cell wall dry weight. Chitin is only a minor component accounting for 1.5-6% of yeast cell wall dry weight (Klis *et al.*, 2006). In comparison, the chitin content in the cell walls of filamentous fungi is up to 10-fold higher, amounting to 10-15% of the cell wall dry weight. Further differences in the cell wall composition of fungal species can be found in their glucan polymer compositions. For example, α-glucans are not present in the cell walls of *S. cerevisiae* and *Candida albicans*, whereas they are important cell wall polymers in many filamentous fungal species, including *A. niger* (R. A. Damveld *et al.*, 2005).

In particular, the role of chitinases in hydrolytic weakening of fungal cell walls during maintained nutrient deprived cultures of filamentous fungi has been studied in considerable detail. The most prominent autolytic chitinase is ChiB which has been identified as the major extracellular chitinase during the autolytic phase of carbon starved submerged cultures of *A. nidulans* (Pusztahelyi *et al.*, 2006). Deletion of *chiB* in *A. nidulans* has been shown to reduce

hyphal lysis in aging cultures (Yamazaki *et al.*, 2007). However, the role of *A. fumigatus* ChiB in cell wall weakening during carbon starvation is less clear. Although ChiB has been shown to be the major enzyme contributing to extracellular chitinolytic activity, its deletion did not affect the autolytic phenotype of *A. fumigatus* (Jaques, 2003). During autolysis, chitin is thought to be degraded in two successive steps involving degradation of chitin polymers by chitinases and subsequent degradation of chitin oligomers, mainly chitobiose, by enzymes having β-N-acetylglucosaminidase activities (Kim *et al.*, 2002). One such β-N-acetylglucosaminidase is NagA, which has been shown to be simultaneously early induced with ChiB upon carbon depletion in *A. nidulans* (Pusztahelyi *et al.*, 2006).

Based on the analysis of several developmental mutants of *A. nidulans* including FluG1, $\Delta brlA$, $\Delta flbA$-$\Delta flbD$ and $fadA^{G203A}$, Pósci and colleagues demonstrated that there is a relation between conidiation and autolysis and that both share common regulatory elements (Molnár *et al.*, 2004; Emri *et al.*, 2005b). For example the loss-of-function *fluG* mutant has been reported to have a non-autolytic phenotype with reduced biomass decline, low chitinase and protease activities as well as severely reduced hyphal fragmentation (Emri *et al.*, 2005b).

Outline of the thesis

This thesis aims at elucidating processes that are induced during carbon starvation in submerged cultures of the industrially important filamentous fungus *Aspergillus niger*. Carbon starvation has been achieved by prolonged cultivation in carbon-limited bioreactor batch cultures. During carbon starvation in aging batch cultures, carbon and energy for maintenance of surviving compartments, cryptic re-growth and asexual development are exclusively available by recycling of endogenous and exogenous resources. This is in contrast to cultivations with pulsed or continuous feeding regimes such as fed-batch or retentostat cultures, where requirements of carbon and energy are (partially) met by the fed substrate. The complex physiological changes during carbon-starved batch cultures were studied and described on a systems level covering physiology, morphology, transcriptomics and secretomics.

Chapter 1 provides an introduction to filamentous fungi, their importance as industrial production hosts and pathogens. Some characteristic traits of filamentous fungi contributing to their lifestyle are briefly introduced in general and/or with respect to nutrient (carbon) starvation.

Resources required for the analysis of omics data from *A. niger* were established and described in chapters 2 and 3. Chapter 2 focuses on transcriptomic data analysis which can generally be considered as a multi-step approach including primary quality assessment, normalization, background correction and condensation of raw data followed by computation of

differentially expressed or co-transcribed genes. Using public *A. niger* datasets, basic steps of transcriptomic data analysis with the open source statistical programming language R were described in a step-by-step tutorial and important theoretical background on the required statistics has been provided. In chapter 3, *A. nidulans* Gene Ontology (GO) annotation was mapped to all Aspergilli with published genome sequences and an online tool for GO enrichment analysis (FetGOat: http://www.broadinstitute.org/fetgoat/index.html) was implemented, thus establishing new resources that strongly facilitate omics data analysis.

Subsequently, in Chapter 4 the above tools for omics data analysis were applied in combination with physiological and morphological analyses to investigate carbon starvation in submerged batch cultures of *A. niger* on a systems level. This description provides a framework for detailed analysis of specific processes induced under carbon starvation conditions. Autophagy and conidiation were among the predominantly induced processes. Subsequently, in chapter 5 the role of autophagy during carbon starved batch cultivation was investigated by deletion of essential autophagy genes and phenotypic characterization during surface growth and submerged cultivation in carbon-limited batch cultures. Fluorescent microscopy and automated image analysis provide evidence that autophagy promotes survival by physiological adaptation to carbon starvation.

Chapter 2

The use of open source bioinformatics tools to dissect transcriptomic data

Benjamin M. Nitsche[1], Arthur F.J. Ram[1,2], Vera Meyer[1,2,3]

[1]Institute of Biology, Leiden University, Sylviusweg 72, 2333 BE Leiden, The Netherlands
[2]Kluyver Centre for Genomics of Industrial Fermentation, PO Box 5057, 2600 GA, Delft, The Netherlands
[3]Institute of Biotechnology, Berlin University of Technology, Gustav-Meyer-Allee 25, 13355 Berlin, Germany

Abstract

Microarrays are a valuable technology to study fungal physiology on a transcriptomic level. Various microarray platforms are available comprising both single and two channel arrays. Despite different technologies, preprocessing of microarray data generally includes quality control, background correction, normalization and summarization of probe level data. Subsequently, depending on the experimental design, diverse statistical analysis can be performed, including the identification of differentially expressed genes and the construction of gene co-expression networks. We describe how Bioconductor, a collection of open source and open development packages for the statistical programming language R, can be used for dissecting microarray data. We provide fundamental details that facilitate the process of getting started with R and Bioconductor. Using two publicly available microarray datasets from *Aspergillus niger*, we give detailed protocols on how to identify differentially expressed genes and how to construct gene co-expression networks.

Methods Mol Biol. 2012;835:311-31

Introduction

The open source and open development project Bioconductor (Gentleman *et al.*, 2004) (http://bioconductor.org/) is actively developed and maintained by members of the academic community, thus providing scientists with leading edge computational biology tools. Bioconductor is well suited for the academic environment where it can be used for research and education. Rather than providing a graphical user interface, most Bioconductor packages depend on command line input. Therefore, getting started with Bioconductor requires some effort, especially for those having limited computational background.

In the following, we give a step-by-step tutorial on how Bioconductor can be used for transcriptomic data analysis and provide the reader with the most important theoretical background on the statistics involved. We use two Affymetrix microarray datasets that were recently published for *Aspergillus niger* (Jørgensen *et al.*, 2010; Martens-Uzunova *et al.*, 2006). The datasets as well as all Bioconductor packages are publicly available, allowing the reader to repeat each step of the analysis. We start with a brief description on how the statistical programming language R (R-Team, 2008) (http://www.r-project.org/), Bioconductor core packages and additional Bioconductor packages can be installed. For the identification of differentially expressed genes, we demonstrate how to import CEL files and associate them with phenotypic labels, how to preprocess microarray data and asses its quality, how to perform multi-way comparisons and finally, how to export the data. For the construction of gene co-expression networks, we subsequently import CEL files, assess the data quality and preprocess the CEL files, perform non-specific filtering and construct gene co-expression networks.

Materials

In the examples described thereafter, the open source and open development packages from the Bioconductor project (Gentleman *et al.*, 2004) (http://bioconductor.org/), which use the statistical programming language R (R-Team, 2008) (http://www.r-project.org/), are used for the analysis of transcriptomic data. The following packages available from the Bioconductor homepage are required: affy (Gautier *et al.*, 2004), affycoretools (MacDonald, 2008), affyPLM (Bolstad *et al.*, 2005), limma (Smyth, 2004), genefilter (Gentleman *et al.*, 2006) and makecdfenv (Irizarry *et al.*, 2006).

Both transcriptomic datasets used for demonstration purposes were recently published for *A. niger* and have been deposited at public databases. The first dataset (Jørgensen *et al.*, 2010) used for the identification of differentially expressed genes comprises nine Affymetrix microarrays corresponding to three different time points during maltose-limited retentostat cultivations and is available via its accession number GSE21752 at the NCBI Gene Expression

Omnibus (GEO) database (http://www.ncbi.nlm.nih.gov/geo/) (Barrett *et al.*, 2011). The second dataset (Martens-Uzunova *et al.*, 2006) used for the construction of gene co-expression networks comprises 29 Affymetrix microarrays from multiple time points after transfer of mycelial biomass from fructose to a variety of carbon sources: rhamnose, xylose, sorbitol, galacturonic acid, polygalacturonic acid and sugar beet pectin. The dataset is available at the EMBL ArrayExpress database (http://www.ebi.ac.uk/arrayexpress/) via the accession number E-MEXP-1626.

Both transcriptomic datasets are based on the Affymetrix chip dsmM_ANIGERa_coll 511030F. The corresponding chip description file (CDF) can be downloaded from the NCBI GEO database via the GEO accession number GPL6758.

Methods

Installation

Before installing Bioconductor packages, the statistical programming language R has to be installed. R installation packages and platform specific help files are available for Linux, Mac OS and Windows at the Comprehensive R Archive Network (CRAN: http://www.r-project.org/). After successful installation, the R command window can be accessed via its application icon or by typing R at the command prompt (see **Note 1**). To install the Bioconductor core packages, make sure to have an Internet connection and type at the R command window (see **Note 2**):

```
> source("http://bioconductor.org/biocLite.R")
> biocLite()
```

Further packages have to be installed:

```
> biocLite("affycoretools")
> biocLite("makecdfenv")
> biocLite("limma")
```

For Affymetrix chips, analysis of raw data usually starts with CEL files. They contain the information from intensity calculations of the pixel values from the raw image data (DAT files) obtained with the chip scanner. To be able to import the Affymetrix raw data from CEL files, Bioconductor requires information about the corresponding Affymetrix chip which has to be provided as a chip-specific package. While those packages can be downloaded for many popular Affymetrix chips, they first have to be built for custom-made arrays such as the *A. niger*

chip. The Affymetrix chip description file (CDF) provides all information required for building the package.

To build the CDF package, first download the dsmM_ANIGERa_coll511030F CDF archive file via its GEO accession number GPL6758 from the GEO database (http://www.ncbi.nlm.nih.gov/geo/) and decompress it (see **Note 3**). Create a new directory (from now on referred to as working directory, WD), copy the CDF file to the WD and rename it into "dsmM_ANIGERa_anColl.CDF". At the R command line, define the WD with the function setwd (see **Note 4** and **Note 5**), load the required package makecdfenv with the library command and build the chip specific package with the make.cdf.package function:

```
> setwd("absolute path to WD/")
> library("makecdfenv")
> make.cdf.package("dsmM_ANIGERa_anColl.CDF", species = "Aspergillus niger
  ")
```

The newly built package is saved in a new folder in the WD (WD/dsmmanigeraancollcdf/). Next, open a new command prompt window, change to the WD and install the package (see **Note 1**):

```
> R CMD INSTALL dsmmanigeraancollcdf
```

Computation of differentially expressed genes

The identification of differentially expressed genes will exemplarily be shown on a transcriptomic dataset recently published for *A. niger* (Jørgensen *et al.*, 2010). The data has been deposited at the NCBI GEO database and can be downloaded via its accession number: GSE21752. *A. niger* was cultivated under controlled conditions in carbon-limited retentostat cultures, which is a specific form of continuous cultivation. The biomass was retained in the bioreactor, while old medium was removed and fresh defined medium was fed at a constant rate. With increasing cultivation time, the biomass specific availability of the sole limiting carbon source maltose decreased and the fungus underwent carbon starvation. The RNA used for microarray hybridizations derived from three different time points: Batch phase referred to as day 0 (d0), day 2 and day 8 of retentostat cultivation (d2 and d8, respectively). With three replicate cultures, the number of microarrays adds up to a total of nine. Below, we describe how to identify sets of genes that are differentially expressed comparing d2 versus d0, d8 versus d0 and d8 versus d2.

Importing CEL files into R

Create a new WD and download the raw data (CEL files) from the NCBI GEO database (http://www.ncbi.nlm.nih.gov/geo/) via the dataset accession number GSE21752. Next, decompress (see **Note 3**) the data and copy the CEL files into the WD. Open the R command line, load the packages that will be used for data analysis with the library function and define the WD using the function setwd (see **Note 4** and **Note 5**):

```
> library("affy")
> library("affycoretools")
> library("affyPLM")
> library("limma")
> setwd("absolute path to WD/")
```

Before importing the CEL files into R, generate a file that allocates phenotypic labels to them. It consists of tab-separated columns and should be saved in the WD as a plain text file named "phenotypic_labels.txt". The required sample information can be obtained from the NCBI GEO database via the corresponding dataset accession number (GSE21752). The content of the phenotypic label file should look like:

```
sample    FileName          Target
d0.1      GSM542228.CEL     d0
d0.2      GSM542335.CEL     d0
d0.3      GSM542336.CEL     d0
d2.1      GSM542337.CEL     d2
d2.2      GSM542338.CEL     d2
d2.3      GSM542339.CEL     d2
d8.1      GSM542340.CEL     d8
d8.2      GSM542341.CEL     d8
d8.3      GSM542342.CEL     d8
```

Use the function read.table to import the text file and assign (see **Note 6**) the phenotypic labels to the variable pData, which represents a data frame with row names equal to the unique file names. Subsequently, call the function ReadAffy to import the raw data from all annotated CEL files:

```
> pData <- read.table("phenotypic_labels.txt", row.names = 2, header =
  TRUE)
> rawData <- ReadAffy(filenames = rownames(pData), verbose = TRUE)
```

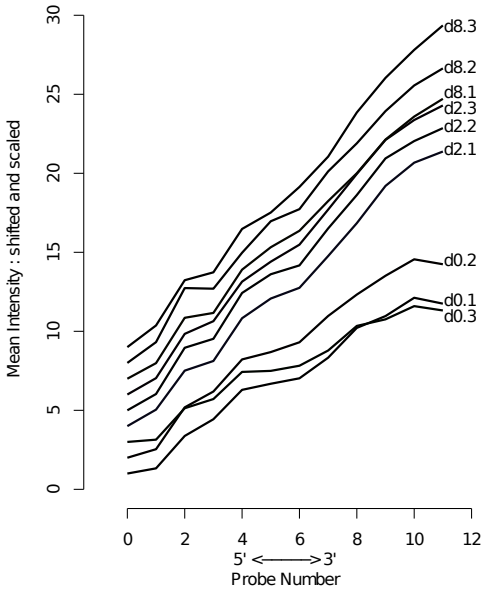

Figure 2.1 — RNA degradation plot
For each array of the retentostat dataset (GSE21752), mean probe intensities are plotted ordered from 5' to 3' end. For assessment of RNA quality, it is important that the 5'/3' intensity ratios are comparable between samples rather than the actual values. Typical 5'/3' ratios depend on the Affymetrix chip used (Bolstad *et al.*, 2005; MacDonald, 2008).

Quality assessment and preprocessing

We recommend checking the average integrity of RNA transcripts, because RNA is very sensitive to degradation by ribonucleases. For this purpose, make a degradation plot showing mean intensities of the probes ordered from 5' to 3' end of their target transcripts. The 5'/3' ratio of mean probe intensities should be comparable between the samples, as shown in Figure 2.1 (see **Note 7**). The following code will create a degradation plot (see **Note 8**):

```
> plotDeg(rawData, filenames = pData$sample)
```

Next, use the Robust Multi-array Average (RMA) package (Irizarry *et al.*, 2003) for preprocessing probe level data. The function rma performs background correction, quantile normalization and robust median polish to summarize intensities of probe sets to expression values. Background correction aims to differentiate specific from non-specific hybridization signals. For this purpose, Affymetrix chips are designed to provide pairs of nearly identical probes for hybridization, so called perfect match (PM) and mismatch (MM) probes. The MM probes are identical to the PM probes, except for their central nucleotide at position 13, which is

changed to its complement. The Affymetrix MAS5.0 algorithm for background correction uses the intensities of both probes to correct for non-specific hybridization signals. However, it has been shown that MM probes in many cases give stronger signals than their corresponding PM probes indicating that besides non-specific also specific hybridization occurs (Naef *et al.*, 2002). Therefore, RMA does not use MM probe intensities but applies a global empirical model for the distribution of PM probe intensities for background correction. Especially for lowly expressed genes, the RMA algorithm for background correction has been shown to be superior to MAS5.0 (Irizarry *et al.*, 2003). Before normalization, differences in probe intensities between arrays are due to biological and technical differences. The later is mainly introduced during labeling and hybridization, which normalization aims to compensate for. After normalization, differences in probe intensities between arrays should in theory exclusively be due to biological differences. The quantile normalization performed by RMA makes probe intensity distributions comparable between the set of arrays under investigation. Finally, RMA fits a robust multi-array model to summarize the probe intensities of each probe set into an expression value. Use the rma function to preprocess the probe level data and compute expression values. The results are organized as an object of the class ExpressionSet. To allocate phenotypic labels to the ExpressionSet object eset, call the function new:

```
> eset <- rma(rawData)
> phenoData(eset) <- new("AnnotatedDataFrame", data = pData)
```

To show the effect of quantile normalization, generate two box plot diagrams for the raw and RMA processed data. First, use the function par to define a new window in which two plots can be placed next to each other (see **Note 9**). Subsequently, generate two box plot diagrams with the function boxplot. The two box plots nicely illustrate the effect of RMA preprocessing. As a result of quantile normalization, the arrays have nearly identical median intensities and comparable intensity distributions after RMA preprocessing compared to the raw data (see Figure 2.2).

```
> par(mfrow = c(1,2))
> boxplot(rawData, las = 2, cex.axis = 0.5, main = "raw data")
> boxplot(eset, las = 2, cex.axis = 0.5, main = "RMA preprocessed data")
```

Next, convert the ExpressionSet object eset, to a matrix with RMA expression values (see **Note 10**) using the function exprs and assign the resulting matrix to the variable e. The matrix has nine columns (one for each CEL file) and 14,554 rows, each containing probe specific RMA expression values. The probes still include Affymetrix control probes beginning with

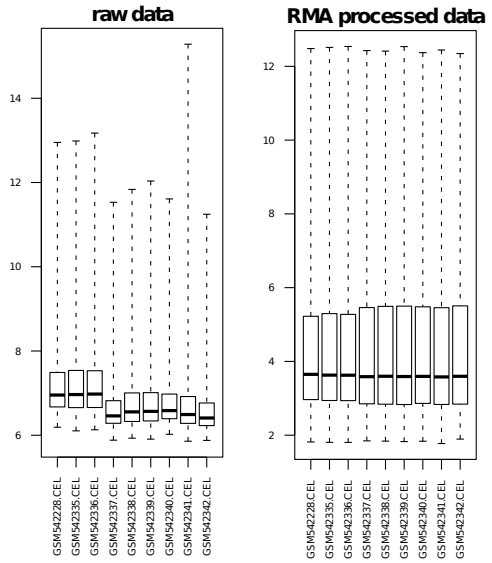

Figure 2.2 – Boxplots of raw and RMA processed data
For each array of the retentostat dataset (GSE21752), boxplots show the log intensity distributions of raw and RMA processed data. As a result of quantile normalization, the log intensity distributions are comparable after RMA processing (Irizarry *et al.*, 2003).

"AFFX". To remove them, use the function grep (see **Note 11**) and obtain an index referring to all probes that are starting with "AFFX". Subsequently create the matrix e.anig containing exclusively *A. niger* specific probes (see **Note 12**):

```
> e <- exprs(eset)
> subIndex <- grep("AFFX", featureNames(eset))
> e.anig <- e[-subIndex,]
```

Before starting the comparative analysis, do a simple test to exclude errors during the allocation of phenotypic labels to the CEL files. Using the function plotPCA, perform a principal component analysis (PCA) and plot the first two principal components against each other. Array data deriving from replicate time points is expected to cluster together. The PCA plot clearly shows that replicate array data from d0, d2 and d8 clusters together and that the three clusters are well separated (see Figure 2.3). Errors during the allocation of phenotypic labels to the CEL files can therefore be excluded.

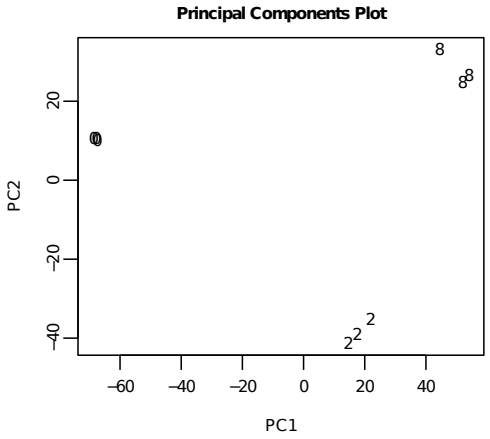

Figure 2.3 – Principle component analysis (PCA)
For each array of the retentostat dataset (GSE21752), the first two principle components are plotted against each other. Ideally, replicate arrays should cluster together and clusters of replicate arrays should be well separated. PCA plots can thus be applied to exclude errors during the allocation of phenotypic labels and to assess the reproducibility.

```
> par(mfrow = c(1,1))
> plotPCA(e.anig, groupnames = labels, pch = c
  ("0","0","0","2","2","2","8","8","8"), col = rep("black",9), legend =
  FALSE)
```

Multi-way comparisons

When analyzing microarray data, multiple-hypothesis testing has to be taken into account (see **Note 13**). Diverse methods have been suggested to correct p-values for multiple testing among which the Benjamini and Hochberg (BH) false discovery rate (FDR) (Benjamini *et al.*, 1995) is commonly used. However, multiple testing correction decreases the statistical power (see **Note 14**), which in many cases is anyway low due to small sample sizes. Different methods have been suggested to compensate for that. A reduction of the number of hypothesis tests to be performed by non-specific filtering of probes with low information content is one possibility. If the non-specific filtering is independent from the following hypothesis tests, it has been shown to increase the statistical power (Bourgon *et al.*, 2010). The standard deviations or mean values of probe intensities over all arrays (neglecting phenotypic labels) could be used for non-specific filtering. An alternative approach could be the computation of moderated (Baron *et al.*, 1986) instead of normal statistics. One such approach is implemented in the eBayes method from the Limma package (Smyth, 2004), where a global variance estimator

borrows information from all genes to infer probe-specific variances. A combination of non-specific filtering and moderated statistics is obviously an interesting approach. However, it has been shown to potentially decrease the statistical power and therefore either, non-specific filtering with normal t-statistics or moderated t-statistics with unfiltered data are recommended (Bourgon *et al.*, 2010).

It is very convenient to use the limma package for multi-way comparisons of microarray data. It can even be used for multi-factorial experimental designs (see **Note 15**). Compute moderated t-statistics on the unfiltered data by calling multiple limma functions. Indicate which experimental conditions should be compared to each other by defining a contrasts matrix with the function makeContrasts:

```
> f <- factor(pData$Target, levels = levels(pData$Target))
> design <- model.matrix(~0 + f)
> colnames(design) <- levels(pData[,2])
> fit <- lmFit(e.anig, design)
> contrasts <- makeContrasts(d2 - d0, d8 - d2, d8 - d0, levels = design)
> fit2 <- contrasts.fit(fit, contrasts)
> fit2 <- eBayes(fit2)
```

To better understand the concept of the contrasts matrix, have a look at how R represents it. Type at the R command line:

```
> contrasts
```

Next, make Venn diagrams to get an overview of the sets of genes that are differentially expressed comparing d2 to d0, d8 to d2 and d8 to d0. First, use the function decideTests to decide whether or not genes are differentially expressed controlling the FDR at 0.005:

```
> results <- decideTests(fit2, adjust.method = "fdr", p.value = 0.005)
```

The results matrix consists of three columns, one for each comparison defined in the contrasts matrix, and rows for each probe. The numbers indicate if a gene is not differentially expressed (0), upregulated (+1) or downregulated (-1). To get an impression of the results matrix, take a look at rows 120 to 130:

```
> results[120:130,]
```

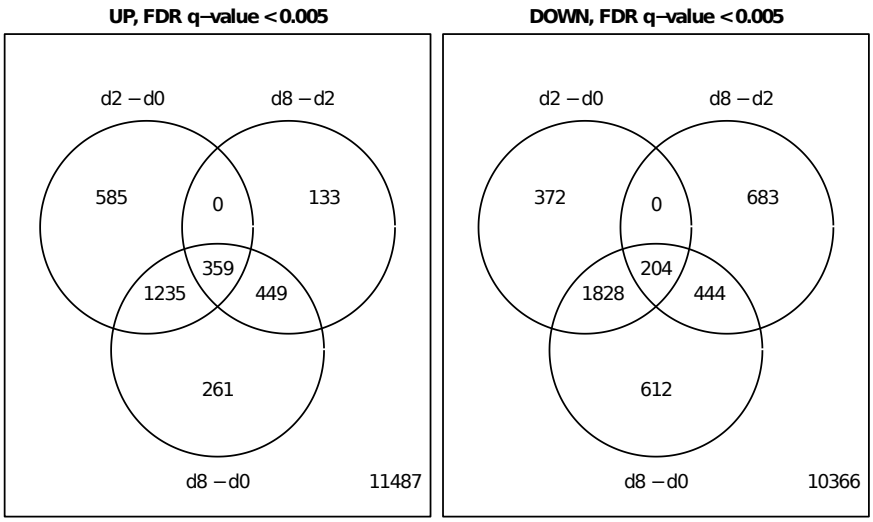

Figure 2.4 – Venn diagrams
Venn diagrams showing the relations between sets of up- and downregulated genes identified comparing day 0 (d0), day 2 (d2) and day 8 (d8) of retentostat cultivation.

Finally, use the information of the results matrix to generate two Venn diagrams (see Figure 2.4) for the up- and downregulated genes:

```
> par(mfrow = c(1,2))
> vennDiagram(results, include = "up", main = "UP, FDR q−value < 0.005",
  cex = 0.8)
> vennDiagram(results, include = "down", main = "DOWN, FDR q−value <
  0.005", cex = 0.8)
```

Next, obtain some of the results from the moderated t-statistics that were computed with the limma package. Extract the p-values and assign them to the matrix p.values (see **Note 16**).

```
> p.values <− fit2$p.value
```

In order to have distinct column names when combining different data later, change the column names of the p.value matrix. Use a for loop (see **Note 17**) to access column by column of the p.value matrix. In each cycle of the for loop, the function paste (see **Note 18**) is used to generate a new column name by preceding the corresponding column name from the contrasts matrix with “pValue”.

```
> for(i in 1:ncol(contrasts)){
>  colnames(p.values)[i] <- paste("pValue.", colnames(contrasts)[i], sep =
   " ")
> }
```

To obtain FDR q-values, use the function p.adjust and correct the p-values for multiple hypothesis testing. For each column of the p.value matrix, apply the Benjamini and Hochberg method to compute FDR q-values, combine them to a new matrix fdr.values using the function cbind (see **Note 19**) and change their column names:

```
> fdr.values <- NULL
> for(i in 1:ncol(p.values)){
>  fdr.values <- cbind(fdr.values, p.adjust(p.values[,i], method = "BH"))
>  colnames(fdr.values)[i] <- paste("qValue.", colnames(contrasts)[i], sep
   = " ")
> }
```

Next, obtain the fold changes applying the limma function topTable (see **Note 20**). Loop through all comparisons defined in the contrasts matrix and call the function topTable to extract the log2 fold changes for the corresponding comparison. Subsequently transform the log2 fold changes to normal scale and appended them to the matrix FCs. Define the column names of the matrix FCs analogously to the examples given above.

```
> FCs <- NULL
> for(i in 1:ncol(contrasts)){
>  toptable <- topTable(fit2, coef = i, number = 15000, adjust.method = "
  BH", sort.by = "none", p.value = 1, lfc = 0)
>  FCs <- cbind(FCs,2^toptable$logFC)
>  colnames(FCs)[i] <- paste("FC.", colnames(contrasts)[i], sep = " ")
> }
```

Besides the RMA expression data for the nine arrays, it is helpful to provide mean expression data for each of the three time points. Make use of the pData matrix, which allocates phenotypic labels to the CEL files to loop through the three time points. Because the dataset consists of triplicates, use the function unique (see **Note 21**) to access each time point only once. In each cycle of the loop, call the function which (see **Note 22**) to obtain an index pointing to the corresponding columns of the expression data matrix. Subsequently, use the function apply (see **Note 23**) to calculate mean expression values and convert the log2 expression data to normal scale. At the end of each loop, extend the matrix mean by the computed mean expression data and define the column names accordingly:

```
> means <- NULL
> for(i in 1:length(unique(pData$Target))){
>  Index <- which(eset$Target == unique(pData$Target)[i])
>  log2.a <- apply(e.anig[,Index],1,mean)
>  a <- 2^(log2.a)
>  means <- cbind(means, a)
>  colnames(means)[i] <- paste("mean.", unique(pData$Target)[i], sep = "
  ")
> }
```

Exporting data

For sharing data, it is wise to export it in such a way that it can be imported into any spreadsheet program. Use the function cbind (see **Note 19**) to combine the RMA and mean expression data as well as fold changes, p-vlaues and FDR q-values into the new matrix export:

```
> export <- cbind(e.anig, means, FCs, p.values, fdr.values)
```

Finally, use the function write.table to save the matrix export as a tab-delimited plain text file "results.txt" in the current WD:

```
> write.table(export, quote = FALSE, row.names = TRUE, col.names = NA, sep
  = "\t", file = "results.txt")
```

Construction of gene co-expression networks

In the following, we give a short demonstration on how gene co-expression networks can be built when starting with raw CEL file data. The transcriptomic dataset used was published in 2006 for *A. niger* (Martens-Uzunova *et al.*) and comprises 29 microarrays, which can be downloaded from the EMBL ArrayExpress database via its accession number: E-MEXP-1626. Briefly, the data derives from shake flask experiments in which fungal biomass from 18 hours pre-grown cultures was transferred to seven carbon sources: rhamnose, xylose, sorbitol, fructose, galacturonic acid, polygalacturonic acid and sugar beet pectin. In total, one reference sample was taken from the pre-culture and subsequently four samples were taken within 24 hours after transfer for each of the seven carbon sources. Thus, no biological replicates are available for the transcriptomic data. The carbon sources cover repressing (fructose) and non-repressing (sorbitol) carbon sources as well as complex carbon sources (polygalacturonic acid

and sugar beet pectin) and common monomeric constituents (rhamnose, xylose and galacturonic acid).

Importing CEL files

Download the expression dataset from the ArrayExpress database (http://www.ebi.ac.uk/arrayexpress/), decompress (see **Note 3**) and copy the CEL files into a new WD. On the R command line, load the required libraries and define the WD:

```
> library("affy")
> library("affyPLM")
> library("affycoretools")
> library("genefilter")
> setwd("absolute path to WD/")
```

Next, use the function ReadAffy to import all CEL files present in the WD. No phenotypic labels need to be associated with the CEL file names, because we are not interested in differential expression between specific conditions.

```
> rawData <- ReadAffy(verbose = TRUE)
```

Quality assessment and preprocessing

The affyPLM package has been suggested for quality assessment of transcriptomic data and detection of outlier arrays (Bolstad *et al.*, 2005). First, fit a linear model to the Affymetrix probe level data using the function fitPLM. Based on the linear model, generate two plots that are particularly helpful to detect outlier arrays. The normalized unscaled standard error (NUSE) and the relative log expression (RLE) plots.

```
> rawDataPLM <- fitPLM(rawData)
> par(mfrow = c(1,2))
> boxplot(rawDataPLM, main = "NUSE", ylim = c(0.95, 1.25), las = 2,
  whisklty = 0, staplelty = 0, cex.axis = 0.5)
> abline(h = 1)
> Mbox(rawDataPLM, main = "RLE", whisklty = 0, staplelty = 0, ylim = c
  (-0.4, 0.4), las = 2, cex.axis = 0.5)
> abline(h = 0)
```

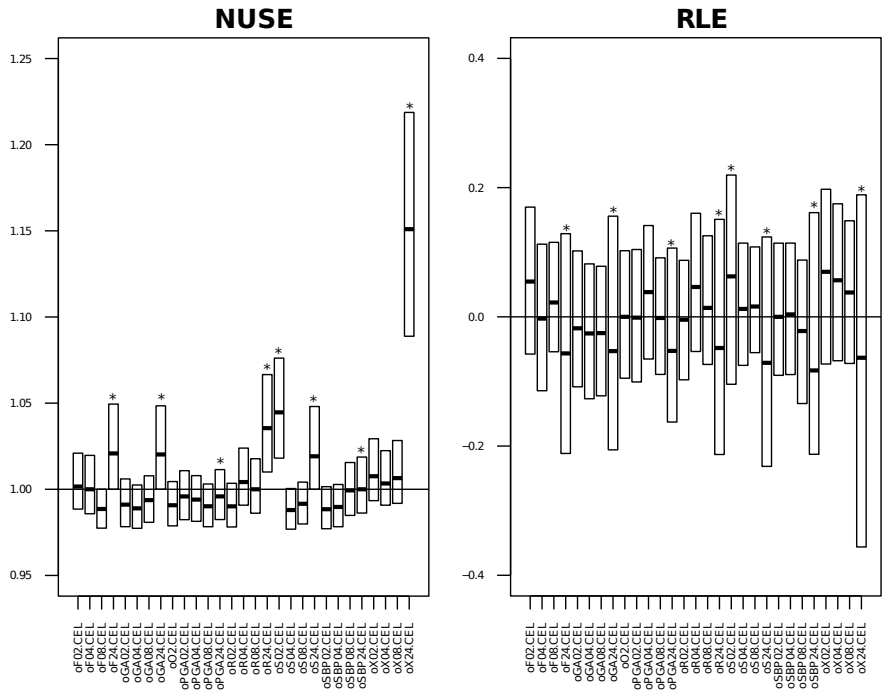

Figure 2.5 – Quality assessment using probe level models (PLM)
Normalized Unscaled Standard Error (NUSE) and Relative Log Expression (RLE) plots for each array of the carbon source transfer experiments (E-MEXP-1626). Outlier arrays (marked with asterisks) can be recognized by their deviation from the remaining arrays (Bolstad *et al.*, 2005).

Problematic arrays can be recognized from the NUSE plot as having elevated and more spread intensities. In the RLE plot, problematic arrays tend to have a larger spread and a median different from zero (Bolstad *et al.*, 2005). Inspecting the NUSE and RLE plots, all seven arrays from the 24 h samples can be considered as outlier arrays (see Figure 2.5). This could be due to secondary effects such as carbon and oxygen limitations during shake flask cultivation that are independent from the carbon sources. Furthermore, the first sorbitol time point appears to be problematic, probably because the fungus requires more time to induce the enzymatic machinery to metabolize it and therefore, during the first time points suffers from carbon limitation. We recommend removing these eight arrays before continuing with further analysis (see **Note 11** and **Note 12**).

```
> problematicArrays <- grep("24|oS04", sampleNames(rawData))
> rawData.sub <- rawData[,-problematicArrays]
```

Using a spike-in and dilution benchmark dataset, it was shown that the RMA algorithm is superior to the Affymetrix MAS5.0 algorithm for the detection of differentially expressed genes (Irizarry *et al.*, 2003). However, as recently reviewed (Usadel *et al.*, 2009), the preprocessing method of choice for gene correlation studies is less clear. With two different approaches (Harr *et al.*, 2006; Lim *et al.*, 2007), it was shown that RMA preprocessing is not suited for gene co-expression studies because of gene correlations introduced as artifacts by the RMA algorithm. For *Escherichia coli*, it was reported that a combination of the MAS5.0 background correction procedure with non-linear normalization (invariantset method) and probe summarization according to Li-Wong (Li *et al.*, 2001) gave the best correlations between co-transcribed operon genes (Harr *et al.*, 2006).

To combine MAS5.0 background correction with non-linear normalization and Li-Wong probe summarization, use the expresso function from the affy package. Assign the results, which are organized as an object of the class ExpressionSet to the variable eset. Subsequently, convert the ExpressionSet object to the expression matrix e and remove all Affymetrix control probes to finally obtain the matrix e.anig:

```
> eset <- expresso(rawData.sub, bgcorrect.method = "mas", pmcorrect.method
   = "mas", normalize.method = "invariantset", summary.method = "liwong")
> e <- exprs(eset)
> subIndex <- grep("AFFX", featureNames(eset))
> e.anig <- e[-subIndex,]
```

Non-specific filtering

For the construction of gene co-expression networks, the expression patterns of every pairwise combination of genes are checked for significant correlation. The number of probe pairs that can be drawn from n probes can be calculated with the binomial coefficient $\binom{n}{2}$ and is equal to $\frac{n!}{n(n-2)!}$. With the function choose, calculate the number of comparisons required for the e.anig matrix:

```
> choose(nrow(e.anig), 2)
```

The number of comparisons is 105,248,286, which will require a lot of computing time and memory. The number of comparisons can be reduced by not taking those genes into consideration that have a low overall variability across all arrays. Removal of all genes with standard deviation (SD) lower than the mode of the distribution of SDs has been suggested (Hahne *et al.*, 2008) as a good threshold for non-specific filtering based on variability (see **Note 24**). First,

calculate row-wise SDs with the rowSds function, determine the mode of the distribution of SDs with the function shorth and select all probes with SDs larger than the mode:

```
> sds <- rowSds(e.anig)
> sds.mode <- shorth(sds)
> e.anig.sub <- e.anig[sds > sds.mode,]
```

After this non-specific filtering step, the pairwise comparisons are reduced by approximately 50%. 10,647 probes are left for which a total of 56,673,981 pairwise comparisons have to be computed.

Building gene co-expression networks

To compute pairwise correlation coefficients, use the function cor. For each pairwise combination of columns from a given matrix, cor computes correlation coefficients as specified by the method parameter. Before the function can be applied, the matrix e.anig.sub has to be transposed using the function t. In the resulting matrix e.anig.sub.t, columns (CEL files) and rows (probes) are interchanged.

```
> e.anig.sub.t <- t(e.anig.sub)
```

The application of different correlation coefficients for the construction of gene co-expression networks has been discussed in a recent review (Usadel *et al.*, 2009). The Pearson correlation coefficient is often used as a measure for gene co-expression. However, it is sensitive to outliers and high correlation coefficients can only be obtained for linear relationships. The Spearman rank correlation coefficient has been supposed as a good alternative. The Spearman correlation coefficient is less sensitive to outliers because it is not directly calculated from the expression values but from ranks of expression values. Whereby, it can also detect correlations for non-linear relationships such as the Michaelis-Menten kinetic. To calculate pairwise Spearman correlation coefficients for the transposed matrix e.anig.sub.t, use the function cor (see **Note 25**):

```
> e.anig.sub.t.cor <- cor(e.anig.sub.t, method = "spearman")
```

The correlation matrix is symmetric with respect to its main diagonal. Row-column combinations define pairs of genes. Probes correlated to themselves are lying on the main diagonal and both halves (above and below the main diagonal) of the matrix contain equal information.

Therefore, only correlation coefficients from one half of the correlation matrix excluding its main diagonal have to be checked and compared to a threshold.

Before checking all pairwise comparisons, set a range of critical correlation coefficients by defining the minimal and maximal correlation coefficients cutoff.min and cutoff.max, as well as the increment cutoff.increment. The code below exemplarily defines a range of critical correlation coefficients, for which five different co-expression networks (with absolute correlation coefficients smaller than 0.70, 0.75, 0.80, 0.85, 0.90 and 0.95) will be constructed within a for loop (see **Note 17**).

```
> cutoff.min <- 0.7
> cutoff.max <- 0.95
> cutoff.increment <- 0.05
```

In order to check one half of the correlation matrix excluding its main diagonal, basically two for-loops have to be initiated. The outer for-loop increments its counter i, used as row index, by 1 starting with the first row until it reaches the last but one row. The inner for-loop increments its counter j, used as column index, by 1 starting at i plus 1 until it reaches the last column. In the inner for-loop, the row and column indices i and j are used to access the corresponding correlation coefficient and compare it to the range of thresholds defined above. For this, a third for-loop is initiated where probe pairs are linked to each other by positive or negative correlations if the correlation coefficient is larger or smaller in case of positive or negative values, respectively. The results are exported to files in the simple interaction format (SIF) format and saved in the WD (see **Note 24**).

```
> for(i in seq(1, nrow(e.anig.sub.t.cor) - 1, 1)){
>  print(i)
>  for(j in seq(i + 1, ncol(e.anig.sub.t.cor), 1)){
>   for(cutoff in seq(cutoff.min, cutoff.max, cutoff.increment)){
>    file.name <- paste("network.", cutoff, ".sif")
>    if(e.anig.sub.t.cor[i,j] > 0 && e.anig.sub.t.cor[i,j] > cutoff){
>     write(paste(row.names(e.anig.sub)[i], "POScorrelation", row.names(e.
  anig.sub)[j], sep = " "), file = file.name, append = TRUE)
>    }
>    if(e.anig.sub.t.cor[i,j] < 0 && e.anig.sub.t.cor[i,j] < (-1) * cutoff
  ){
>     write(paste(row.names(e.anig.sub)[i], "NEGcorrelation", row.names(e.
  anig.sub)[j], sep = " "), file = file.name, append = TRUE)
>    }
>   }
>  }
> }
```

The resulting SIF files can be imported into Cytoscape (Shannon *et al.*, 2003), an open source platform for network analysis and visualization. Cytoscape provides a graphical user interface and various plug-ins for network analysis exist, such as MCODE (Bader *et al.*, 2003) for the identification of clusters of highly connected genes or BinGO (Maere *et al.*, 2005) for enrichment analysis of Gene Ontology terms.

Notes

1. If R cannot be called from every directory at the command line, the directory containing its executable has to be added to the PATH environment variable. Details are depending on the operating system.

2. For R code and command line commands, each new line begins with a "larger-than" symbol (>). For copy and pasting the code to the corresponding command prompt, the "larger-than" symbols have to be removed.

3. For Windows systems, the open source program 7-zip (http://www.7-zip.org/) can be used for decompression.

4. In general, most R and Bioconductor functions/packages are well documented. Typing a question mark directly in front of any function at the R command line should open a short documentation (for example `?mean` opens the documentation for the function mean). Furthermore, many packages provide additional documentations (so-called vignettes) containing executable examples. When putting two question marks directly in front of any word, a list can be obtained with functions matching that word (for example `??mean` lists all functions matching the word mean).

5. The function `setwd` can be used to define the WD. The forward slash (/) is used as path separator. It is most robust, to define the absolute path. While on Mac OS and Linux, `setwd("/Users/someUser/Documents/someWD/")` could for example be used, it could look something like `setwd("C:/Documents and Settings/someWD/")` on a Windows system.

6. In R, values can be assigned to variables using <- or ->, which are assigning a value on their right to a variable on their left, or vice versa.

7. There is no critical slope indicating RNA degradation since different chip architectures result in different chip specific slopes. Rather than the actual values of the slopes, it is important that the slopes are comparable for different samples (Bolstad *et al.*, 2005; MacDonald, 2008).

8. Plots can be exported to PDF files by simply preceding the plot command(s) with pdf("desired_filename.pdf"). With dev.off(), the PDF file is finalized and saved in the current WD. If multiple plots are generated after initializing the PDF document, they will be appended to each other resulting in a single PDF file.

9. The function par can be used to set diverse graphical parameters among which mfrow can be used to define the number of rows and columns. Defining par(mfrow = c(i, j)) before plotting graphs will define i rows and j columns allowing to place i times j plots on one page or window.

10. Unlike most other preprocessing procedures, RMA expression values are in log(2) scale.

11. The function grep can be applied on a vector and returns an index of elements that match a given pattern.

12. To obtain parts of vectors or matrixes, subscripts can be used in R. Subscripts are given in squared brackets directly behind the corresponding variable. With v[3], the 3rd element from the one dimensional vector v can be obtained. For matrixes, the squared brackets contain two subscripts separated by a comma. The first subscript refers to the row and the second to the column. For the matrix m, the value of the 5th row and the 2nd column can be obtained by m[5,2]. Furthermore, the values of the 5th row and columns 2 to 5 can be obtained by m[5,2:5]. With m[5,c(2,4,5)], the values of the 5th row and columns 2, 4 and 5 can be obtained. By using negative subscripts, elements can be dropped from a vector or matrix. In addition, subscripts can consist of logical expressions (for example > or <) and subscripts can also be used for sorting. Many more details can be found in basic R documentations.

13. If one performs 10,000 independent t-tests on a set of 10,000 genes to identify differentially expressed genes applying a critical p-value of 0.05, the number of false positives (Type I error α) accounts to 500 (5% of 10,000). Without an adjustment for multiple testing, the Type I error rate is not controlled at the level indicated by the p-value, especially because the majority of genes is not expected to be differentially expressed in microarray studies.

14. The Type II error β accounts for false negatives and the statistical power is defined as $1 - \beta$.

15. The code can easily be adapted for similar analysis. The only lines that have to be changed are line 4 and line 5. Please consult the documentation of the limma package to understand the different commands in more detail.

16. The $ operator can be used in R to obtain a component from an object.

17. For loops can by applied to generalize or automate repeating blocks of code. For loops consist of two parts. The first part, which is enclosed by brackets initiates the loop by setting the loop counter, comparing it to a defined limit and incrementing it in each cycle. The second part of the loop, the body, is enclosed by curly brackets and contains the code to be executed in each cycle until the loop counter reaches the defined limit. By initializing a loop with (i in 1:ncol(contrasts)), the loop counter i is defined to start at 1, being incremented in each cycle by 1 until it is equal to the number of columns of the contrasts matrix. Alternatively, the function seq can be used to define the range of the loop counter i as follows (seq(start value, end value, increment)).

18. The function paste can be used to concatenate strings. The argument sep defines how the strings are separated. Calling paste("one", "two", sep = "-") results in "one-two".

19. The function cbind is used here to append matrixes or columns from matrixes together. The number and the order of rows have to be identical, because cbind does not take row names into consideration. If that his not the case, the function merge can be used.

20. The limma function topTable can be used to list the top-ranked genes from the limma analysis based on fold change, FDR or other criteria. Besides other information, the function topTable returns the logarithmic fold changes for the corresponding comparisons. In this example, the argument sort.by = "none" represses any sorting, because the data will be combined with other data based on the original row order using the function cbind later. The argument coef specifies which comparison of the contrasts matrix is of interest.

21. The function unique can be used to remove redundant elements from a vector.

22. To check within a logical expression if two arguments are equal, a double equal sign (==) has to be used. If only a single equal sign (=) is used, the argument on the right site gets assigned to the variable on the left.

23. The function apply can be used to apply a function to rows or columns of a matrix. While apply(x, 1, mean) computes column-wise mean values for all rows, apply(x, 2, mean) computes row-wise mean values for all columns of the matrix x.

24. Depending on the available computational resources, one might consider not to perform any non-specific filtering or to apply a more severe threshold. We recommend applying a range of filter settings and comparing the resulting co-expression networks.

25. With the method parameter for the cor function, different correlation coefficients can easily be calculated. Should R give an error message related to problems with memory allocation, apply a more stringent threshold for non-specific filtering to reduce the number of pairwise combinations.

Acknowledgments

This work was supported by a grant of SenterNovem IOP Genomics project IGE07008. Part of this work was carried out within the research programme of the Kluyver Centre for Genomics of Industrial Fermentation, which is part of the Netherlands Genomics Initiative/Netherlands Organization for Scientific Research. We thank T.G. Homan for discussions and proof reading of the manuscript.

Chapter 3

New resources for functional analysis of omics data for the genus Aspergillus

Benjamin M. Nitsche[1], Jonathan Crabtree[2], Gustavo C. Cerqueira[3], Vera Meyer[1,4,5], Arthur F.J. Ram[1,4], Jennifer R. Wortman[3]

[1]Institute of Biology, Leiden University, Sylviusweg 72, 2333 BE Leiden, The Netherlands
[2]Institute for Genome Sciences, University of Maryland School of Medicine, Baltimore, MD 20850, USA
[3]Microbial Informatics, Broad Institute, 320 Charles Street, MA 02141, USA
[4]Kluyver Centre for Genomics of Industrial Fermentation, PO Box 5057, 2600 GA, Delft, The Netherlands
[5]Institute of Biotechnology, Berlin University of Technology, Gustav-Meyer-Allee 25, 13355 Berlin, Germany

Abstract

Background: Detailed and comprehensive genome annotation can be considered a prerequisite for effective analysis and interpretation of omics data. As such, Gene Ontology (GO) annotation has become a well accepted framework for functional annotation. The genus *Aspergillus* comprises fungal species that are important model organisms, plant and human pathogens as well as industrial workhorses. However, GO annotation based on both computational predictions and extended manual curation has so far only been available for one of its species, namely *A. nidulans*.

Results: Based on protein homology, we mapped 97% of the 3,498 GO annotated *A. nidulans* genes to at least one of seven other *Aspergillus* species: *A. niger*, *A. fumigatus*, *A. flavus*, *A. clavatus*, *A. terreus*, *A. oryzae* and *Neosartorya fischeri*. GO annotation files compatible with diverse publicly available tools have been generated and deposited online. To further improve their accessibility, we developed a web application for GO enrichment analysis named FetGOat and integrated GO annotations for all *Aspergillus* species with public genome sequences. Both the annotation files and the web application FetGOat are accessible via the Broad Institute's website (http://www.broadinstitute.org/fetgoat/index.html). To demonstrate the value of those new resources for functional analysis of omics data for the genus *Aspergillus*, we performed two case studies analyzing microarray data recently published for *A. nidulans*, *A.niger* and *A. oryzae*.

Conclusions: We mapped *A. nidulans* GO annotation to seven other Aspergilli. By depositing the newly mapped GO annotation online as well as integrating it into the web tool FetGOat, we provide new, valuable and easily accessible resources for omics data analysis and interpretation for the genus *Aspergillus*. Furthermore, we have given a general example of how a well annotated genome can help improving GO annotation of related species to subsequently facilitate the interpretation of omics data.

BMC Genomics. 2011 Oct 5;12:486

Background

Gene Ontology (GO) is a framework for functional annotation of gene products aiming to provide a unique vocabulary for living systems (Ashburner *et al.*, 2000). It comprises Biological Process (BP), Molecular Function (MF) and Cellular Component (CC) ontologies. GO terms are organized as directed acyclic graphs (DAG) meaning that GO terms are connected as nodes by directed edges defining hierarchical parent-child relationships. As a consequence, the specificity of GO terms increases with increasing distance from their root node. Enrichment analysis of GO terms is a well accepted approach to dissecting omics data in a non-biased manner. It has been used in many studies to highlight major trends in genomic, transcriptomic or proteomic datasets and describe them with a controlled vocabulary (Jørgensen *et al.*, 2010; Lin *et al.*, 2009; Twine *et al.*, 2011; Ryan *et al.*, 2010). If the frequency of specific GO terms in a list of genes or proteins is higher than expected by chance, it is likely that these enriched GO terms are related to the biological processes under investigation.

The genus *Aspergillus* covers a group of filamentous fungi that includes saprophytes, human and plant pathogens as well as species being exploited in biotechnology. Whereas *A. nidulans* has been comprehensively studied and used as model organism, *A. niger*, *A. oryzae* and *A. terreus* are important industrial workhorses for the production of various enzymes and organic acids. In medical research, *A. fumigatus* and *Neosartorya fischeri* have been intensively studied because of their importance as allergens and pathogens of immunocompromised patients. The aflatoxin producing fungus *A. flavus* is well known to cause spoilage of a great variety of agricultural goods. With genome sequences publicly available for eight of its species, the genus *Aspergillus* provides an important group of related fungal species for comparative genomics (Jones, 2007). The exceptional role of this genus in the genomics of filamentous fungi is further emphasized by a community sequencing project (CSP#350), which has recently been initiated by the DOE Joint Genome Institute (JGI), aiming to sequence nine additional *Aspergillus* species. However, despite the importance of the genus *Aspergillus, A. nidulans* has so far been the only species with a genome-scale GO annotation inferred from both orthology mapping and intense manual curation (Wortman *et al.*, 2009; Galagan *et al.*, 2005; Arnaud *et al.*, 2010), thus providing a valuable resource for the analysis of omics data.

In this work, we have generated a new central repository for functional analysis of omics data for the genus *Aspergillus* using GO annotation. Firstly, we extended the GO annotation of *A. nidulans* to all *Aspergillus* species with publicly available genome sequences and generated annotation files compatible with diverse publicly available tools for GO enrichment analysis. Secondly, we further improved the accessibility of the GO annotation for the genus *Aspergillus* by integrating it into a web tool for GO enrichment analysis and graph visualization named Fisher's exact test Gene Ontology annotation tool (FetGOat). Finally, we performed two case

studies to demonstrate the value and flexibility of the newly generated resources for functional analysis of omics data for the genus *Aspergillus*.

Results

Mapping of GO annotation

A. nidulans is the only *Aspergillus* species for which comprehensive GO annotation based on both computational prediction and extended manual curation of gene-specific literature is available (Arnaud *et al.*, 2010). It constitutes a valuable resource for GO enrichment analysis, which has proven to be a powerful tool for dissecting omics data, for example sets of differentially expressed genes. The GO annotation of *A. nidulans* available at the Aspergillus Genome Database (AspGD) (Arnaud *et al.*, 2010) covers 33% (3,498) of its predicted transcripts and associates them with 3,340 GO terms. Including all parental nodes, the list of GO terms extends to 5,508 comprising 3,061 (55%) BP, 1,753 MF (32%) and 694 (13%) CC terms.

To extend this valuable resource to other species of its genus, we mapped the *A. nidulans* GO annotation to all *Aspergillus* strains with published genome sequences (see Table 3.1). Groups of orthologous and close paralogous proteins were compiled with the Sybil comparative analysis package (Crabtree *et al.*, 2007), which applies a modified reciprocal best-hit approach comprising two clustering cycles. Roughly 89% (99,679) of all predicted proteins from the ten analyzed *Aspergillus* strains constituted 13,179 Jaccard ortholog clusters. For *A. nidulans*, 9,250 of its predicted proteins were organized in Jaccard ortholog clusters, meaning that roughly 80% of all *A. nidulans* proteins were linked to at least one ortholog of another *Aspergillus* species. Of the 3,498 GO annotated *A. nidulans* genes, 97% were contained in Jaccard ortholog clusters, meaning that their associated annotations could be mapped to at least one other *Aspergillus* species (see Figure 3.1). Overall, mapping resulted in an average of 3,484 GO annotated tran-

Table 3.1 – Mapping of *A. nidulans* GO annotation

		Transcripts		
Species	**Strain**	**Predicted**	**GO annotated (%)**	**GO terms**
A. nidulans	FGSC A4	10546	3498 (33)	5508
A. fumigatus	AF2937	9846	3443 (35)	5445
A. fumigatus	A1163	10109	3450 (34)	5446
A. flavus	NRRL 3357	13487	3574 (26)	5463
A. niger	CBS 513.88	14366	3540 (25)	5430
A. niger	ATCC 1015	11200	3487 (31)	5412
A. oryzae	RIB40	12319	3502 (28)	5434
A. terreus	NIH 2624	10402	3414 (33)	5406
A. clavatus	NRRL 1	9379	3403 (36)	5449
N. fischeri	NRRL 181	10728	3543 (33)	5445

Summary of mapping *A. nidulans* GO annotation to seven other Aspergilli. The number of predicted transcripts were obtained from the Central Aspergillus Data REpository (CADRE) (Mabey *et al.*, 2004).

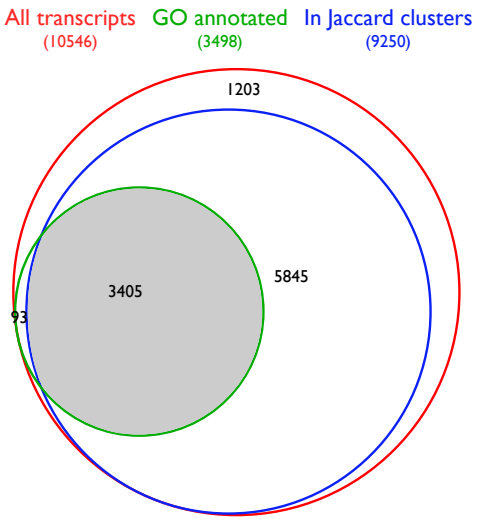

Figure 3.1 — Mapping of *A. nidulans* GO annotation to Jaccard ortholog clusters
Area-proportional Venn diagram (Hulsen *et al.*, 2008) showing fractions of all *A. nidulans* transcripts (red) annotated by GO (green) and/or associated with Jaccard ortholog protein clusters (blue). The intersection of all circles (gray), comprising 3,405 transcripts, was used to infer *A. nidulans* GO annotation to seven other *Aspergillus* species.

scripts per genome ranging from 3,403 (*A. clavatus*) to 3,574 (*A. flavus*). On average, their GO annotations comprise 5,436 terms, (see Table 3.1). These numbers correspond well to the GO annotation of *A. nidulans* and indicate that the majority (97%) of the *A. nidulans* GO annotated genes could be efficiently mapped to the other Aspergilli.

Availability of GO resources for the genus *Aspergillus*

The newly mapped GO annotations were deposited at the Broad Institute's website (http://www.broadinstitute.org/fetgoat/index.html). Different annotation file formats were generated that can be used with diverse public tools for GO enrichment analysis, such as: the Gene Set Enrichment Analysis tool (GSEA) (Subramanian *et al.*, 2005), the functional annotation suite Blast2GO (Conesa *et al.*, 2005), the Cytoscape plug-in BiNGO (Maere *et al.*, 2005) and the Bioconductor package TopGO (Adrian *et al.*, 2010). To further improve its accessibility, we have implemented Fisher's exact test (Fisher, 1922), a well-accepted approach for GO enrichment analysis, in the web application FetGOat and integrated the newly mapped GO annotations. FetGOat can be accessed via a web interface at the Broad Institute's website (http://www.broadinstitute.org/fetgoat/index.html). It combines GO annotations for all *Aspergillus* species with public genome sequences and a widely used statistical methodology to identify overrepresented GO terms. Via the web interface, a list of gene identifiers can be

uploaded to the server and statistical parameters can easily be adjusted with end-user computational skills. After completion of the analysis on the server-side, the enrichment results are sent by Email. The results consist of plain text and spreadsheet files as well as scalable vector graphics representing graphs of enriched GO terms.

Case studies

To demonstrate the flexibility and value of the newly generated resources for omics data analysis, we performed two case studies analyzing transcriptomic datasets recently published for the genus *Aspergillus*. In the first case study, we demonstrate that the generated resources can be used with various methods for enrichment analysis. We analyze a set of maltose-induced genes from *A. niger* using FetGOat and two alternative tools for enrichment analysis to subsequently compare their results. In the second case study, we highlight the advantage of having GO annotations that are as comprehensive as possible available for different species. We use FetGOat to analyze sets of glycerol-induced genes derived from a three-species microarray study to highlight major differences in the transcriptional responses for *A. nidulans*, *A. niger* and *A. oryzae*.

Maltose-induced genes

The first dataset reflects the transcriptomic responses of *A. niger* to growth in maltose and xylose-limited chemostat cultures at identical growth rates. From manual analysis of roughly 700 upregulated genes, Jørgensen *et al.* (2009) concluded a concerted induction of secretory pathway genes in maltose compared to xylose-limited cultures.

Using three alternative approaches, we repeated the analysis of the maltose induced genes in an automated and un-biased manner to subsequently compare their enrichment results. First, we performed the analysis using the web application FetGOat. We identified 73 enriched GO terms, which were reduced to 19 most-specific GO terms by removing redundant higher hierarchy terms with less detailed annotations. In correspondence to the findings by Jørgensen *et al.*, the enriched GO terms are related to important steps involved in protein secretion: Translocation to the endoplasmic reticulum, glycosylation and transport between the endoplasmic reticulum and the Golgi apparatus (see Table 3.2).

For comparison of FetGOat with alternative programs, we used the generated annotation files and repeated the enrichment analysis with two publicly available tools, Blast2GO (Conesa *et al.*, 2005) and GSEA (Subramanian *et al.*, 2005). The numbers of enriched GO terms found with Blast2GO and GSEA are in the same range compared to the results from FetGOat, they identified 76 and 47 enriched GO terms, respectively. To compare the enrichment results from

Table 3.2 – FetGOat enrichment analysis of maltose-induced genes

				Transcripts	
GO term	**Description**	**FDR**	**Ontology**	**Induced**	**Predicted**
Translocation to ER					
GO:0031204	posttranslational protein targeting	2.7E-04	BP	6	6
GO:0031207	Sec62/Sec63 complex	6.1E-03	CC	3	3
GO:0005787	signal peptidase complex	6.1E-03	CC	3	3
GO:0006616	SRP-dependent cotranslational protein targeting	1.7E-02	BP	4	5
GO:0051605	protein maturation by peptide bond cleavage	1.6E-02	BP	5	8
Glycosylation in ER					
GO:0005788	endoplasmic reticulum lumen	3.3E-03	CC	4	5
GO:0008250	oligosaccharyltransferase complex	6.9E-03	CC	4	6
GO:0006487	protein amino acid N-linked glycosylation	4.2E-02	BP	8	24
GO:0016758	transferase activity, transferring hexosyl groups	3.4E-02	MF	14	54
Transport between ER and golgi					
GO:0030126	COPI vesicle coat	1.3E-02	CC	4	7
GO:0030127	COPII vesicle coat	6.9E-03	CC	4	6
GO:0006888	ER to Golgi vesicle-mediated transport	4.8E-03	BP	22	92
GO:0030173	integral to Golgi membrane	12.0E-02	CC	5	12
Starch metabolism					
GO:0005982	starch metabolic process	4.2E-02	BP	5	10
Miscellaneous					
GO:0006066	alcohol metabolic process	4.2E-02	BP	33	199
GO:0003756	protein disulfide isomerase activity	8.2E-03	MF	4	4
GO:0006083	acetate metabolic process	4.2E-02	BP	7	19
GO:0015812	gamma-aminobutyric acid transport	4.2E-02	BP	6	14
GO:0015935	small ribosomal subunit	5.6E-03	CC	12	44

Most specific GO terms identified by FetGOat as being enriched in the maltose-induced gene set. GO terms were grouped in five arbitrary categories: Translocation into endoplasmic reticulum (ER), glycosylation in ER, transport between ER and golgi, starch metabolism and miscellaneous.

the three tools, we computed semantic similarity scores with the G-SESAME tool (Du *et al.*, 2009). For both FetGOat and Blast2GO, the enrichment statistic is based on Fisher's exact test and thus their results are theoretically expected to be identical resulting in a semantic similarity score of 1. A similarity score of 0.983 confirms that their results are virtually identical, with minor differences that are likely due to differences in their implementations. In contrast to FetGOat (and Blast2GO), the GSEA results are based on running-sum statistics computed from the complete expression dataset. Therefore, the similarity between their results can be expected to be less. Accordingly, G-SESAME determined a smaller semantic similarity score of 0.863 for the results obtained with FetGOat and the GSEA tool.

In addition to the GO terms identified by both Fisher's exact test based tools, GSEA computed an enrichment of GO terms related to oxidative phosphorylation (GO:0006119), carbohydrate transport (GO:0008643) and glucosidase activity (GO:0015926). Comparing maltose to xylose limitation, an enrichment of those GO terms fits our expectations. Under maltose-limitation, *A. niger* breaks down the disaccharide into its monomer glucose by enzymes having glucosidase activity. Subsequently, glucose is taken up by carbohydrate transporters, which can be expected to be different from those required for the uptake of xylose. Finally, 1 mole of glucose yields more ATP than 1 mole of xylose, thereby explaining an induction of oxidative phosphorylation.

These differences in the enrichment results are potentially inherited by the statistics applied by Jørgensen *et al.* to define the set of maltose-induced genes. In contrast to the GSEA tool, which analyzes the complete expression data, FetGOat and Blast2GO are depending on a-priori performed statistics that were applied to generate subsets of genes or proteins of interest. Jørgensen *et al.* used the Affymetrix MAS 5.0 algorithm for data preprocessing in combination with the student's t-test to define their set of maltose-induced genes. In current literature, this approach is critically discussed (Irizarry *et al.*, 2003; Bourgon *et al.*, 2010). To assess the effect of those a-priori applied statistics on the differences between the results from FetGOat and the GSEA tool, we generated an alternative set of maltose-induced genes. We computed RMA expression data (Irizarry *et al.*, 2003) from the raw data (CEL files) and subsequently applied a moderated t-statistic (Smyth, 2004) to identify upregulated genes (data not shown). Interestingly, FetGOat also identified enriched GO terms related to glucosidase activity and carbohydrate transport for this alternative set of maltose-induced genes. However, no enrichment of genes related to oxidative phosphorylation was found. Genes annotated with the GO term oxidative phosphorylation were only marginally induced and their FDR values were rather high (data not shown). Interestingly, similar differences between Fisher's exact test based methods and the GSEA tool were reported in another study. In muscle tissue from diabetics, the GSEA tool identified a joint downregulation of genes related to oxidative phosphorylation compared to healthy controls, while no enrichment was found in the set of downregulated genes (Mootha *et al.*, 2003). For tightly regulated essential cellular processes that show only minor fold changes, the GSEA tool seems to be superior to gene-by-gene differential expression studies.

Glycerol-induced genes

In the second case study, we used FetGOat to analyze transcriptomic data generated by Salazar *et al.* (2009). With a three-species microarray, the authors studied the transcriptomic responses of *A. nidulans*, *A. niger* and *A. oryzae* to growth in glycerol and glucose-limited batch cultures. The authors identified 4,139 glycerol-induced genes comprising 679, 2,240 and 1,040 genes from *A. nidulans*, *A. niger* and *A. oryzae*, respectively. Based on tri-directional best blast hits, 81 orthologous gene clusters were shown to be upregulated in each of the species. Using the *A. niger* (strain ATCC 1015) GO annotation, Salazar *et al.* analyzed the set of conserved upregulated genes and identified enriched BP terms, which are related to amino acid metabolism, gluconeogenesis, hexose and alcohol biosynthetic processes.

First, we repeated the enrichment analysis similar to Salazar *et al.* on the set of 81 upregulated and conserved genes. With the web application FetGOat, we individually performed

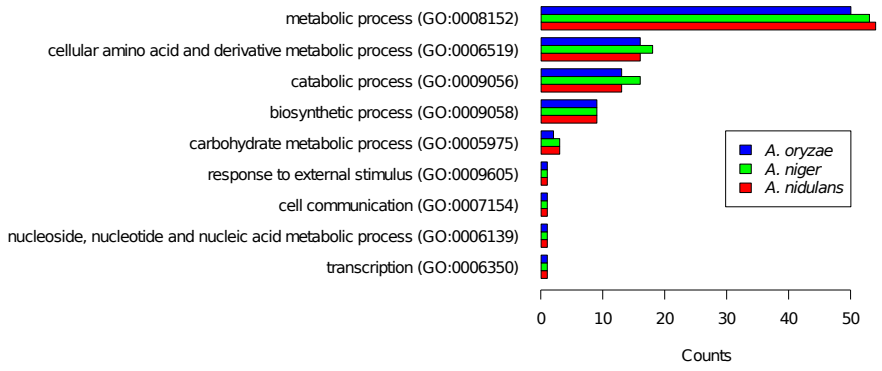

Figure 3.2 – Comparative GO enrichment analysis of conserved glycerol-induced orthologous gene sets
Comparative enrichment analysis of 81 glycerol-induced and conserved genes of the three species *A. nidulans*, *A. niger* and *A. oryzae* (Salazar *et al.*, 2009). Using FetGOat, enrichment analysis of BP terms was performed independently for each of the orthologous gene sets. For comparison, the enriched GO terms were mapped to a GO Slim annotation and the occurrences of the corresponding GO terms were counted with the CateGOrizer tool (Hu *et al.*, 2008)

enrichment analysis using GO annotations of *A. nidulans*, *A. niger* (strain ATCC 1015) and *A. oryzae*. FetGOat identified 58, 57 and 54 enriched BP terms, respectively. To summarize the enrichment results for the three Aspergilli and compare them with each other, we mapped the GO terms to a GO Slim annotation and counted the occurrences of related GO terms. As expected from analyzing orthologous gene sets, the counts for the GO Slim terms were nearly identical, independent of which of the three Aspergilli the enrichment analysis was performed for (see Figure 3.2). To further assess the similarity of the three lists of enriched GO terms, we used the G-SESAME tool (Du *et al.*, 2009) and computed pair-wise semantic similarity scores for *A. nidulans* vs. *A. niger*, *A. nidulans* vs. *A. oryzae* and *A. niger* vs. *A. oryzae* of 0.991, 0.992 and 0.993, respectively. The similarity of the three enrichment results indicates that the newly mapped GO annotations for *A. niger* and *A. oryzae* are well comparable with each other and the *A. nidulans* GO annotation.

Corresponding to the enrichment results from Salazar *et al.*, FetGOat identified enriched GO terms that are related to pyruvate and (aromatic) amino acid metabolism. Unlike Salazar *et al.*, FetGOat did not identify BP terms related to gluconeogenesis. This difference can be explained by an improvement of the GO annotation. While only three genes were annotated with the BP term gluconeogenesis (GO:0006094) in the GO annotation used by Salazar *et al.*, it is a total of 28 genes in the newly mapped GO annotation for *A. niger* (ATCC 1015 strain). For both annotations, one out of the upregulated conserved genes is annotated by the BP term gluconeogenesis, thus explaining why Salazar *et al.* identified it as an enriched BP term and FetGOat did not.

Next, we aimed to identify differences in the tendencies of the transcriptional responses to glycerol for the three Aspergilli. With FetGOat, we individually performed enrichment analysis on each of the complete sets of upregulated genes and found 35, 100 and 65 enriched BP terms for *A. nidulans*, *A. niger* and *A. oryzae*, respectively. The differences in the number of enriched BP terms correspond to the differences in the number of upregulated genes. To summarize and compare the results with each other, we mapped the GO terms to a GO-Slim annotation and counted their occurrences (see Figure 3.3). This summary clearly shows different tendencies in the transcriptomic responses of the three Aspergilli. Most strikingly, a number of GO-Slim terms were identified as being enriched for *A. niger* but not for the other two Aspergilli. Many of the associated GO terms are directly or indirectly related to nutrient limitation such as conidiation, secondary metabolic processes and cell death. Furthermore, FetGOat found an enrichment of the BP term response to nutrient levels (GO:0031667) for *A. nidulans* (nine upregulated genes) and *A. niger* (30 upregulated genes) but not *A. oryzae*. In contrast, GO terms related to energy generation and peroxisomal organization were enriched for *A. oryzae* but not for the other two Aspergilli. FetGOat further computed an enrichment of the BP term carbohydrate transport (GO:0008643) specifically for *A. oryzae*. Interestingly, the different transcriptional trends correspond well with the physiological data. The capacities to grow on glycerol differ significantly for the three Aspergilli. With a maximum specific growth rate of 0.05 h^{-1}, which is one-fourth of its maximum specific growth rate on glucose, *A. niger* grew the worst on glycerol. In contrast, *A. oryzae* showed the fastest growth (0.30 h^{-1}), which is equal to approximately 80% of its maximum specific growth rate on glucose. *A. nidulans* is in between and grew with roughly 50% of its glucose specific speed.

Discussion

A detailed and comprehensive genome annotation can be considered a prerequisite for the analysis and interpretation of omics data. GO provides a framework for functional annotation and has been proven to be a valuable tool for omics data analysis, especially in combination with enrichment statistics. Currently, the GO reference genome project (Gaudet, 2009) provides the most comprehensive manually curated GO annotation for twelve model organisms and is intended to serve as a reference for automated mapping of GO annotation to organisms other than these major models. From the reference genome projects, *Saccharomyces cerevisiae* and *Schizosaccharomyces pombe* are most closely related to the genus *Aspergillus*.

A. nidulans has so far been the only *Aspergillus* species with comprehensive genome scale GO annotation based on both orthology mapping to *S. cerevisiae* and extensive manual curation of gene-specific literature (Arnaud *et al.*, 2010). We have thus mapped the *A. nidulans*

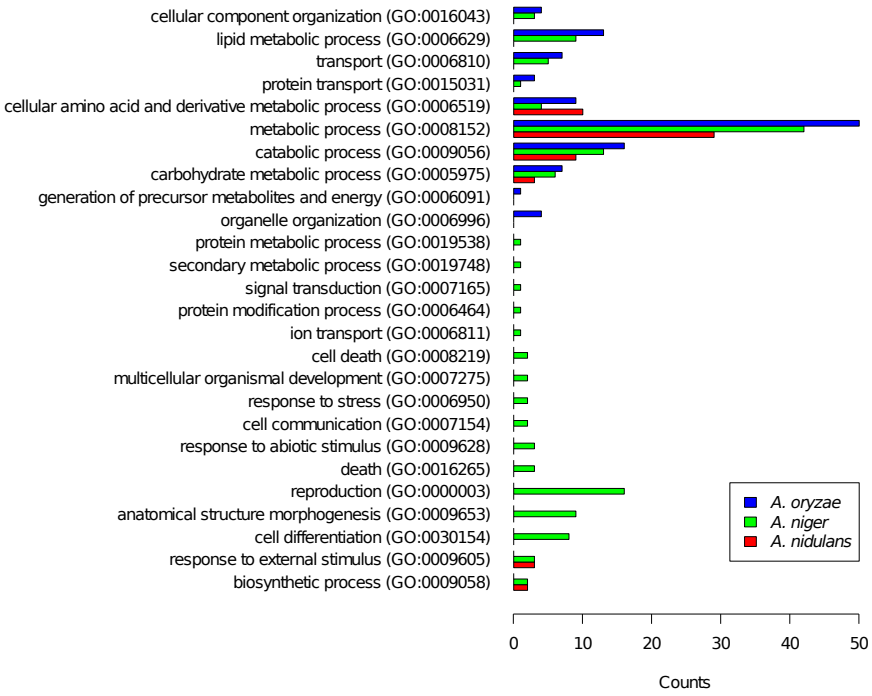

Figure 3.3 — Comparative GO enrichment analysis of individual glycerol-induced gene sets
FetGOat was used for comparative enrichment analysis of the complete glycerol-induced gene sets of the three species *A. nidulans*, *A. niger* and *A. oryzae* (Salazar *et al.*, 2009). For comparison, the enriched GO terms were mapped to a GO Slim annotation and the occurrences of the corresponding GO terms were counted with the CateGOrizer tool (Hu *et al.*, 2008).

GO annotation to all other *Aspergillus* species (see Table 3.1) with published genomes. With 79% of all *A. nidulans* genes being organized in Jaccard ortholog clusters covering 97% of all its GO annotated genes, we demonstrated that this approach is promising for mapping GO annotation between closely related genomes such as those of the genus *Aspergillus*. Nevertheless, the newly generated GO annotations have exclusively been inferred by computational analysis and thus their quality can be expected to be lower compared to the extensively manually curated *A. nidulans* GO annotation. The ortholog clustering approach as implemented in the Sybil comparative analysis package (Crabtree *et al.*, 2007) has worked well for a number of comparative genome studies (Carlton *et al.*, 2008; McDonagh *et al.*, 2008; Fedorova *et al.*, 2008; Brayton *et al.*, 2007; Ghedin *et al.*, 2007; Dunning Hotopp *et al.*, 2006; El-Sayed *et al.*, 2005a; El-Sayed *et al.*, 2005b; Gardner *et al.*, 2005; Joardar *et al.*, 2005), but does have limitations, especially when there are a large number of strains and/or percentage of repetitive proteins. Additionally, we recognize that the optimal choice of an ortholog detection method depends

on the purpose of the analysis. This graph based approach is robust if looking at closely related species, but may not be the best choice when considering large numbers of more distantly related genomes.

The GO annotations for ten *Aspergillus* strains (see Table 3.1) have been made available at the Broad Institute's website (http://www.broadinstitute.org/fetgoat/index.html) and will be updated regularly as the GO annotations for the various *Aspergillus* species continue to improve through manual and computational efforts. To improve the applicability of the GO annotations, they are provided in different file formats that can be used with various freely available GO enrichment tools, e.g. Blast2GO (Conesa *et al.*, 2005), TopGO (Adrian *et al.*, 2010), GSEA (Subramanian *et al.*, 2005) and BinGO (Maere *et al.*, 2005). Thereby, functional analysis of *Aspergillus* omics data by GO enrichment analysis is strongly facilitated. The availability of different annotation file formats makes it feasible to use different tools and compare them with each other.

To further improve the accessibility of the extended annotations, we developed the web application FetGOat and integrated the GO annotation for all *Aspergillus* species with public genome sequences. FetGOat basically resembles the functionality of other publicly available enrichment tools. However, for the *Aspergillus* research community, FetGOat is a valuable addition to existing programs because it uniquely combines an intuitive web interface, GO annotations for all Aspergilli with public genome sequences and a frequently applied statistical method for the identification of enriched GO terms.

To demonstrate the use of those newly generated resources for functional analysis of omics data, we applied them in two case studies to re-analyze recently published microarray data in an automated and un-biased manner. As shown for the first dataset, the enrichment results are in correspondence to the main conclusions from Jørgensen *et al.* (2009). We found an induction of processes related to secretion, glycosylation and starch degradation (see Table 3.2). In addition, we used the dataset from Jørgensen *et al.* to compare the enrichment results of FetGOat to those obtained with two well established publicly available tools, Blast2GO and GSEA. The three tools apply two different methods for enrichment analysis. While Blast2GO and FetGOat compute a Fisher's exact test statistic to identify GO terms that are over-represented in subsets of genes derived e.g. from transcriptomic or proteomic data, the GSEA tool computes running sum statistics on (non-filtered) expression data to identify a-priori defined groups of genes that show joined differential expression. The results from FetGOat are virtually identical to the results obtained with Blast2GO demonstrating the correctness of FetGOat. As expected, the similarity between the results from FetGOat and the GSEA tool is less, while their results are still well comparable. For a large part, both tools are highlighting the same transcriptional trends. However, the GO term oxidative phosphorylation was exclusively identified as being

enriched by the GSEA tool. Taking into account that 1 mole of glucose yields more ATP than 1 mole of xylose, an induction of the oxidative phosphorylation machinery during growth in maltose-limited cultures can be expected. Because the fold-changes of the corresponding genes were very small and their statistical significances were low, no enrichment could be found in the set of maltose-induced genes as assessed by Fisher's exact test. Similar results were found in another study, in which the GSEA tool detected a joined transcriptional downregulation of genes related to oxidative phosphorylation in tissue from diabetics vs. control (Mootha *et al.*, 2003). For tightly regulated essential genes, which show only marginal differential expression, the GSEA tool seems to be superior to gene-by-gene differential expression approaches. However, we would like to emphasize that this is rather caused by the a-priori performed statistics than by the Fisher's exact test itself. A combination of clustering based on gene expression profiles combined with Fisher's exact test enrichment statistics will potentially allow to draw similar conclusions as with the GSEA tool. The causality between an increased ATP yield for maltose and an upregulation of secretion related genes remains to be investigated. However, it is an interesting new hypothesis for further investigations.

For the second dataset from Salazar *et al.* (2009), we first performed GO enrichment analysis on the set of 81 conserved and glycerol-induced genes used in the original study. We could partly reproduce the enrichment results. However, we didn't find an enrichment of genes annotated with the GO term gluconeogenesis. A comparison of the GO annotation used by Salazar *et al.* and our newly mapped GO annotation revealed that this is due to an improvement of the newly mapped GO annotation, which includes many more genes annotated with the GO term gluconeogenesis. As expected from analyzing orthologous gene sets, we showed that the enrichment results are nearly identical, independent of which of the three Aspergilli they were obtained for. Furthermore, we separately performed enrichment analysis for the three Aspergilli analyzing their complete sets of up regulated genes and highlighted major differences in their responses to glycerol vs. glucose limitation. Thereby, we were able to draw additional conclusions explaining their different capabilities to grow on glycerol. Especially for the three-species microarray platform, FetGOat in combination with the newly mapped GO annotation forms a new, valuable and flexible resource for omics data analysis. Applied at an early stage of data analysis, GO enrichment analysis can thus strongly facilitate subsequent manual data interpretation.

While GSEA is an attractive alternative to Fisher's exact test based tools such as FetGOat and Blast2GO, it lacks flexibility because it is restricted to transcriptomic data and can only compare two conditions at a time. Furthermore, its application is more sophisticated, because microarray specific chip annotation files as well as phenotypic labels have to be provided for analysis. Tools such as FetGOat and Blast2GO can be applied to any set of genes or proteins

deriving from genomic, transcriptomic or proteomic studies. They can for example be used to perform GO enrichment analysis on a set of proteins commonly secreted under certain conditions. Improving the power of the statistics applied to obtain gene sets of interest will consequently improve the strength of Fisher's exact test based enrichment analysis. For transcriptomic data analysis, moderated statistics or non specific filtering have for example been shown to improve the statistical power (Bourgon *et al.*, 2010).

The choice of a tool for GO enrichment analysis depends on the type of data, the available resources and personal preferences. Certainly, most of the enrichment results will be redundant between the tools. With the different GO annotation files generated in this study, various freely available tools can easily be used and compared with each other. Especially for the genus *Aspergillus*, FetGOat stands out with respect to the ease of use and the integration of comprehensive and regularly updated GO annotations. The power of FetGOat lies in its flexibility. Any set of genes/proteins from any *Aspergillus* strain with published genome sequence can be investigated for enrichment of GO terms. FetGOat is not restricted to the genus *Aspergillus* as it can be extended to include GO annotations from any organism of interest.

Conclusions

We have mapped the *A. nidulans* GO annotation to the genomes of seven other *Aspergillus* species and made the GO annotations available in different file formats. We furthermore developed the web tool FetGOat, which can be used for GO enrichment analysis of omics data from all *Aspergillus* strains with published genome sequences. Both, the mapped GO annotations and FetGOat were successfully applied in two case studies and are available at the Broad Institute's website (http://www.broadinstitute.org/fetgoat/index.html). Moreover, we have given a general example of how a well annotated genome can help improving GO annotation of related species to subsequently facilitate the interpretation of omics data.

Methods

Ortholog and paralog identification

Clusters of orthologous proteins from ten *Aspergillus* strains (see Table 3.1) were generated with Sybil (Crabtree *et al.*, 2007). The Sybil comparative analysis package currently utilizes the following two-step clustering method, which is a modification of the standard reciprocal best match approach. First, an all-vs-all protein similarity matrix is computed by searching each of the predicted polypeptides within the genomes being compared against all polypeptides. BLASTP is currently used for these searches, with an E-value cut off of 1E-5. Polypeptides

from each individual species are clustered independently using only BLASTP hits that had a sequence identity score of at least 80%. The BLASTP matches that meet these criteria are used to compute a Jaccard similarity coefficient (Jaccard, 1908) for each distinct pair of polypeptides in the same genome. Given two polypeptides P1 and P2 the Jaccard similarity coefficient is defined as:

$$J(P1, P2) = \frac{\text{matches to } P1 \cap P2}{\text{matches to } P1 \cup P2}$$

Using default parameters, any pair of polypeptides with a Jaccard coefficient > 0.6 is connected in a graph representation. The connected components of this graph are referred to as "Jaccard Clusters" and are analogous to paralogous protein clusters within each species. Subsequently, the reciprocal best-hit phase of the clustering algorithm identifies pairs of Jaccard clusters such that: (1) The clusters are from different genomes. (2) The highest-scoring BLASTP match of at least one polypeptide in each of the clusters is to a polypeptide in the other cluster. A graph is constructed, with an edge drawn between two nodes (Jaccard clusters) if and only if they are bidirectional best BLASTP matches of each other. The connected components of this graph are considered ortholog groups in downstream analysis and will be referred to as "Jaccard orthlogous clusters".

Mapping *A. nidulans* GO annotation

GO annotation for *A. nidulans* (gene_association.aspgd version: 1.256) was obtained from the Aspergillus Genome Database (AspGD: http://www.aspgd.org) (Arnaud *et al.*, 2010) and is based on orthology mapping between *A. nidulans* and *S. cerevisiae* as well as extensive manual curation based on gene specific *A. nidulans* literature. GO terms for Jaccard ortholog clusters and their associated proteins were inferred from *A. nidulans* GO annotation such that each protein belonging to the same Jaccard ortholog cluster shares identical GO terms. For each of the analyzed strains (see Table 3.1), individual GO annotation files were generated in different formats.

Enrichment analysis

GO enrichment analyses were performed applying two different statistical tests: Fisher's exact test (Fisher, 1922) and Kolmogorow-Smirnov statistics (Subramanian *et al.*, 2005; Hollander *et al.*, 1999). If not stated differently, p-values were corrected according to Benjamini and Hochberg (Benjamini *et al.*, 1995) and a critical False Discovery Rate (FDR) q-value of 0.05 was applied. For the Fisher's exact test based enrichment analysis of GO terms, we developed the web application FetGOat, which calculates one-tailed p-values and corrects them

for multiple hypothesis testing according to the Benjamini & Hochberg method. In addition to FetGOat, Blast2GO (Conesa *et al.*, 2005) was used to compute enriched GO terms via Fisher's exact test as implemented in GOSSIP (Bluthgen *et al.*, 2005). For the identification of enriched GO terms based on the Kolmogorov-Smirnov statistic, the GSEA tool (Subramanian *et al.*, 2005) was used. The corresponding GO annotation files for Blast2GO and the GSEA tool were generated in this study and are available at the Broad Institute's website (http://www.broadinstitute.org/fetgoat/index.html).

Mapping to GO slim annotation

To summarize GO enrichment results, we mapped the enriched GO terms to a GO Slim annotation (Ashburner *et al.*, 2000), which is a reduced version of the complete annotation with less detailed high-level GO terms, and counted the occurrences (single occurrence option) of GO Slim terms as well as related lower hierarchy terms using the CateGOrizer tool (Hu *et al.*, 2008).

Authors contributions

BMN implemented a data analysis pipeline to map GO annotation to Jaccard clusters and generate annotation files, developed FetGOat, performed further data analysis and wrote the manuscript. JC and JRW generated Jaccard clusters. GCC integrated FetGOat at the Borad Institute's website. JRW, AFJR and VM were involved in writing the manuscript. All authors read and approved the final manuscript.

Acknowledgments

This work was supported by grants of the SenterNovem IOP Genomics project (IGE07008) and the National Institute of Allergy and Infectious Diseases at the US National Institutes of Health (R01 AI077599). Part of this work was carried out within the research programme of the Kluyver Centre for Genomics of Industrial Fermentation, which is part of the Netherlands Genomics Initiative/Netherlands Organization for Scientific Research.

Chapter 4

The carbon starvation response of Aspergillus niger during submerged cultivation: Insights from the transcriptome and secretome

Benjamin M. Nitsche[1,2], Thomas R. Jørgensen[1,3,4], Michiel Akeroyd[5], Vera Meyer[2,3], Arthur F.J. Ram[1,3]

[1] Institute of Biology, Leiden University, Sylviusweg 72, 2333 BE Leiden, The Netherlands
[2] Institute of Biotechnology, Berlin University of Technology, Gustav-Meyer-Allee 25, 13355 Berlin, Germany
[3] Kluyver Centre for Genomics of Industrial Fermentation, PO Box 5057, 2600 GA, Delft, The Netherlands
[4] Present address: Novo Nordisk, Protein Expression, 2760 Måløv, Denmark
[5] DSM Biotechnology Center, Beijerinck Laboratory, PO Box 1, 2600 MA Delft, The Netherlands

Abstract

Background: Filamentous fungi are confronted with changes and limitations of their carbon source during growth in their natural habitats and during industrial applications. To survive life-threatening starvation conditions, carbon from extra- and intracellular resources becomes mobilized to fuel fungal self-propagation. Key to understand the underlying cellular processes is the system-wide analysis of fungal starvation responses in a temporal and spatial resolution. The knowledge deduced is important for the development of both new antifungal strategies and optimized industrial production processes.

Results: This study describes the physiological, morphological and genome-wide transcriptional changes caused by prolonged carbon starvation during submerged batch cultivation of the filamentous fungus *Aspergillus niger*. Bioreactor cultivation supported highly reproducible growth conditions and monitoring of physiological parameters. Changes in hyphal growth and morphology were analyzed at distinct cultivation phases using automated image analysis. The Affymetrix GeneChip platform was used to establish genome-wide transcriptional profiles for three selected time points during prolonged carbon starvation. Compared to the exponential growth transcriptome, about 50% (7,292) of all genes displayed differential expression during at least one of the starvation time points. Enrichment analysis of Gene Ontology, Pfam domain and KEGG pathway annotations uncovered autophagy and asexual reproduction as major global transcriptional trends. Induced transcription of genes encoding hydrolytic enzymes was accompanied by increased secretion of hydrolases including chitinases, glucanases, proteases and phospholipases as identified by mass spectrometry.

Conclusions: This study is the first system-wide analysis of the carbon starvation response in a filamentous fungus. Morphological, transcriptomic and secretomic analyses identified key events important for fungal survival and their chronology. The dataset obtained forms a comprehensive framework for further elucidation of the interrelation and interplay of the individual cellular events involved.

BMC Genomics. 2012 Aug 8;13:380 (with minor modifications)

Background

Aspergillus niger is a ubiquitous filamentous fungus. According to its saprophytic lifestyle, *A. niger* is capable of secreting large amounts of various plant polysaccharide degrading enzymes. Its naturally high secretion capacity has long been exploited in industrial biotechnology for the production of homologous and heterologous proteins as well as organic acids (Pel *et al.*, 2007; Andersen *et al.*, 2011; Archer, 2000). Many of its products have acquired the GRAS status, meaning that they are generally considered as safe food ingredients (Schuster *et al.*, 2002). However, besides its positive economic relevance as an industrial workhorse, *A. niger* is a common storage mold causing spoilage of agricultural goods and contamination of food and feedstocks with mycotoxins (Pitt *et al.*, 1997; Mogensen *et al.*, 2010). Although to a much lesser extent than other species of its genus, *A. niger* is an opportunistic pathogen, which can cause invasive aspergillosis in immunocompromised patients (Person *et al.*, 2010).

A. niger is exclusively known to propagate via an asexual life cycle which finally leads to the formation of black airborne mitotic spores. Core genes involved in signal transduction and conidiophore development in the model fungus *A. nidulans* (Adams *et al.*, 1998) have also been identified in *A. niger* (Pel *et al.*, 2007), suggesting that the regulation of asexual development is conserved. The first step in conidiophore development is the activation of the transcriptional regulator BrlA which induces the expression of a number of conidiation-specific genes. BrlA expression is autoregulated, resulting in a strong accumulation of its mRNA during asexual development (Adams *et al.*, 1998). Although most conidiation studies are performed at a substrate/air interface, conidiation can also be induced in submerged cultures by nutrient limitation such as severe carbon limitation (Broderick *et al.*, 1981; Schrickx *et al.*, 1993; Jørgensen *et al.*, 2010). Under these conditions, carbon is liberated from extra- and intracellular sources to fuel fungal self propagation. Consequently, the fungal mycelium becomes highly heterogeneous, bearing empty compartments and those that are committed to conidiation (White *et al.*, 2002; Jørgensen *et al.*, 2010). While this strategy is beneficial for self-propagation and the exploitation of new substrate sources during saprophytic growth, it may result in a decrease of the active biomass fraction during carbon-limited industrial production processes.

Only a few studies have been conducted to investigate different aspects of aging carbon-limited fungal cultures. As discussed in the review by White *et al.* (2002), most of them focus on physiological and morphological aspects. The generic term autolysis has been frequently used to summarize the involved processes. Hallmarks of autolysis are decreasing biomass, hyphal fragmentation, release of ammonia and increased extracellular hydrolase activity (White *et al.*, 2002). For different fungal species, the involvement of hydrolases, especially chitinases and glucanases but also proteases has been investigated in great detail (McNeil *et al.*, 1998; McIntyre *et al.*, 2000; Emri *et al.*, 2005b). An early and strong transcriptional induction in

response to carbon starvation was shown in *A. nidualns* for the two hydrolases ChiB and NagA, which have been intensively studied because of their role in the degradation of the cell wall component chitin (Pusztahelyi *et al.*, 2006). In addition to the description of physiological and biochemical hallmarks of aging fungal cultures, several approaches have been developed to quantify the decreasing fraction of active hyphal compartments in aging mycelium by (semi-) automated image analysis (White *et al.*, 2002).

An increasing number of publications highlights the importance of programmed cell death (PCD) in aging fungal cultures (Hamann *et al.*, 2008; Etxebeste *et al.*, 2010; Emri *et al.*, 2008; White *et al.*, 2002). PCD is generally classified into three types which are referred to as apoptosis (type I), autophagy (type II) and necrosis (type III) (Lockshin *et al.*, 2004). Their physiological roles are very complex and their relationships are not completely understood. While apoptosis and necrosis are explicitly associated with cell death, autophagy is also a normal physiological process important for cellular homeostasis by lysosomal degradation and recycling. The cellular functions of autophagy have been proposed to exert roles that are both causative of and protective against cell death (Lockshin *et al.*, 2004; Giansanti *et al.*, 2011; Edinger *et al.*, 2004).

Improving our understanding of processes induced by carbon starvation and their dynamic interactions is important to further optimize industrial production processes. Further, advancing knowledge in this field will potentially result into new antifungal strategies for medicine and agriculture. The aim of this study is to provide a system-wide description of the carbon starvation response of the filamentous fungus *A. niger*. Submerged carbon-limited bioreactor batch cultures were performed and maintained starving up to six days after carbon depletion. In addition to describing the physiology and morphology, we analyzed the secretome and established genome-wide transcriptional profiles for three distinct starvation phases. Besides specifically dissecting expression data for groups of selected genes including proteases, chitinases and glucanases, we performed enrichment analysis to dissect the complex transcriptional changes.

Our investigation shows that carbon starvation in submerged cultures caused complex morphological changes and cellular differentiation including emergence of empty hyphal ghosts, secondary growth of thin non-branching filaments on the expense of older hyphal compartments and formation of conidiating structures. Concomitantly, autophagy and conidiation pathway genes were clearly induced on the transcriptional level. We propose that metabolic adaptation to carbon starvation is mediated by autophagy and that cell death rather than hydrolytic weakening of the fungal cell wall can be considered a hallmark of aging carbon starved *A. niger* cultures.

Results

Physiology of carbon starved cultures

The *A. niger* wild-type strain N402 (Bos *et al.*, 1988) was cultivated under controlled conditions in bioreactors to study its response to carbon starvation during prolonged submerged batch cultivation (Figure 4.1A-B). The defined medium had a pH of 3 and was balanced such, that carbon (maltose) was the growth limiting nutrient. During exponential growth ($\mu_{max} = 0.24 h^{-1}$), pH 3 was maintained by alkaline addition (Figure 4.1B), which linearly correlated with the biomass accumulation and was previously shown to reflect ammonium uptake during balanced growth on minimal medium (Hrdlicka *et al.*, 2004). The end of the exponential growth phase was detected by an increase of the dissolved oxygen signal (Figure 4.1B) and depletion of the carbon source was confirmed by measurements of maltose and glucose concentrations (not shown). The corresponding time point (defined as t=0) was used to synchronize replicate cultures insuring that samples were taken from equivalent physiological phases. The biomass concentration peaked at $5 g \cdot kg^{-1}$ culture broth (Figure 4.1A).

After maltose was exhausted, pH 3 was maintained by acid addition (Figure 4.1B). The metabolic activity of the culture decreased in response to the lack of an easily accessible carbon and energy source as indicated by the CO_2 production and O_2 consumption rates (Figure 4.1B). Protease activity rapidly increased and was already detected within three hours after maltose depletion. During the later starvation phase (up to 140 hours), the protease activity remained constant; however, extracellular protein levels doubled within 16 hours after carbon depletion and remained constant thereafter. Towards the end of the starvation phase, the cell mass decreased by nearly 60% (Figure 4.1A). Importantly, CO_2 and O_2 levels in the exhaust gas indicated that the cultures were still metabolically active, even 140 hours after depletion of the carbon source (Figure 4.1B).

Morphological differentiation during carbon starvation

Throughout the entire cultivation, *A. niger* displayed a dispersed morphology. During exponential growth, the mycelium remained intact and no damaged or empty hyphae were observed (Figure 4.2A). Early after depletion of maltose and onset of starvation, empty hyphal compartments emerged and the diameter of growing hyphae significantly decreased (Figure 4.2B). Throughout prolonged starvation, the fraction of empty hyphal compartments increased, but the cell wall exoskeleton appeared to remain intact (Figure 4.2B-D). Fragmented, broken hyphal ghosts were rarely observed. Outgrowing thin filaments emerged, which continued elongating in a non-branching manner. Towards the later starvation phases (60 hours

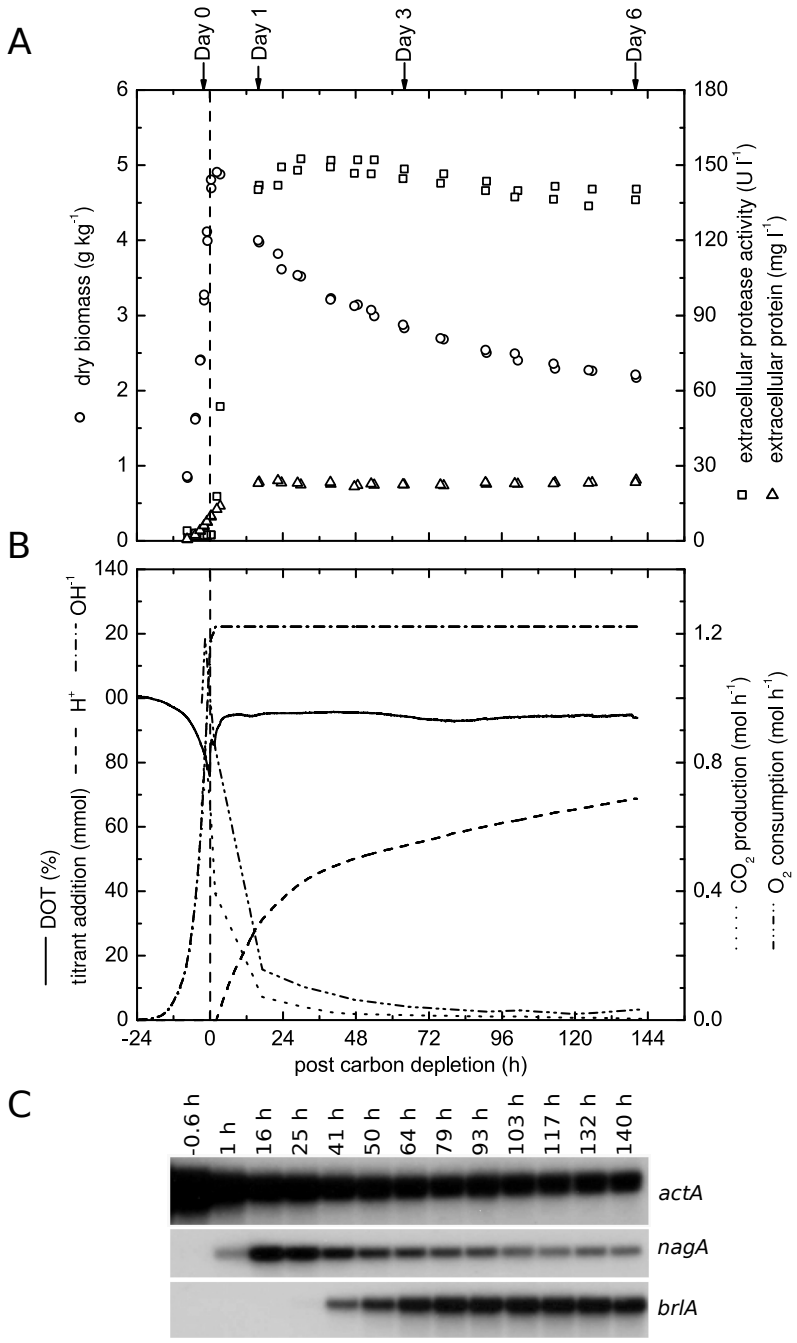

Figure 4.1 — Physiology and expression profiles of aging carbon-limited batch cultures
(A) Growth curve combined with profiles for extracellular protease activity and extracellular protein concentrations. (B) Summary of physiological parameters including dissolved oxygen tension (DOT), titrant addition, O_2 consumption and CO_2 production rates. (C) Northern analysis for the gamma-actin encoding gene *actA* (An15g00560), the β-N-acetylglucosaminidase *nagA* (An09g02240) and the regulator of conidiation *brlA* (An01g10540).

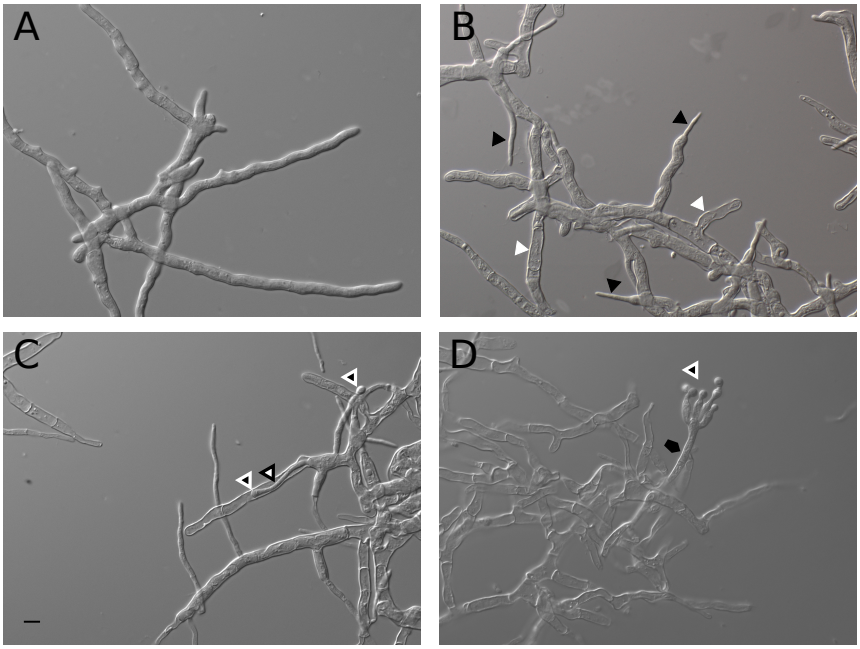

Figure 4.2 – Hyphal morphology during four distinct cultivation phases
(A) Intact hyphae from the exponential growth phase with an average diameter of approximately 3 μm. (B) 16 hours after carbon depletion empty hyphal compartments emerged (white triangles) and new hyphae with a significantly reduced average diameter of approximately 1 μm appeared (black triangles). (C) 60 hours after carbon depletion, the number of empty hyphal compartments increased and thin hyphae elongated in a non-branching manner. First reproductive structures emerged (white-edged triangles). Thin hyphae even grew cryptically inside empty hyphal ghosts (black-edged triangle). (D) Even 140 hours after carbon depletion, surviving compartments were present (black pentagon) often bearing morphologically reduced reproductive structures (white-edged triangle). The mycelial network consisted largely of empty hyphal ghosts but hyphal fragmentation was rarely observed. The scale bar refers to 5 μm.

post carbon depletion), morphologically crippled asexual reproductive structures appeared (Figure 4.2C-D). Even 140 hours after exhaustion of the carbon source, surviving compartments were present, which often showed outgrowing hyphae bearing asexual reproductive structures (Figure 4.2D). Secondary growth of thin hyphae was even observed within empty hyphal ghosts (Figure 4.2C).

Similar to our results, morphological data from *A. oryzae* (Pollack *et al.*, 2008) indicate a sharp transition between thick and thin compartments (Figure 4.2B) in response to carbon starvation, suggesting that hyphal diameters can be used to distinguish populations of old and young hyphae formed during primary growth on the supplied carbon source and secondary growth fueled by carbon recycling, respectively. To visualize the transition dynamics from thick (old) to thin (young) hyphae in response to carbon starvation, an image analy-

sis algorithm was developed to analyze hyphal diameter distributions of the cytoplasm filled mycelial fraction. Microscopic pictures from samples of various cultivation time points were analyzed and probability density curves were plotted for the distributions of hyphal diameters (Figure 4.3). Diameters from exponentially growing hyphae resembled a normal distribution with a mean of approximately 3 μm. In response to carbon starvation, a second population of thinner hyphae with a mean diameter of approximately 1 μm emerged. Throughout the course of starvation, there was a gradual transition from thick (old) to thin (young) hyphae for the cytoplasm filled fraction, suggesting that compartments of older hyphae originating from the exponential growth phase gradually underwent cell death and became empty while a new population of thin hyphae started to grow on the expense of dying compartments.

Transcriptomic response to carbon starvation

To follow transcriptomic changes during carbon starvation, total RNA was extracted from biomass harvested at different time points during batch cultivation. Although difficulties to isolate intact RNA from aging cultures were reported for *A. nidulans* (Emri *et al.*, 2006), we

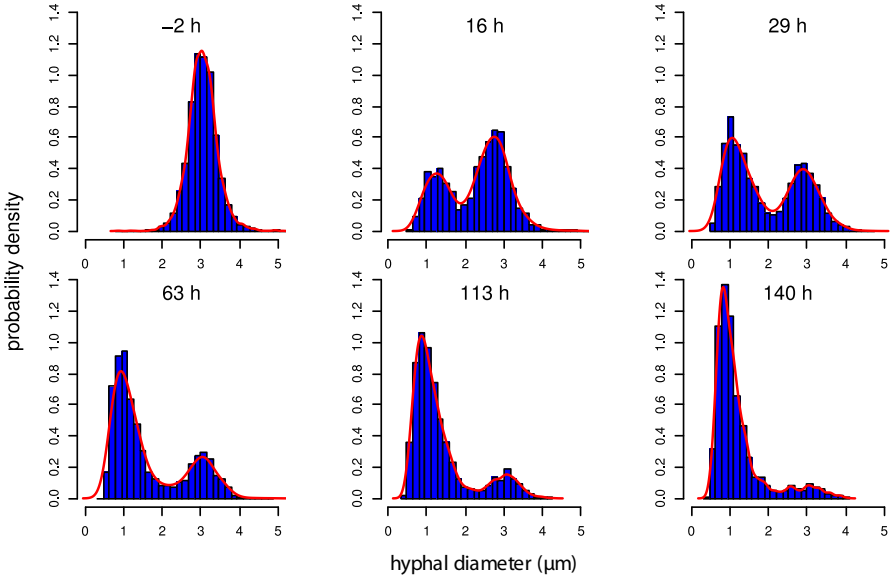

Figure 4.3 – Hyphal population dynamics
For six distinct time points, probability density curves of hyphal diameters are shown. Two hours prior to carbon depletion, a single population of hyphae with a mean diameter of approximately 3 μm was detected. After carbon depletion, a second population with a significantly reduced mean diameter of approximately 1 μm started to emerge. Throughout the course of starvation, the ratio of thin/thick hyphae gradually increased, indicating secondary growth on the expense of dying compartments.

could isolate total RNA of high quality from samples up to 140 hours after depletion of the sole carbon source, as assessed by lab on chip quality control (data not shown) and Northern analysis (Figure 4.1C). Transient expression levels of the gamma-actin encoding gene *actA* (An15g00560), the glycosyl hydrolase *nagA* (An09g02240) and the regulator of asexual sporulation *brlA* (An01g10540) are exemplarily shown in Figure 4.1C. While *nagA* can be considered an early response gene whose expression peaked 16 hours after exponential growth, *brlA* expression was induced later and remained constant after reaching a plateau at 64 hours of carbon starvation. Expression levels of *actA* decreased considerably after exponential growth but remained constant during later cultivation phases.

RNA samples from four distinct cultivation phases were subjected to genome-wide transcriptional profiling: Exponential growth phase, 16 hours (day 1), 60 hours (day 3) and 140 hours (day 6) post carbon depletion. Differentially expressed genes were identified by a moderated t-test (Smyth, 2004) applying a critical FDR q-value of 0.005. Compared to the exponential growth phase, 7,292 of totally 13,989 genes (52%) were identified as differentially expressed during at least one of the starvation time points (Additional file 1). 1,722 genes were conjointly upregulated, whereas 2,182 genes were conjointly downregulated during carbon starvation (Figure 4.4). Enrichment analyses using Gene Ontology (GO) (Ashburner *et al.*, 2000), Pfam domain (Bateman *et al.*, 2004) and Kyoto Encyclopedia of Genes and Genomes (KEGG) (Kanehisa *et al.*, 2010) pathway annotations were performed to uncover major transcriptional trends. For *A. niger*, all three annotations are based on computational inference. Among them, GO annotation can be considered to have the best quality because it was inferred from the computationally and manually curated GO annotation of the closely related species *A. nidulans* (Nitsche *et al.*, 2011).

The GO enrichment results are summarized in Figure 4.5 (see Additional file 2 for complete GO enrichment results). They cover 20% (668) and 33% (1,334) of all up- and downregulated genes, respectively. Among the genes induced under carbon starvation, common and time-dependent overrepresentation of GO terms was observed. While GO terms related to e.g. catabolic (autophagy, cytoplasm to vacuole targeting (CVT) pathway, fatty acid oxidation and trehalose catabolism) and reproductive (conidiation and mitotic cell cycle) processes were generally enriched, other processes responded in a time-dependent manner constituting early, intermediate or late responses. Among the transiently enriched processes were non-glycolytic fermentation and PCD (day 1), cell wall organization (day 3), regulation of transcription from RNA polymerase II promoter (day 3 and 6) as well as reactive oxygen metabolism (day 6). In contrast to the upregulated genes, the downregulated gene sets did not display any time-dependent differences with respect to the significantly overrepresented GO terms. The com-

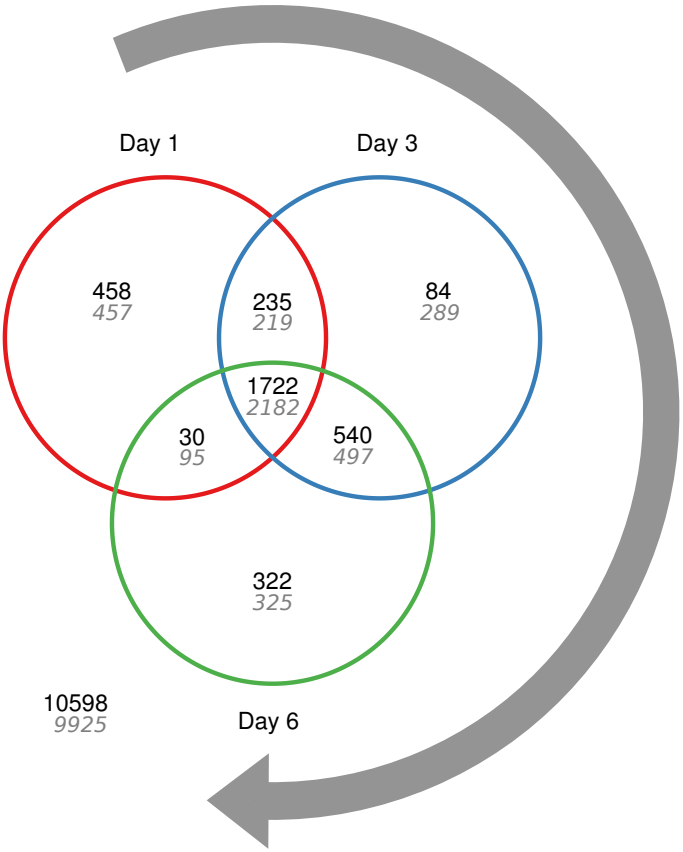

Figure 4.4 — Venn Diagram of genes differentially expressed during carbon starvation
Venn diagram showing numbers of up- and downregulated genes in black and gray, respectively. Differential expression (FDR q-value < 0.005) was assessed by comparison of expression profiles from day 1, 3 and 6 of carbon starvation with expression profiles from the exponential growth phase.

monly downregulated processes included transcription from RNA polymerase I promoter, ribosome biogenesis, translation and respiration.

Pfam domain and KEGG pathway enrichment results are summarized in the supplemental data (Additional files 3 and 4). Although the three annotations have different sources, structures and levels of complexity, the individual enrichment results confirm each other. Only in a few cases, Pfam domain and KEGG pathway enrichment analyses provided additional information beyond the GO enrichment results. For example, among the upregulated genes at day 1, 3 and 6, those having a putative sugar transporter domain (PF00083) were strongly enriched (49, 40, 39 predicted genes out of 110, respectively). In consideration of the severe carbon limitation, it can be assumed that these predicted sugar transporters comprise high-affinity sugar

UP

Day 1	Day 3	Day 6	GO term	Description
■	■	■	GO:0000080	G1 phase of mitotic cell cycle
■	■	■	GO:0043648	dicarboxylic acid metabolic process
■	■	■	GO:0015850	organic alcohol transport
■	■	■	GO:0000422	mitochondrion degradation
■	■	■	GO:0075306	regulation of conidium formation
■	■	■	GO:0006468	protein amino acid phosphorylation
■	■	■	GO:0034727	piecemeal microautophagy of nucleus
■	■	■	GO:0070887	cellular response to chemical stimulus
■	■	■	GO:0019395	fatty acid oxidation
■	■	■	GO:0000160	two-component signal transduction system (phosphorelay)
■	■	■	GO:0005993	trehalose catabolic process
■	■	■	GO:0043603	cellular amide metabolic process
■	■	■	GO:0019751	polyol metabolic process
■	■	■	GO:0032258	CVT pathway
■	■	■	GO:0034498	early endosome to Golgi transport
■	■	■	GO:0007231	osmosensory signaling pathway
■	■	■	GO:0009063	cellular amino acid catabolic process
■	■	■	GO:0007039	vacuolar protein catabolic process
■	■	■	GO:0000045	autophagic vacuole assembly
■	□	□	GO:0019662	non-glycolytic fermentation
■	□	□	GO:0012501	programmed cell death
■	■	□	GO:0006081	cellular aldehyde metabolic process
■	■	□	GO:0015718	monocarboxylic acid transport
□	■	□	GO:0007047	cellular cell wall organization
□	■	□	GO:0051173	positive regulation of nitrogen compound metabolic process
□	■	■	GO:0032569	gene-specific transcription from RNA polymerase II promoter
□	■	■	GO:0045860	positive regulation of protein kinase activity
□	■	■	GO:0000165	MAPKKK cascade
□	□	■	GO:0048468	cell development
□	□	■	GO:0007186	G-protein coupled receptor protein signaling pathway
□	□	■	GO:0006800	oxygen and reactive oxygen species metabolic process
□	□	■	GO:0000747	conjugation with cellular fusion
□	□	■	GO:0001403	invasive growth in response to glucose limitation
□	□	■	GO:0000122	negative regulation of transcription from RNA polymerase II promoter
□	□	■	GO:0007124	pseudohyphal growth

DOWN

Day 1	Day 3	Day 6	GO term	Description
■	■	■	GO:0006360	transcription from RNA polymerase I promoter
■	■	■	GO:0045039	protein import into mitochondrial inner membrane
■	■	■	GO:0000027	ribosomal large subunit assembly
■	■	■	GO:0006555	methionine metabolic process
■	■	■	GO:0009108	coenzyme biosynthetic process
■	■	■	GO:0006418	tRNA aminoacylation for protein translation
■	■	■	GO:0000463	maturation of LSU-rRNA from tricistronic rRNA transcript
■	■	■	GO:0030150	protein import into mitochondrial matrix
■	■	■	GO:0000472	endonucleolytic cleavage from (SSU-rRNA, 5.8S rRNA, LSU-rRNA)
■	■	■	GO:0006733	oxidoreduction coenzyme metabolic process
■	■	■	GO:0000447	endonucleolytic cleavage in ITS1 to separate tricistronic rRNA transcript
■	■	■	GO:0006407	rRNA export from nucleus
■	■	■	GO:0051258	protein polymerization
■	■	■	GO:0015986	ATP synthesis coupled proton transport
■	■	■	GO:0033108	mitochondrial respiratory chain complex assembly
■	■	■	GO:0042026	protein refolding
■	■	■	GO:0000154	rRNA modification
■	■	■	GO:0031204	posttranslational protein targeting to membrane, translocation
■	■	■	GO:0071038	nuclear polyadenylation-dependent tRNA catabolic process
■	■	■	GO:0006547	histidine metabolic process
■	■	■	GO:0006614	SRP-dependent cotranslational protein targeting to membrane
■	■	■	GO:0009067	aspartate family amino acid biosynthetic process
■	■	■	GO:0042274	ribosomal small subunit biogenesis
■	■	■	GO:0006450	regulation of translational fidelity
■	■	■	GO:0006007	glucose catabolic process
■	■	■	GO:0009060	aerobic respiration

Figure 4.5 – Summary of GO enrichment results
Summary of GO enrichment results for the up- and downregulated gene sets of day 1, 3 and 6 of carbon starvation. Statistically significant overrepresentation (FDR < 0.05) is indicated in black.

transporters. Indeed, *mstA* (An12g07450) and *mstF* (An02g00590) encoding two high-affinity sugar/H^+symporters (Kuyk *et al.*, 2004) were significantly upregulated at day 1 and 3 as well as day 1, 3 and 6, respectively. Furthermore, the cytochrome P450 domain (PF00067) was significantly enriched among genes upregulated at day 1. The biochemical roles of the majority of cytochromes P450 are unknown but many are expected to be involved e.g. in the formation of pigments, antioxidants and secondary metabolites (Kelly *et al.*, 2009). Two of the 44 enriched cytochrome P450 domain proteins are physically associated with distinct (putative) secondary metabolite clusters, of which one is the fumonisin cluster (Pel *et al.*, 2007). Obviously, induction of the fumonisin cluster constitutes an early and orchestrated response to carbon starvation. Transcript levels for 11 of the 14 predicted open reading frames were exclusively elevated at day 1, including the putative transcription factor encoded by An01g06900 (Additional file 5).

In addition, PCD-associated genes were specifically overrepresented (q−value < 0.033) during the early adaptive phase at day 1 of carbon starvation. The encoded proteins include two predicted metacaspases (An09g04470, An18g05760) and a Poly(ADP-ribose) polymerase homologue (An18g01170). Four proteins sharing NACHT domains combined with ankyrin or WD40 domain repeats (An11g08920, An01g08000, An01g01380, An07g01930) and three proteins with a NB-ARC domain (An07g01850, An02g07340,An10g00600) were upregulated as well (Additional file 6).

As implied by the enrichment results for both GO and KEGG pathway annotations, carbon starvation coordinately induced the expression of genes involved in autophagic processes. To date, more than 30 autophagy (*atg*) genes have been identified for *Saccharomyces cerevisiae* and other fungi (Kanki *et al.*, 2011; Xie *et al.*, 2007), 23 of which have a predicted ortholog in *A. niger*. All except one were detected as significantly upregulated during at least one of the starvation time points (see Table 4.1). The expression level of *atg8* (An07g10020), encoding a lipid-conjugated ubiquitin-like protein that controls the expansion of pre-autophagosomes (Xie *et al.*, 2008), was the highest among all *atg* genes. At day 3 it reached 75% of the actin expression level during exponential growth. Despite this concerted induction during carbon starvation, it is clearly evident from the expression data that autophagic processes also play an important role during exponential growth, because *atg* gene expression levels ranged from 0.6% (*atg12*: An11g06920) to 24% (*atg8*: An07g10020) when compared with the actin gene expression level (Table 4.1).

The induction of hydrolases, including proteases and glycosyl hydrolases, has been proposed as a key event in aging fungal cultures (White *et al.*, 2002). During carbon starvation, glycosyl hydrolases are involved in both the liberation of carbon from fungal cell wall polymers and cell wall remodeling. We identified those upregulated genes that putatively encode glycosyl hy-

Table 4.1 – Transcriptome data of predicted autophagy genes

		Identifiers		
Gene	**(Predicted) function**	***S. cerevisiae***	***A. nidulans***	***A. niger***
atg1	Ser/thr kinase	S000003148	AN1632	An04g03950
atg2	Membrane protein	S000005186	AN5491	An08g10270
atg3	E2-like conjugating enzyme	S000005290	AN11004	An03g04380
atg4	Cysteine protease	S000005167	AN3470	An11g11320
atg6	Subunit of phosphatidylinositol 3-kinase complexes	S000006041	AN10213	An16g07540
atg7	Ubiquitine activating enzyme	S000001214	AN7428	An02g14900[4]
atg8	Autophagosomal membrane protein	S000000174	AN5131	An07g10020
atg9	Transmembrane protein	S000002308	AN3734	An06g01500
atg10	E2-like conjugating enzyme	S000003965	AN10728	An18g06610
atg11	Adapter protein pexophagy and CVT pathway	S000006253	AN2887	An02g07380
atg12	Ubiquitin-like modifier	S000000421	AN1760	An11g06920
atg13	Regulatory subunit of Atg1 signalling complex	S000006389	AN2076	An11g04460
atg15	Vacuolar lipase	S000000664	AN5919	An03g02820
atg16	Atg12-Atg5-Atg16 complex	S000004769	AN0090	An18g02220
atg17	Scaffold protein of Atg1 signalling complex	S000004415	AN6360	An02g04820
atg18	Phosphoinositide binding protein	S000001917	AN0127	An18g03070
atg20	Sorting nexin family member	S000002271	AN6351	An02g01390
atg22	Vacuolar integral membrane protein	S000000543	AN7437	An02g14810
			AN7591	An09g03630
			AN5876	An02g03340
atg24	Sorting nexin	S000003573	AN3584	An01g08520
atg26	UDP-glucose:sterol glucosyltransferase	S000004179	AN4601	An07g06610
atg27	Type I membrane protein	S000003714	AN0861	An01g13390
atg28	Coiled-coil protein		AN1701	An04g03260
atg29	Recruitment of proteins to the pre-autophagosomal structure	S000006087	AN4832	An02g13480

(1) mRNA abundance relative (%) to the gamma-actin (An15g00560) encoding transcript during exponential growth

(2) Fold changes and FDR q-values for comparisons with transcriptome data from the exponential growth phase

(3) Exponential growth phase

(4) ORF truncated by contig borders

Expression data[1]				Fold changes[2]			FDR q-values[2]		
Exp[3]	Day 1	Day 3	Day 6	Day 1	Day 3	Day 6	Day 1	Day 3	Day 6
1.3	3.2	2.9	2.4	2.4	2.2	1.8	2.5E-07	1.1E-06	1.5E-05
3.9	8.2	8.2	7.8	2.1	2.1	2.0	2.8E-08	2.9E-08	6.8E-08
1.0	2.9	2.7	2.9	2.9	2.6	2.9	1.8E-08	6.1E-08	1.9E-08
4.6	15.5	16.8	17.3	3.4	3.6	3.7	3.8E-10	2.1E-10	1.6E-10
1.0	1.0	1.0	0.8	1.0	1.0	0.8	8.3E-01	8.2E-01	5.0E-02
1.5	5.6	5.1	3.0	3.8	3.5	2.0	5.7E-08	1.3E-07	6.4E-05
23.8	69.1	75.0	69.7	2.9	3.2	2.9	3.1E-10	1.5E-10	3.1E-10
1.0	8.0	6.6	5.8	8.0	6.6	5.8	4.1E-11	1.3E-10	3.0E-10
1.2	1.4	1.4	1.2	1.1	1.2	1.0	1.0E-01	3.2E-02	7.3E-01
2.3	5.2	6.1	4.0	2.2	2.6	1.7	6.2E-08	8.3E-09	5.8E-06
0.6	0.8	0.7	0.6	1.4	1.2	1.0	6.4E-03	9.4E-02	7.9E-01
0.8	1.1	1.1	1.2	1.4	1.4	1.6	3.3E-02	2.0E-02	6.6E-03
2.6	7.1	6.0	5.5	2.7	2.3	2.1	5.3E-09	4.7E-08	1.9E-07
1.7	3.5	3.3	2.9	2.1	2.0	1.8	7.1E-05	1.1E-04	6.7E-04
1.6	3.5	4.2	4.7	2.2	2.7	3.0	8.6E-09	9.4E-10	2.6E-10
2.0	1.8	2.8	2.6	0.9	1.4	1.3	3.7E-01	1.4E-03	4.7E-03
4.5	7.7	8.4	9.0	1.7	1.8	2.0	6.1E-06	1.1E-06	3.3E-07
5.7	10.1	9.2	8.9	1.8	1.6	1.6	5.3E-07	4.0E-06	6.8E-06
1.6	1.4	2.0	3.1	0.9	1.3	2.0	3.9E-01	2.0E-02	8.6E-06
1.9	1.3	1.0	1.0	0.7	0.5	0.6	8.7E-04	3.5E-06	1.3E-05
2.8	4.9	4.8	4.9	1.7	1.7	1.7	2.0E-06	3.3E-06	2.3E-06
3.8	10.3	9.8	7.6	2.7	2.6	2.0	2.7E-09	5.8E-09	2.2E-07
1.1	1.7	1.5	1.5	1.6	1.4	1.4	2.8E-06	1.8E-04	6.8E-05
1.0	1.9	1.9	2.2	1.9	2.0	2.2	5.9E-06	3.7E-06	6.5E-07
1.0	2.5	2.4	2.7	2.4	2.3	2.6	3.2E-08	6.2E-08	1.2E-08

drolases active on fungal cell wall polymers such as chitin, glucan and mannan (Table 4.2) by mining publicly accessible data (Pel *et al.*, 2007; Cantarel *et al.*, 2009). The expression profiles allow a general classification into early and late response genes. In agreement with literature (Pusztahelyi *et al.*, 2006), the chitinolytic genes *chiB* (An02g07020) and *nagA* (An09g02240) were among the highest induced early response genes. The rapid transient induction of *nagA* as shown by Northern analysis (Figure 4.1C) exemplarily corroborates the microarray data. In addition to the chitinolytic hydrolases, the group of intensely induced early response hydrolases includes the α-glucanase *agnB* (An07g08640), multiple β-glucanases and one mannanase. Besides a number of glycosyl hydrolases that were only marginally induced during the later time points, the chitinases *cfcI* (An02g13580) and *ctcB* (An09g05920) showed strong specific induction during the two later time points. It is thus tempting to speculate that *cfcI* and *ctcB* are rather involved in cell wall remodeling during asexual development than liberation of carbon from cell wall polymers.

The second group of hydrolases, namely proteases, fulfills diverse physiological functions ranging from signaling to nutrient recycling. In accordance to the rapidly increasing extracellular protease activity after carbon depletion (Figure 4.1A), an early transcriptional induction of extracellular proteases was observed (Table 4.3). Compared to exponential growth, the expression levels of the two major secreted proteases *pepA* and *pepB* (Mattern *et al.*, 1992) were increased by more than 130 fold at day 1. Additionally, roughly 20 further predicted secreted proteases were induced during carbon starvation with transcript level changes ranging from 2 to 40. In agreement, expression of the main transcriptional regulator of proteases PrtT (Punt *et al.*, 2008) was strongly upregulated. Furthermore, transcript levels of about 20 proteases lacking predicted signal peptide sequences were identified as significantly elevated (Table 4.3), suggesting considerable intracellular proteolytic activities during carbon starvation.

Northern (Figure 4.1C), microscopic (Figure 4.2C-4.2D) and GO enrichment (Figure 4.5) analyses clearly indicated that conidiation is one of the main responses provoked by carbon starvation. Transcriptomic data of a subset of genes predicted to be involved in asexual development in *Aspergillus* is shown in Table 4.4. Expression profiles of orthologous genes belonging to the two core regulatory pathways identified in *A. nidulans*, STUNTED (*stuA* → *wetA*) and BRISTLE (*brlA* → *abaA* → *wetA*) (Miller *et al.*, 1991; Fischer, 2002) suggest conservation of these regulatory pathways between the two Aspergilli. Whereas the first pathway is induced early upon achievement of asexual developmental competence (day 1), induction of the latter pathway is delayed (day 3). Among the fluffy genes *flbA-E* encoding upstream regulators of BrlA (Adams *et al.*, 1998), only *flbC* and *flbD* were clearly induced. Remarkably, although only little asexual differentiation occurred, hydrophobins were among the most intensely induced genes (Table 4.4). In a global ranking based on highest expression levels at day 6, the

three predicted hydrophobins encoded by An03g02400, An08g09880 and An03g02360 were at positions one, five and six, respectively. In agreement, conidial pigmentation genes including *olvA* were strongly induced (Table 4.4).

Secretomic response to carbon starvation

To identify extracellular hydrolases secreted at various cultivation time points, mass spectrometric analyses of tryptically digested proteins precipitated from culture filtrates were performed. Neither chitin, α-glucan nor mannan active hydrolases were detected in the culture broth during exponential growth (Table 4.2). In agreement to its high transcript levels during carbon starvation, NagA (An09g02240) was the most abundant extracellular hydrolase involved in chitin degradation at day 1, 3 and 6. However, the chitinase ChiB was, in contrast to its strong transcriptional upregulation, only marginally detected in filtrates at day 1. Both observations correspond well to the presence and absence of predicted signal peptide sequences for NagA and ChiB, respectively. Interestingly, ChiB of *A. niger* showed only low extracellular abundance, whereas the *A. nidulans* ChiB (AN4871) was identified as the major extracellular autolytic chitinase during carbon starvation (Pusztahelyi *et al.*, 2006). The absence of ChiB in the culture broth of *A. niger* could explain why hyphal ghosts remained intact but were reported to fragment in aging cultures of *A. nidulans* (Emri *et al.*, 2004). In concordance with its expression profile, the α-glucanase AgnB (An07g08640) was detected extracellularly at day 1 and 3. While GelD (An09g00670) was the only reliably detected β-glucanase during exponential growth, various β-glucanases with predicted signal peptide sequences were detected at day 1, 3 and 6 of carbon starvation. Among the predicted mannanases, only An04g09650 was reliably detected in filtrates at later time points (day 3 and 6).

In agreement with increasing extracellular protease activity and expression profiles, a number of proteases with predicted signal peptide sequences were identified in culture filtrates of day 1, 3 and 6 (Table 4.3). Among them, PepA (An14g04710), the major extracellular protease (Mattern *et al.*, 1992), was most abundant. However, although PepB (An01g00530) has a predicted signal peptide sequence and showed strong transcriptional induction, it was not detected in culture filtrates. Transcriptionally induced proteases lacking predicted signal peptide sequences were not detected in culture filtrates, with the only exception of An01g00370 (Table 4.3). Similar results have been previously reported for *A. niger* by Braaksma *et al.* (2010), who proposed that the high extracellular abundance of An01g00370 is likely a result of non-classical secretion rather than lysis.

The secretome during starvation conditions was clearly enriched by an additional group of proteins with strong similarity to phospholipases. Together the four putative phospholipases,

Table 4.2 — Transcriptome and secretome data of predicted glycosyl hydrolases

					Transcriptome			
					Expression data[2]			
Identifier	Gene	CAZy[1]	(Predicted) function	SP[5]	Exp[6]	Day 1	Day 3	Day 6
Chitin								
An09g02240	*nagA*	GH20	β-1,6-N-acetylglucosaminidase	1	1.1	64	52	48
An02g07020	*chiB*	GH18	chitinase	0	1.6	73	77	84
An01g05360	*cfcD*	GH18	chitinase	0	1.2	10	11	10
An01g01920		GH20	β-1,6-N-acetylglucosaminidase	1	0.5	2	1	2
An02g02340	*csmB*	GT2	chitin synthase	0	7.7	19	25	22
An09g02290	*chsD*	GT2	chitin synthase	0	4.4	10	11	10
An09g04010	*chsB*	GT2	chitin synthase	0	7.5	16	16	17
An08g05290	*chsG*	GT2	chitin synthase	1	0.5	1	1	0
An02g02360	*csmA*	GT2	chitin synthase	0	2.9	5	6	4
An02g13580	*cfcI*	GH18	chitinase	1	0.6	1	24	43
An09g05920	*ctcB*	GH18	chitinase	1	0.5	1	16	42
α-*glucan*								
An07g08640	*agnB*	GH71	α-glucanase	1	0.5	33	27	6
An15g04760	*agnE*	GH71	α-glucanase	1	0.4	0	2	1
An09g03100	*agtA*	GH13	α-glucan transferase	1	6.2	14	15	18
An02g03260	*agsD*	GH13/GT5	α-glucan synthase	1	0.4	0	1	1
β-*glucan*								
An01g03090		GH81	β-glucanase	1	1.1	34	56	57
An02g13180		GH55	β-glucanase	1	0.4	4	2	3
An01g04560		GH16	β-glucanase	1	1.2	10	23	31
An18g04100		GH28	β-glucanase	1	0.8	4	16	17
An01g11010	*crhD*	GH16	β-glucanase	1	21.3	92	61	44
An07g04650	*bgtC*	GH17	β-glucanase	0	1.4	6	7	6
An01g12450	*bxgA*	GH55	β-glucanase	1	7.5	26	23	34
An11g01540		GH16	β-glucanase	1	1.0	2	1	1
An10g00400	*gelA*	GH72	β-1,3-glucosyl transferase	1	12.6	20	52	50
An09g00670	*gelD*	GH72	β-1,3-glucosyl transferase	1	48.0	75	59	69
An02g00850		GH16	β-glucanase	1	1.5	2	6	9
An06g01550	*fksA*	GT48	β-1,3-glucan synthase	0	62.6	71	78	91
An08g03580	*bgtA*	GH17	β-glucanase	1	0.7	1	1	2
An02g09050	*gelG*	GH72	β-1,3-glucosyl transferase	1	0.6	1	2	6
An16g02850		GH16	β-glucanase	1	1.4	1	5	3
An06g01530		GH17	β-glucanase	1	0.6	1	1	3
An02g03980	*kslA*	GH16	β-glucanase	0	0.5	0	1	2
Mannan								
An07g07700		GH76	α-1,6-mannanase	1	1.4	30	35	27
An01g06500	*dfgD*	GH76	α-1,6-mannanase	1	0.5	3	5	6
An14g03520	*dfgC*	GH76	α-1,6-mannanase	1	3.6	7	6	7
An04g09650		GH76	α-1,6-mannanase	1	0.3	1	0	0
An02g02660	*dfgG*	GH76	α-1,6-mannanase	1	0.8	1	1	1
An18g01410	*dfgA*	GH76	α-1,6-mannanase	1	0.7	1	1	2

(1) Families from the Carbohydrate-Active Enzyme (CAZy) database (Cantarel *et al.*, 2009)

(2) mRNA abundance relative (%) to the gamma-actin (An15g00560) encoding transcript during exponential growth

(3) Fold changes and FDR q-values for comparisons with transcriptome data from the exponential growth phase

(4) Protein abundance in filtrates: (-) not detected; (+) $<$ 5 ng/ml; (++) $<$ 50 ng/ml; (+++) $<$ 250 ng/ml; (++++) $<$ 1 μg/ml; (+++++) $<$ 4 μg/ml; (++++++) $>$ 4 μg/ml; (*) biological and/or technical relative standard deviation above 100 and 50, respectively

(5) Signal peptide sequence prediction (Braaksma *et al.*, 2010)

(6) Exponential growth phase

data									
Fold changes[3]			FDR q-values[3]			Secretome data[4]			
Day 1	Day 3	Day 6	Day 1	Day 3	Day 6	Exp[6]	Day 1	Day 3	Day 6
57.4	46.4	43.5	2.4E-12	5.0E-12	5.6E-12	-	++++	+++++	+++++
45.0	47.2	51.5	3.9E-14	4.1E-14	3.4E-14	-	++	-	-
8.1	8.9	7.7	2.8E-12	1.9E-12	3.7E-12	-	-	-	-
3.1	2.5	3.6	5.6E-08	9.3E-07	1.5E-08	-	-	+++	++
2.5	3.2	2.9	1.8E-09	1.0E-10	2.9E-10	-	-	-	-
2.3	2.6	2.3	5.1E-09	1.4E-09	8.0E-09	-	-	-	-
2.1	2.1	2.2	4.1E-08	4.7E-08	1.9E-08	-	-	-	-
1.6	1.3	1.0	1.6E-04	1.5E-02	7.5E-01	-	-	-	-
1.6	2.0	1.5	2.1E-03	4.9E-05	6.5E-03	-	-	-	-
2.3	41.6	73.5	1.2E-02	3.9E-09	6.9E-10	-	-	-	-
1.3	33.8	90.2	1.2E-01	2.1E-11	1.2E-12	-	-	-	+++*
68.7	57.7	13.4	8.4E-15	1.3E-14	1.2E-12	-	+++	++	-
1.0	3.6	1.7	7.2E-01	1.5E-08	1.6E-04	-	-	-	-
2.3	2.4	2.8	3.2E-04	1.9E-04	4.0E-05	-	-	-	-
1.0	2.3	1.5	9.5E-01	1.9E-06	1.4E-03	-	-	-	-
29.8	49.3	50.5	1.1E-14	4.3E-15	3.7E-15	-	-	-	-
11.1	6.1	8.1	5.4E-11	1.7E-09	2.9E-10	-	+++	+++*	++*
8.2	19.8	26.5	1.4E-11	3.3E-13	1.1E-13	-	+++*	++++	++++*
5.9	21.0	22.8	1.3E-07	2.5E-10	1.8E-10	-	-	-	-
4.3	2.9	2.1	1.2E-09	6.3E-08	4.6E-06	+++*	+++++	+++++	+++++
4.0	5.0	4.3	2.6E-09	5.3E-10	1.6E-09	+*	-	-	-
3.5	3.0	4.5	6.4E-08	2.9E-07	7.6E-09	++*	++++	+++++	+++++
2.1	1.0	0.6	6.2E-06	9.9E-01	2.5E-04	++*	++++	++++	++++*
1.6	4.1	4.0	4.3E-05	1.6E-10	2.1E-10	+++*	++	-	-
1.6	1.2	1.4	3.3E-05	1.5E-02	2.2E-04	+++	++++*	+++++*	+++++
1.4	3.8	6.1	1.9E-03	1.3E-09	3.4E-11	-	-	-	++
1.1	1.2	1.4	7.0E-02	2.7E-03	1.7E-05	-	-	-	-
1.1	1.9	2.8	4.3E-01	1.5E-05	9.9E-08	-	-	-	-
1.0	3.6	9.0	9.3E-01	2.5E-06	4.6E-09	-	-	-	-
0.8	3.6	2.3	1.3E-01	4.8E-09	7.7E-07	-	-	-	-
0.8	2.3	4.4	2.5E-02	1.9E-07	2.3E-10	-	-	-	-
0.8	2.4	4.7	4.2E-03	1.5E-08	2.0E-11	-	-	-	-
20.8	24.7	18.8	7.1E-13	4.5E-13	1.1E-12	-	+++	-	-
5.8	8.4	10.9	2.3E-10	2.9E-11	7.0E-12	-	-	-	-
1.9	1.8	1.9	1.1E-07	5.8E-07	1.9E-07	-	++*	+++*	-
1.8	1.3	1.3	4.0E-05	3.4E-02	2.3E-02	-	+++*	+++*	+++
1.6	1.4	1.1	4.7E-03	3.5E-02	4.7E-01	-	-	-	-
0.8	1.5	2.7	2.4E-01	4.1E-03	1.9E-06	-	-	-	-

Table 4.3 – Transcriptome and secretome data of predicted protein hydrolases

			Transcriptome			
			Expression data[1]			
Identifier	**Gene**	**(Predicted) function**	**Exp[4]**	**Day 1**	**Day 3**	**Day 6**
SP[5] present						
An01g00530	*pepB*	A4 family peptidase	0.6	84.9	32.5	113.9
An14g04710	*pepA*	Aspartyl protease	1.4	180.1	34.7	70.5
An01g01750		Subtilisin-like serine protease	1.1	45.8	9.8	8.9
An02g01550		Secreted serine protease	2.4	63.2	25.3	6.0
An08g04640		Lysosomal pepstatin insensitive protease	1.1	16.2	8.0	10.6
An06g00190		Lysosomal pepstatin insensitive protease	2.3	31.5	27.2	25.9
An03g01010		Lysosomal pepstatin insensitive protease	1.2	14.9	3.2	4.2
An02g04690		Serine-type carboxypeptidase I	6.4	64.7	31.7	34.9
An12g05960		Dipeptidyl peptidase II	1.0	9.2	4.1	2.7
An07g08030	*pepF*	Serine carboxypeptidase	0.8	7.0	4.2	6.3
An11g06350		Carboxypeptidase	1.1	8.3	3.6	1.7
An09g03780	*pepD*	Subtilisin-like serine protease	0.5	3.0	0.6	0.7
An12g03300		Aspartic protease	0.7	3.4	0.5	0.4
An15g06280		Aspartic proteinase [truncated ORF]	5.8	25.2	33.2	22.4
An16g09010		Carboxypeptidase I [putative frameshift]	0.6	2.2	3.6	4.7
An14g00620		Aminopeptidase	5.3	20.4	14.7	14.3
An07g03880	*pepC*	Serine proteinase	31.1	111.2	101.5	91.5
An07g10060		Proteinase B inhibitor	4.2	13.1	17.0	19.5
An02g07210	*pepE*	Aspartic protease	30.4	83.9	57.8	57.2
An15g07700		Aspergillopepsin II precursor	1.3	3.5	3.3	4.4
An18g01320		Extracellular protease precursor	21.9	54.8	14.7	4.9
An02g13740		Gly-X carboxypeptidase precursor	1.9	4.4	4.2	4.4
An03g01660		Vacuolar aminopeptidase Y	9.1	19.2	17.4	17.5
An08g08750	*cpY*	Carboxypeptidase	33.8	67.9	53.8	51.3
An14g03250		Aspergillopepsin II	0.7	1.2	0.9	1.6
An07g10410		Metalloprotease	1.2	1.3	7.5	16.1
SP[5] absent						
An01g00370		Aspergillopepsin	0.8	89.0	16.8	10.0
An02g00090		Prolidase	0.4	20.4	22.7	7.6
An14g02080		Prolidase	1.8	18.0	6.8	4.1
An09g02830		Acylaminoacyl-peptidase	4.3	39.7	18.0	9.9
An17g00390		Aminopeptidase	4.6	27.7	10.2	7.4
An18g03980		Glutamate carboxypeptidase II	3.2	19.0	13.8	13.7
An01g01720		Bleomycin hydrolase	0.6	3.3	1.4	1.0
An07g06490		Insulin-degrading enzyme	0.4	2.1	1.1	1.1
An11g05920		Prolidase	0.9	4.6	1.5	1.3
An11g02950		Calpain family cysteine protease	0.9	3.6	3.2	1.7
An01g14920		Metallopeptidase	0.5	1.8	1.3	1.1
An11g01970		Pyroglutamyl peptidase	2.1	8.2	6.0	6.8
An14g01530		Subtilisin-like serine proteases	0.5	2.0	1.1	0.7
An09g06800		Leucyl aminopeptidase	10.9	40.3	37.7	33.4
An12g01820		Ubiquitin carboxyl-terminal hydrolase	0.8	2.6	1.7	1.1
An01g08470		Ubiquitin carboxyl-terminal hydrolase	1.8	5.9	7.5	7.4
An04g00410		Dipeptidyl peptidase III	17.0	51.9	37.8	29.6
An16g08150		Dipeptidyl-peptidase V	10.5	26.0	17.4	17.2
An18g02980		Endopeptidase	4.6	10.4	8.3	8.2
An04g06940	*prtT*	Transcriptional activator of proteases	5.4	58.4	35.2	24.9

(1) mRNA abundance relative (%) to the gamma-actin (An15g00560) encoding transcript during exponential growth

(2) Fold changes and FDR q-values for comparisons with transcriptome data from the exponential growth phase

(3) Protein abundance in filtrates: (-) not detected; (+) $<$ 5 ng/ml; (++) $<$ 50 ng/ml; (+++) $<$ 250 ng/ml; (++++) $<$ 1 μg/ml; (+++++) $<$ 4 μg/ml; (++++++) $>$ 4 μg/ml; (*) biological and/or technical relative standard deviation above 100 and 50, respectively

(4) Exponential growth phase

(5) Signal peptide sequence prediction (Braaksma *et al.*, 2010)

data									
Fold changes[2]			FDR q-values[2]			Secretome data[3]			
Day 1	Day 3	Day 6	Day 1	Day 3	Day 6	Exp[4]	Day 1	Day 3	Day 6
148.1	56.7	198.8	1.4E-16	9.1E-16	5.9E-17	-	-	-	-
130.2	25.1	51.0	1.9E-13	2.2E-11	2.2E-12	+++*	++++++	++++++	++++++
40.0	8.6	7.7	2.3E-14	9.5E-12	1.5E-11	-	+++	++++	+++
26.0	10.4	2.5	8.6E-10	4.8E-08	9.8E-04	++*	++++	++++*	-
14.3	7.1	9.3	4.0E-12	1.5E-10	3.2E-11	+*	++++	+++++	++++
13.4	11.6	11.0	1.1E-10	2.3E-10	2.8E-10	+++*	++++	+++++	++++
12.7	2.7	3.6	1.2E-09	4.8E-05	3.6E-06	+*	+++*	+++*	+++*
10.1	4.9	5.4	9.7E-10	8.4E-08	4.2E-08	++	++++*	+++++	+++++
9.0	4.0	2.6	2.8E-11	7.3E-09	4.8E-07	-	+++*	++++	++++
8.6	5.2	7.7	1.2E-11	2.7E-10	2.2E-11	-	++*	+++	+++*
7.9	3.4	1.6	5.0E-11	2.1E-08	5.0E-04	-	-	-	-
5.8	1.1	1.4	2.2E-11	1.6E-01	2.4E-03	-	-	-	-
5.0	0.7	0.7	1.1E-08	1.2E-02	1.0E-02	++*	+++		
4.3	5.7	3.8	4.1E-09	6.1E-10	1.2E-08	++*	+++*	++++*	++++*
4.0	6.4	8.4	2.5E-09	8.8E-11	1.8E-11	-	-	+++*	+++
3.8	2.8	2.7	4.6E-09	1.3E-07	1.8E-07	-	-	-	-
3.6	3.3	2.9	8.5E-12	2.2E-11	6.3E-11	++*	-	-	-
3.1	4.1	4.7	1.1E-08	1.1E-09	3.5E-10	+++*	-	-	-
2.8	1.9	1.9	1.4E-10	3.3E-08	3.9E-08	-	++++	+++*	++*
2.7	2.6	3.4	3.5E-07	5.2E-07	3.1E-08	-	-	-	-
2.5	0.7	0.2	1.8E-05	1.5E-02	6.8E-08	+++*	++++	+++++*	++++
2.3	2.2	2.4	9.5E-09	2.1E-08	8.6E-09	-	-	-	-
2.1	1.9	1.9	3.1E-09	1.9E-08	1.5E-08	++*	-	-	-
2.0	1.6	1.5	1.0E-08	1.3E-06	4.2E-06	++*	-	-	-
1.7	1.3	2.2	2.5E-04	3.0E-02	3.1E-06	-	+++*	-	-
1.1	6.5	13.9	2.9E-01	8.3E-11	1.6E-12	-	-	-	-
110.2	20.8	12.3	3.6E-14	4.9E-12	3.9E-11	++*	+++++	+++++	+++++
53.2	59.4	19.8	1.2E-14	1.0E-14	1.9E-13	-	-	-	-
9.7	3.7	2.2	4.4E-09	2.8E-06	3.8E-04	-	-	-	-
9.2	4.2	2.3	1.8E-12	3.0E-10	1.6E-07	-	-	-	-
6.0	2.2	1.6	3.2E-11	5.1E-07	1.2E-04	-	-	-	-
5.9	4.3	4.3	3.3E-12	3.3E-11	3.4E-11	-	-	-	-
5.4	2.3	1.7	1.6E-10	8.4E-07	1.0E-04	-	-	-	-
5.2	2.7	2.7	8.5E-11	2.9E-08	3.7E-08	-	-	-	-
5.0	1.6	1.4	5.2E-08	9.1E-03	5.3E-02	-	-	-	-
4.3	3.7	2.0	9.8E-10	3.4E-09	6.0E-06	-	-	-	-
3.9	2.8	2.3	1.1E-09	4.0E-08	4.1E-07	-	-	-	-
3.9	2.8	3.2	1.0E-11	2.4E-10	6.2E-11	-	-	-	-
3.7	2.1	1.3	9.9E-09	7.0E-06	2.6E-02	-	-	-	-
3.7	3.5	3.1	1.3E-11	2.5E-11	8.2E-11	-	-	-	-
3.4	2.2	1.5	8.1E-10	2.0E-07	4.4E-04	-	-	-	-
3.3	4.2	4.1	6.1E-10	8.3E-11	9.6E-11	-	-	-	-
3.1	2.2	1.7	9.6E-10	5.6E-08	3.4E-06	-	-	-	-
2.5	1.7	1.6	4.3E-09	4.1E-06	4.9E-06	-	-	-	-
2.3	1.8	1.8	4.0E-09	2.0E-07	2.6E-07	-	-	-	-
10.8	6.5	4.6	5.7E-12	9.8E-11	1.0E-09	-	-	-	-

Table 4.4 – Transcriptome data of predicted conidiation genes

			Expression data[1]				Fold changes[2]			FDR q-values[2]		
ORF	Gene	(Predicted) function	Exp[3]	Day 1	Day 3	Day 6	Day 1	Day 3	Day 6	Day 1	Day 3	Day 6
Fluffy genes												
An14g03390	*fluG*	Synthesis of small extracellular factor	1.9	1.0	1.3	1.8	0.5	0.7	0.9	3.1E-08	3.7E-05	3.0E-01
An02g03160	*flbA*	Regulator of G-protein signalling	0.9	0.8	0.9	1.2	0.9	1.0	1.4	3.3E-01	7.9E-01	5.4E-04
An15g03710	*flbB*	Transcription factor	2.6	2.5	2.1	2.5	1.0	0.8	1.0	6.6E-01	3.6E-02	7.8E-01
An02g05420	*flbC*	Transcription factor	1.1	2.4	4.5	8.2	2.1	4.0	7.2	4.0E-05	3.3E-08	5.1E-10
An01g04830	*flbD*	Transcription factor	1.3	8.2	6.3	9.0	6.3	4.8	6.9	1.0E-09	7.3E-09	6.2E-10
An08g07210	*flbE*	Activator functionally associated with FlbB	1.9	2.0	3.4	4.5	1.1	1.8	2.4	3.7E-01	2.3E-06	2.7E-08
An08g06130	*fadA*	Heterotrimeric G-protein α-subunit	15.2	18.8	18.4	19.8	1.2	1.2	1.3	2.0E-03	4.0E-03	2.6E-04
Conidiophore development												
An01g10540	*brlA*	Transcription factor	0.4	0.4	13.4	17.0	1.1	37.0	46.8	8.5E-01	3.5E-10	1.7E-10
An01g03750	*abaA*	Transcription factor	1.1	1.0	14.1	31.9	0.9	12.6	28.6	1.7E-01	3.1E-12	1.3E-13
An01g08900	*wetA*	Transcription factor	0.8	0.8	1.5	4.2	0.9	1.8	5.1	4.6E-01	5.1E-06	3.2E-11
An02g02150	*medA*	Transcription factor	1.6	3.6	3.8	2.5	2.2	2.3	1.5	6.2E-08	2.8E-08	7.1E-05
An05g00480	*stuA*	Transcription factor	12.5	28.0	49.7	48.7	2.2	4.0	3.9	5.3E-07	1.0E-09	1.2E-09
Pigmentation genes and hydrophobins												
An03g02400	*hypC*	Hydrophobin	0.6	0.6	261.2	333.0	1.1	436.9	557.1	8.7E-01	4.0E-10	2.4E-10
An08g09880		Hydrophobin	0.5	0.5	180.5	229.9	1.1	360.5	459.1	8.9E-01	5.0E-10	3.0E-10
An03g02360	*hypB*	Hydrophobin	0.5	0.4	162.4	214.5	0.9	345.1	455.8	7.3E-01	5.8E-10	3.2E-10
An14g05350	*olvA*	Hydrolase involved in pigmentation	1.6	11.1	153.3	205.4	6.8	94.2	126.2	8.2E-07	3.7E-11	1.8E-11
An01g13660	*yA*	Laccase invovled in pigmenation	0.8	1.0	46.1	20.6	1.2	56.5	25.3	3.6E-01	2.3E-11	3.0E-10
An14g05370	*brnA*	Multicopper oxidase involved in pigmentation	0.7	0.5	33.0	39.9	0.7	46.3	55.9	3.1E-01	1.8E-09	9.6E-10
An01g10940	*hypA*	Hydrophobin	0.4	0.4	12.3	15.0	0.8	29.3	35.6	5.1E-01	1.3E-09	6.4E-10
An07g03340	*hypE*	Hydrophobin	1.9	2.4	26.9	62.3	1.3	14.4	33.4	3.9E-01	9.6E-08	3.8E-09
An09g05730	*fwnA*	Polyketide synthase involved in pigmentation	2.4	1.2	18.8	36.0	0.5	7.7	14.7	2.6E-03	3.6E-08	1.4E-09
An09g05530	*hypG*	Hydrophobin	0.5	0.4	0.8	1.7	0.8	1.5	3.3	2.4E-02	4.4E-04	2.1E-09

(1) mRNA abundance relative (%) to the gamma-actin (An15g00560) encoding transcript during exponential growth

(2) Fold changes and FDR q-values for comparisons with transcriptome data from the exponential growth phase

(3) Exponential growth phase

An16g01880, An09g02180, An01g14940 and An02g13220 constituted on average about 7% of all detected extracellular proteins during day 1, 3 and 6. All except An02g13220 were transcriptionally induced during carbon starvation. This high abundance of predicted phospholipases during carbon starvation might be indicative for a role of membrane lipids as alternative carbon source during secondary growth.

Discussion

The present study is the first system-wide description of the carbon starvation response in a filamentous fungus. The application of bioreactor technology allowed highly reproducible culture conditions and physiological synchronization of replicate batch cultures. The use of minimal medium with maltose as the sole limiting nutrient, constant pH, sufficient aeration and homogeneously dispersed mycelial biomass reduced biological and technical variations to a minimum and allowed us to highlight those differences in gene expression, which were in direct relation to carbon starvation.

Submerged growth in bioreactors is fundamentally different from the natural fungal life style. While fungi experience spatio-temporal gradients of various ambient factors such as nutrients, temperature and pH in their natural habitats, these gradients can be reduced to temporal gradients during submerged cultivation. In an ideally mixed bioreactor, all dispersed hyphae experience identical environmental conditions and temporal profiles can be monitored and controlled by process parameters. Accordingly, many evolutionary acquired traits contributing to the natural fungal life style such as the formation of substrate exploring hyphae, secretion of certain hydrolases, cell death and conidiation are dispensable during industrial processes and might even negatively affect production yields.

In this study *A. niger* showed general hallmarks of autolysis (White *et al.*, 2002) during prolonged carbon starvation. However, in contrast to *A. nidulans* (Emri *et al.*, 2004), *A. niger* hyphae did not undergo substantial fragmentation. While an increasing number of hyphal compartments became empty after carbon depletion, microscopic analysis showed that hyphal cell wall skeletons remained mainly intact. Thus disintegration of aging mycelia appears rather to be initiated by intracellular activities such as cell death and/or endogenous recycling of neighboring compartments leading to empty hyphal ghosts than by extracellular hydrolysis of fungal cell walls (Figure 4.6). This assumption is supported by studies in *A. nidulans*, where autolytic fragmentation of hyphae and cell death were described as simultaneous but independently regulated processes (Emri *et al.*, 2005a). While deletion of the major carbon catabolite repressor CreA in *A. nidulans* resulted in increased hydrolase activities and mycelial fragmentation during carbon starvation, the viability of *A. nidulans* was not affected (Emri *et al.*, 2006).

Consistently, we observed hyphal fragmentation and an enhanced decline of the biomass in bioreactor cultures during the starvation phase only when the pH control was switched off leading to an elevated pH of approximately 5.8 towards the end of cultivation (Nitsche *et al.* unpublished data). We thus propose that hydrolytic weakening of the fungal cell wall and hyphal fragmentation is a secondary effect, which occurs after initial cell death events and only under favorable conditions (Figure 4.6).

In flow chamber experiments with *A. oryzae*, Pollack *et al.* (2008) followed single hyphae and studied their response to glucose depletion. Similar to our results, they observed secondary growth fueled by carbon recycling, which was morphologically characterized by the formation of hyphae with significantly reduced diameters. For *A. niger* and *A. oryzae* (Pollack *et al.*, 2008; Agger *et al.*, 1998; Müller *et al.*, 2000) hyphal diameters were shown to linearly correlate with the specific growth rate, hence the reduction of hyphal diameters reflects the slow rate of secondary growth during the starvation phase. Focusing on non-empty compartments, we analyzed hyphal population dynamics from statistically valid sample sizes for different cultivation time points (Figure 4.3). Our data showed that older hyphae with larger diameters grown during carbon-sufficient conditions gradually became empty, giving rise to a new population of thinner hyphae. Carbon for this secondary phase of growth might have been liberated from extra- and/or intracellular sources. In agreement with another study of *A. niger* (Braaksma *et al.*, 2010), our secretomic data revealed that the relative contribution of lysis was very limited, even under starvation conditions. Compared to exponential growth, no relative accumulation of proteins without predicted signal peptide sequences was observed in culture filtrates. However, because these results could also be explained by an equilibrium between proteolytic degradation and leakage of cytoplasmic proteins, it still remains to be shown whether intracellular resources are endogenously recycled by neighboring compartments or first leak into the culture broth where they are subsequently taken up by surviving compartments (Figure 4.6).

One process known to be important for endogenous recycling of cytoplasmic content in eukaryotes is macroautophagy. In filamentous fungi, it is thought to play an important role in nutrient trafficking along the hyphal network promoting foraging of substrate exploring hyphae and conidiation (Shoji *et al.*, 2006; Kikuma *et al.*, 2007). However, besides endogenous recycling of nutrients, autophagy in general is clearly associated with cell death and is discussed to have protective roles related to the degradation of e.g. damaged mitochondria or unfolded proteins (Lockshin *et al.*, 2004; Kanki *et al.*, 2008; Kimura *et al.*, 2011) (Figure 4.6). It is strongly evident from our transcriptomic data that the induction of autophagic processes is a hallmark of carbon-starved aging fungal cultures. To which extend autophagic processes play a role in

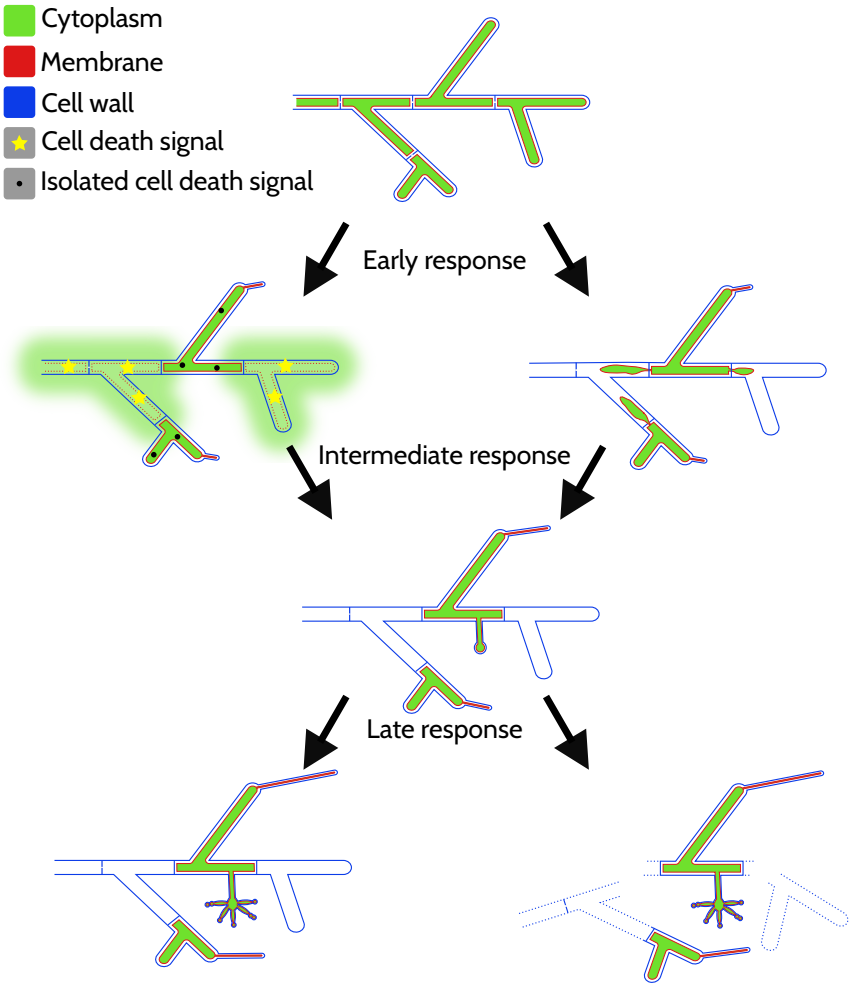

Figure 4.6 — Model for the carbon starvation response in *A. niger*
Schematic representation of major early, intermediate and late processes during prolonged submerged carbon starvation. During the early phase of starvation, secondary growth fueled by carbon recycling is initiated as characterized by the formation of thin hyphae. Two mechanisms resulting in empty hyphal compartments are depicted. On the left side, apoptotic/necrotic signals lead to cell death of compartments. Cytoplasmic content leaks into the culture broth. Surviving compartments are protected by autophagic processes isolating/inactivating cell death signals. On the right side, endogenous recycling of neighboring compartments by autophagic processes leads to the formation of empty hyphal ghosts. Cytoplasmic content does not leak into the culture broth. During the intermediate phase, earlier processes continue and first reproductive structures emerge. Towards later phases, these processes proceed resulting in few surviving compartments often bearing reproductive structures and elongating thin hyphae. Depending on the strain (e.g. $\Delta creA$) and cultivation conditions (e.g. elevated pH), a largely empty non fragmented mycelial network remains (left side) or fragmentation of empty hyphal ghosts occurs by hydrolytic weakening of cell walls (right side).

the protection against apoptotic/necrotic PCD, endogenous recycling and autophagic PCD remains to be shown in future studies.

The liberation of carbon from polymers such as fungal cell wall carbohydrates and secreted proteins is indicated by increased expression of glycosyl hydrolases and proteases as well as by increased extracellular protease activity. Strikingly, the major secreted protease PepA (Mattern *et al.*, 1992) was the second most abundant extracellular protein during carbon starvation, which was only excelled by protein levels of the maltose-induced alpha-glucosidae GlaA (An03g06550) secreted during exponential growth (see Table 4.3). Although transcripts of the ChiB/NagA chitinolytic system accumulated simultaneously during carbon starvation as described previously for *A. nidulans* (Pusztahelyi *et al.*, 2006), only NagA could be identified extracellularly in high relative abundances (see Table 4.2). While the low relative abundance of ChiB in filtrates from day 1 is in agreement with the absence of a predicted signal peptide sequence, it conflicts with results obtained in *A. nidulans* (Pusztahelyi *et al.*, 2006), where it was identified as the major extracellular autolytic chitinase. Interestingly, despite its extracellular abundance, also *A. nidulans* ChiB lacks a signal peptide prediction. Whether *A. nidulans* ChiB is released by non-classical secretion or lysis remains to be shown. It is tempting to speculate that cell wall degrading hydrolases lacking a signal peptide sequence are part of the fungal PCD program and accumulate intracellularly in dying compartments to be subsequently released upon cell death for recycling of the remaining hyphal ghost. In view of the natural emerse growth of fungi, this could be a successful strategy for survival - released hydrolases will remain localized to hyphal ghosts and not become diluted as under submerged conditions. Future studies will be necessary to elucidate whether intracellular localization, retention at the cell wall, protein instability or inefficient translation explain the low abundance of ChiB in filtrates of *A. niger*.

Carbon starvation provoked asexual reproduction of *A. niger*, which was clearly evident by the formation of condiospores (Figure 4.2D) and by expression of respective conidiation-related genes (Table 4.4). This elaborate developmental program requires liberation and recycling of carbon to proceed in aging batch cultures (Figure 4.6). Increased heterogeneity and compartmentalization of the hyphal network resulting in empty, cryptically growing and conidiating compartments implies an ordered form of fungal cell death ensuring self-propagation to survive life-threatening starvation conditions. In *A. nidulans* it was shown that disruption of the *flbA* gene, encoding a regulator of G-protein signaling acting upstream of BrlA, resulted in an enhanced autolytic phenotype (Adams *et al.*, 1998). Hence, vegetative growth, autolysis and conidiation are closely interwoven processes and future factorial genome-wide transcriptomic studies of wild-type and developmental mutants will allow deconstruction of fungal cell death and its link to developmental processes.

Conclusions

This study provides a comprehensive description of the carbon starvation response of the filamentous fungus *A. niger* during submerged cultivation. The impact of secondary growth by carbon recycling was indicated by hyphal population dynamics illustrating a gradual transition from old to young hyphae. The induction of autophagic and reproductive processes was clearly evident by major genome-wide transcriptional trends. Hydrolases with strong transcriptional induction during carbon starvation include ChiB, NagA, AgnB, PepA and PepB. Importantly, fragmentation of empty hyphal ghosts was not observed, thus constituting direct evidence that autolysis in aging submerged cultures of *A. niger* is rather initiated by cell death than by hydrolytic weakening and fragmentation of cell walls.

Methods

Strain, inoculum and media compositions

Conidial suspensions for inoculation of bioreactor cultures were prepared by growing the *A. niger* laboratory strain N402 (*cspA1* derivative of ATCC9029) (Bos *et al.*, 1988) on solidified (1.5% agar) complete medium (CM) for three days at 30°C in the dark. Spores were harvested with sterile physiological salt solution (0.9% NaCl) and filtered through Myracloth (Calbiochem, San Diego, CA, USA) to retain mycelial debris and solidified medium. CM contained per liter: 10 g glucose, 6 g $NaNO_3$, 1.5 g KH_2PO_4, 0.5 g KCl, 0.5 g $MgSO_4 \cdot 7H_2O$, 1 g casamino acids, 5 g yeast extract and 1 ml trace metal solution. The pH was adjusted to 5.8 with NaOH. The trace metal solution, modified from Vishniac *et al.* (1957), contained per liter: 10 g EDTA, 4.4 g $ZnSO_4 \cdot 7H_2O$, 1.01 g $MnCl_2 \cdot 4H_2O$, 0.32 g $CoCl_2 \cdot 6H_2O$, 0.315 g $CuSO_4 \cdot 5H_2O$, 0.22 g $(NH_4) \cdot 6Mo_7O_{24} \cdot 4H_2O$, 1.47 g $CaCl_2 \cdot 2H_2O$ and 1 g $FeSO_4 \cdot 7H_2O$. Minimal medium (MM) for bioreactor cultivations contained per liter: 4.5 g NH_4Cl, 1.5 g KH_2PO_4, 0.5 g KCl, 0.5 g $MgSO_4 \cdot 7H_2O$ and 1 ml trace metal solution. The pH was set to 3 with HCl. After autoclavation, 16 ml of heat-sterilized 50% (w/v) maltose monohydrate solution were added per kg of MM.

Bioreactor cultivation

Inoculation and culture conditions

Batch cultures were performed in 6.6 L BioFlo3000 bioreactors (New Brunswick Scientific) as previously described by Jørgensen *et al.* (2010). Briefly, autoclaved bioreactor vessels were filled with 5 L (kg) sterile MM. During cultivation at 30°C, the controller was set to maintain pH 3

by addition of titrants (2 M NaOH and 1 M HCl). Sterile air was supplied at a rate of 1 L min^{-1}. Prior to inoculation, 1.5 ml of 10% (w/v) filter-sterilized yeast extract was added to enhance conidial germination. Cultures were inoculated with freshly harvested spore suspensions to give 10^9 conidia per liter. To reduce the loss of hydrophobic conidia during germination, the stirrer speed was set to 250 rpm and the culture was aerated via the headspace during the first six hours after inoculation. Subsequently, the stirrer speed was increased to 750 rpm, 0.5 ml of polypropyleneglycol P2000 was added as antifoam agent and air was supplied via the sparger.

Online measurements

O_2 and CO_2 partial pressures of the exhaust gas were analyzed with a Xentra 4100C analyzer (Servomex BV, Netherlands). Dissolved oxygen tension (DOT) and pH were measured electrochemically with autoclavable sensors (Mettler Toledo).

Sample preparations

Culture broth was harvested at regular intervals from batch cultures and mycelial biomass was retained by vacuum filtration using glass microfiber filters (Whatman). Both biomass and filtrate were quickly frozen in liquid nitrogen and subsequently stored at -80°C. Dry biomass concentrations were gravimetrically determined from lyophilized mycelium originating from a known mass of culture broth. Culture broth for microscopic analysis was quickly frozen in liquid nitrogen and stored at -80°C. For LC-MS/MS analysis, 1 ml of Sigmafast protease inhibitor cocktail (S8830, Sigma Aldrich) was added to 30 ml of culture filtrate and BSA was spiked as internal standard (1:10, BSA/total expected protein, w/w) before freezing in liquid nitrogen and storage at -80°C.

Protease activity assay

Extracellular protease activity measurements were performed similarly to a previously described method by Braaksma *et al.* (2009) using N,N-dimethylated BSA as substrate. Measurements were performed in 96 well microtiter plates. 30 μl sample were incubated with 80 μl of 0.5% (w/v) N,N-dimethylated BSA in McIlvaine's citric acid-phosphate buffer, pH 3, for 30 min at 37°C. Reactions were stopped by addition of 190 μl fresh TNBSA borate buffer solution prepared by adding 50 μl of 5% 2,4,6,-trinitrobenzene sulfonic acid (TNBSA; Pierce) to 10 ml of borate buffer with 0.5 g l^{-1} Na_2SO_3, pH 9.3. TNBSA reacts with primary amines yielding a yellow chromophore that was measured at 405 nm after 10 min. Blank measurements for sample background correction were obtained by incubation of filtrates with citric

acid buffer not containing N,N-dimethylated BSA. Non proteolytic release of amines from N,N-dimethylated BSA was assessed by incubation of N,N-dimethylated BSA without filtrate sample. 1 U of protease activity was defined as the activity which, within 1 min under the described incubation conditions, produces a hydrolyzate with an absorption equal to that of 1 μmol glycine at 405 nm.

Extracellular protein quantification

Extracellular protein concentrations in culture filtrates were determined using the Quick Start Bradford Protein Assay (Bio-Rad) according to the manufacturer's instructions.

Microscopy and image analysis

Microscopic samples were slowly defrosted on ice. For differential interference contrast microscopy (DIC) an Axioplan 2 instrument (Zeiss) with a 100x oil immersion objective was used and micrographs were captured with an DKC-5000 digital camera (Sony). For the automated determination of hyphal diameters, samples were fixed and stained in a single step by mixing them at a 1:1 ratio with Lactophenolblue (Fluka). Sets of 40 micrographs were taken per sample with an DM IL LED (Leica) microscope using a 40x objective and an ICC50 camera (Leica). The microscope and camera settings were optimized to obtain micrographs with strong contrast. To measure hyphal diameters from micrographs of dispersed mycelia in an automated manner, the following six-step image analysis algorithm was developed and implemented as a macro for the open source program ImageJ (Abràmoff *et al.*, 2004): (1) Convert micrographs to binary images; (2) Copy binary images and outline all objects; (3) Copy binary images and skeletonize all objects; (4) Clean skeletons by removing all intersections; (5) Combine outline and skeleton images; (6) Fragment skeletons and orthogonally measure from the center of each skeleton fragment the distance to the outline.

RNA extraction, gene chip hybridization and Northern analysis

To minimize the chance of RNA degradation, frozen biomass was directly ground in liquid nitrogen and subsequently total RNA was isolated using the Trizol reagent (Invitrogen) according to the manufacturer's instructions. Prior to gene chip hybridization, samples were purified on NucleoSpin RNA II columns (Machery-Nagel) including a DNAse I treatment. Lab on chip quality control, labeling, Affymetrix chip (dsmM_ANIGERa_coll511030F) hybridization and scanning were performed at ServiceXS (Leiden, The Netherlands) according to the GeneChip Expression Analysis Technical Manual (Affymetrix inc., 2002). Northern analysis

using [α^{32}P]-dCTP-labelled probes was performed as previously described by R. a. Damveld *et al.* (2005) using 1.8 μg of RNA per sample. A standard loading control such as 18S rRNA was not used. Equal loading was concluded from smoothly increasing/decreasing time course profiles. Templates for random primer labeling were amplified from genomic DNA of N402 using the following primer pairs: *actA* (An15g00560): 5'-atctcccgtgtcgacatgg-3' and 5'-gcggtg gacgatcgagg-3'; *nagA* (An09g02240): 5'-cccgcgcgaggtatattcac-3' and 5'-cctgggcgtcagtcagatt t-3'; *brlA* (An01g10540): 5'-ggtaacatgtccgatcgcctg-3' and 5'-gcaactttcctggagggctg-3'.

Transcriptome data analysis

RNA samples from four cultivation phases were subjected to genome-wide transcriptional profiling: Exponential growth phase, 16 hours (day 1), 60 hours (day 3) and 140 hours (day 6) post carbon depletion. While the expression data for the exponential growth phase was derived from triplicate cultures, expression data for the three post-exponential time points was obtained from duplicate cultures. Transcriptomic data were analyzed with the statistical programming language R (R-Team, 2008). The following packages of the open source and open development project Bioconductor (Gentleman *et al.*, 2004) were used: affy (Gautier *et al.*, 2004), affycoretools (MacDonald, 2008), affyPLM (Bolstad *et al.*, 2005) and limma (Smyth, 2004). Affymetrix probe level data was imported from .CEL files and preprocessed with the Robust Multi-array Average (RMA) (Irizarry *et al.*, 2003) algorithm as implemented in the affy package. To improve background correction and data normalization, six additional .CEL files corresponding to day 2 and day 8 of carbon-limited retentostat cultivations of *A. niger* (Jørgensen *et al.*, 2010), available at the Gene Expression Omnibus (GEO) database (http://www.ncbi.nlm.nih.gov/geo/) under accession number: GSE21752, were included in the RMA preprocessing step. Prior to the computation of differentially expressed genes, 65 Affymetrix control probes and 204 probes targeting genetic elements were removed from the expression matrix. For 277 transcripts targeted by multiple probes, mean expression values were calculated from the RMA expression data of all associated probes. Subsequently, RMA expression data for the 13,989 transcripts were analyzed with the limma package comparing day 1, 3 and 6 of carbon starvation with the exponential growth phase. The Benjamini & Hochberg False Discovery Rate (FDR) (Benjamini *et al.*, 1995) was controlled at 0.005. A minimal fold change criterion was not applied, as fold changes are not necessarily related to biological relevance (R. A. v. d. Berg *et al.*, 2010; R. A. v. d. Berg *et al.*, 2006)

Annotation enrichment analyses

Enrichment analysis of Gene Ontology (GO) (Ashburner *et al.*, 2000) terms was performed using the Fisher's exact test Gene Ontology annotation tool (FetGOat: http://www.broadinstitute.org/fetgoat/index.html) (Nitsche *et al.*, 2011) applying a critical Benjamini & Hochberg FDR q-value of 0.05. In order to compare and summarize enriched GO terms, we aimed to identify common most-specific GO terms for the sets of up- and downregulated genes, and thus implemented the following algorithm in the programming language Perl: (1) Combine all enriched GO terms from the input sets; (2) Reduce redundancy from higher hierarchy terms by keeping only the most-specific (most-distant) GO terms; (3) For each remaining most-specific GO term, check all parental GO terms, sorted by increasing distance from the corresponding child term, for the presence in the input sets; (4) If a parental GO terms is present in all input sets denote it as common most-specific, if any other equally distant parental terms are present in all input sets, denote them as common most-specific as well and continue with the next most-specific GO term; (5) If none of the parental GO terms are present in all input sets, denote the corresponding most-specific GO term as non-common most-specific; (6) After completing the analysis of all most-specific GO terms, reduce redundancy from the set of common most-specific terms by removing all their parental terms; (7) Output the sets of common most-specific and non-common GO terms. Fisher's exact test based enrichment analysis of Kyoto Encyclopedia of Genes and Genomes (KEGG) pathway (Kanehisa *et al.*, 2010) and Pfam domain (Bateman *et al.*, 2004) annotations were performed using in-house developed Perl scripts. The Benjamini & Hochberg FDR was controlled at 0.05. KEGG pathway annotation (file: ang_pathway.list, version from 22.06.2011) for *A. niger* was downloaded from the KEGG homepage (http://www.genome.jp/kegg/). Pfam domain annotation for *A. niger* was generated by analyzing the predicted proteome of *A. niger* strain CBS 513.88 (Pel *et al.*, 2007) with the PfamScan Perl script (ftp://ftp.sanger.ac.uk/pub/databases/Pfam/Tools/PfamScan.tar.gz).

Secretome analysis

Sample pretreatment

8 ml of 100% (w/v) trichloracetic acid was added to frozen filtrate samples, which were subsequently completely defrosted by shaking at 4°C. Precipitated proteins were spun down and washed twice with ice-cold acetone. Precipitated protein pellets were air-dried, solubilized in 8 M urea (50 μl) and diluted 10x with 100 mM NH_4HCO_3. Reduction, alkylation of cysteines and digestion with trypsin were performed according to Thakur *et al.* (2011). Another aliquot of trypsine (2.5 μl 0.25 mg ml^{-1} pH 3) was added after overnight digestion followed by in-

cubation for three hours at 37°C to ensure complete digestion. Samples were acidified to 1% formic acid.

LC-MS/MS analysis

The protein digests were analyzed in triplicate on an Accela-LTQ-Velos, using a 85 min data dependent LC-MS/MS run, 0-80 min 5-40% B, 80-82 min 40-60% B, 82-83 min 60% B, 83-85 min 5% B (Buffer A 0.1% formic acid in water, buffer B 0.1% formic acid in acetonitrile, both UHPLC grade, Biosolve, Valkenswaard, The Netherlands). Peptide separation was achieved by 25 μl injection on a C18 column (Zorbax SB-C18 2.1x50 mm, Agilent, Santa Clara, CA, USA) using a guard column (Poroshell 300 SB-C3 2.1x12.5 mm, Agilent, Santa Clara, CA, USA) at 50°C and a flow rate of 0.4 ml min^{-1}. The data dependent MS method consisted of an enhanced MS scan 300-2000 m/z and MS/MS on the top 10 peaks.

Data analysis

The peptide datasets were searched against the *A. niger* database, which was manually modified to contain the sequences of trypsin and BSA, using the Sorcerer 2 Sequest search engine (SageN, San Diego, CA, USA). The search opted for carbamidomethylation (C), oxidation (M) and deamidation (NQ) as variable modifications. The Sequest results were processed using the APEX program (Lu *et al.*, 2007) according to the author's description in order to obtain estimates of the protein quantities. Proteins identified with protein probability > 0.9 were considered as significant.

Microarray data accession number

Microarray data for the post-exponential time points have been made available at the GEO database (Barrett *et al.*, 2011) (http://www.ncbi.nlm.nih.gov/geo/) under accession number GSE39559. Microarray data from the exponential growth phase were previously made available at the GEO database under accession number GSE21752.

Authors contributions

BMN performed batch cultivations, protease activity measurements, microscopic and Northern analysis. BMN developed and implemented algorithms for image and GO analysis, conducted transcriptomic data analysis and wrote the manuscript. MA did LC MS/MS analysis.

AFJR, VM and TRJ were involved in writing the manuscript. All authors read and approved the final version of the manuscript.

Acknowledgements

This work was supported by grants of the SenterNovem IOP Genomics project (IGE07008). Part of this work was carried out within the research programme of the Kluyver Centre for Genomics of Industrial Fermentation, which is part of the Netherlands Genomics Initiative/Netherlands Organization for Scientific Research. We thank Maurien Olsthoorn and Yin Qing-Yuan from DSM for scientific advice and Andre Vente from DSM for technical assistance. Peter Punt from TNO kindly provided us with the N,N-dimethylated BSA substrate for measurements of proteolytic activities.

Additional Files

Additional file 1 --- Expression data
Genome-wide transcript profiles, fold changes and FDR q-values

Additional file 2 --- GO enrichment
GO enrichment analysis of genes up-/downregulated at day 1, 3 and 6

Additional file 3 --- Pfam enrichment
Pfam domain enrichment analysis of genes up-/downregulated at day 1, 3 and 6

Additional file 4 --- KEGG pathway enrichment
KEGG pathway enrichment analysis of genes up-/downregulated at day 1, 3 and 6

Additional file 5 --- Expression data fumonisin cluster
Transcript profiles, fold changes and FDR q-values for the fumonisin cluster

Additional file 6 --- Expression data PCD genes
Transcript profiles, fold changes and FDR q-values for putative PCD associated genes

Additional file 7 --- Secretome data
Estimated protein abundances in culture filtrates at day 1, 3 and 6

Chapter 5

Autophagy promotes survival in aging submerged cultures of the filamentous fungus Aspergillus niger

Benjamin M. Nitsche[1,2,§], Anne-Marie van Welzen[1,3,§], Gerda Lamers[1,3], Vera Meyer[2,3], Arthur F.J. Ram[1,3]

[1]Institute of Biology, Leiden University, Sylviusweg 72, 2333 BE Leiden, The Netherlands
[2]Institute of Biotechnology, Berlin University of Technology, Gustav-Meyer-Allee 25, 13355 Berlin, Germany
[3]Kluyver Centre for Genomics of Industrial Fermentation, PO Box 5057, 2600 GA, Delft, The Netherlands
[§]Both authors equally contributed to the manuscript

Abstract

Autophagy is a well conserved catabolic process constitutively active in eukaryotes that is involved in maintaining cellular homeostasis by targeting of cytoplasmic content and organelles to vacuoles. Autophagy is strongly induced by limitation of nutrients including carbon, nitrogen and oxygen and is clearly associated with cell death. We previously demonstrated that the accumulation of empty hyphal compartments and cryptic growth in carbon starved submerged batch cultures of *A. niger* were accompanied by a joint transcriptional induction of autophagy genes. In this study we examined the role of autophagy by deleting the *atg*1, *atg*8 and *atg*17 orthologs in *A. niger* and phenotypically analyzing the deletion strains in surface and submerged cultures. Our results indicate that *atg*1 and *atg*8 are essential for efficient autophagy, whereas deletion of *atg*17 has little to no effect on autophagy. Depending on the kind of oxidative stress confronted with, autophagy deficiency renders *A. niger* either more resistant or more sensitive to oxidative stress. Fluorescence microscopy showed that mitochondrial turnover upon carbon depletion in submerged cultures is severely blocked in autophagy impaired mutants. Furthermore, automated image analysis demonstrated that autophagy promotes survival in maintained carbon starved cultures of *A. niger*. Taken together, our results suggest that besides its function in nutrient recycling, autophagy plays important roles in physiological adaptation by organelle turnover and protection against cell death upon carbon depletion in submerged cultures.

Submitted to Applied and Molecular Biotechnology

Introduction

The filamentous fungus *Aspergillus niger* is an important and versatile cell factory commonly exploited for the industrial-scale production of a wide range of enzymes and organic acids. Although numerous studies have been conducted aiming at improving our knowledge of degradative cellular activities that determine product yields in *A. niger* including secretion of proteases and the unfolded protein response (Peberdy, 1994; MacKenzie *et al.*, 2005; Jørgensen *et al.*, 2009; Mattern *et al.*, 1992; Braaksma *et al.*, 2009), the possible role of autophagy in relation to protein production has yet not been studied in this industrially important fungus.

Autophagy is an intracellular degradation process functioning in the delivery of cytoplasmic proteins and organelles to the vacuole for macromolecule turnover and recycling (Bartoszewska *et al.*, 2011b; Inoue *et al.*, 2010). During autophagy, cellular components are sequestered and transported to lytic compartments in double-membrane vesicles, termed autophagosomes. The outer membrane of the autophagosome fuses with the vacuolar membrane, whereupon a single membrane vesicle is released into the lumen. Following lysis of the autophagic membrane and degradation of its content by hydrolytic enzymes, the breakdown products are transported back into the cytoplasm for reuse by the cell.

The autophagy pathway is highly conserved from yeast to higher eukaryotes and is tightly regulated (Bartoszewska *et al.*, 2011b). To date, more than 30 autophagy-related (*atg*) genes have been identified for *Saccharomyces cerevisiae* and other fungi (Kanki *et al.*, 2011; Xie *et al.*, 2007). One key player controlling the levels of autophagy is the autophagy-related protein ATG1, which is a serine/threonine protein kinase (Bartoszewska *et al.*, 2011b; Inoue *et al.*, 2010). Upon induction of autophagy, this kinase interacts with ATG17, ATG29 and ATG31 in an ATG13-dependent manner, forming the ATG1-kinase complex and initiating the formation of autophagosomes (Cheong *et al.*, 2008; Kabeya *et al.*, 2005). Deletion of the *atg*1 ortholog in *Podospora anserina* abolished autophagy and caused several developmental defects (Pinan-Lucarré *et al.*, 2005). Mutants displayed fewer aerial hyphae and did not form protoperithecia. Similar phenotypic traits were observed in *P. anserina* Δ*atg*8 mutants (Pinan-Lucarré *et al.*, 2005). ATG8 is coupled to the membrane lipid phosphatidylethanolamine (PE) forming an essential component of autophagic vesicle membranes (Bartoszewska *et al.*, 2011b; Inoue *et al.*, 2010). The *atg*8 gene has also been deleted in the filamentous fungus *Aspergillus oryzae*. The resulting mutants were defective in autophagy and formed no aerial hyphae and conidia (Kikuma *et al.*, 2006).

Autophagy plays an important role in cellular homeostasis by efficient removal of damaged organelles. For filamentous fungi it has been shown that endogenous recycling of cellular products by autophagy facilitates foraging of hyphae and fuels conidiation under nutrient starvation (Shoji *et al.*, 2006; Shoji *et al.*, 2011; Richie *et al.*, 2007). The hyphae that are formed

during this starvation-induced (cryptic) re-growth show fewer new branches and a significant decrease in hyphal diameter (Pollack *et al.*, 2008). In the older portions of the mycelium vacuolation increases dramatically following starvation, resulting in fragmentation and eventually dying of the hyphae.

We have shown previously that the morphological response to carbon starvation in submerged batch cultures of the filamentous fungus *A. niger*, including emergence of empty hyphal ghosts and thinner non-branching hyphae, is accompanied by the concerted induction of genes related to autophagy (Nitsche *et al.*, 2012a). To gain insights into the role of autophagy during submerged carbon starvation, *A. niger* autophagy mutants were generated by deletion of *atg*1, *atg*8 and *atg*17 gene orthologs. The mutants were phenotypically characterized during growth in surface and submerged cultures applying nutrient limitation and oxidative stress. Cytological effects of autophagy deficiency were assessed by investigation of fluorescent reporter strains allowing the visualization of cytoplasm, vacuoles and mitochondria. Our results indicate that autophagy plays important roles in metabolic adaptation to carbon starvation during submerged growth and thereby promotes the survival of pre-starvation formed hyphae.

Material and Methods

Strains, media and molecular techniques

Aspergillus strains used (Table 5.1) were grown at 30°C on solidified (20 $g \cdot l^{-1}$ agar) minimal medium (MM) (Alic *et al.*, 1991) or complete medium (CM) containing 0.5% (w/v) yeast extract and 0.1% (w/v) casamino acids in addition to MM. The pH of synthetic medium for bioreactor cultivations was adjusted to 3 and contained per liter: 4.5 g NH_4Cl, 1.5 g KH_2PO_4, 0.5 g KCl, 0.5 g $MgSO_4 \cdot 7H_2O$ and 1 ml trace metal solution (modified from Vishniac *et al.* (1957)). After autoclavation the synthetic media was supplemented with filter-sterilized 0.003% (w/v) yeast extract and 0.8% (w/v) glucose. Cloning was performed according to the methods described by Sambrook *et al.* (2001) using *Escherichia coli* strain DH5α. Transformation of *A. niger* was performed as described by Meyer *et al.* (2010). Hygromycin resistant transformants were isolated from plates supplemented with 200 $\mu g\ ml^{-1}$ hygromycin and 50 $\mu g\ ml^{-1}$ caffeine. MM for sensitivity plate assays was solidified with 2% (w/v) agar and supplemented with H_2O_2 or menadione as indicated.

Table 5.1 — Strains used

Strain	Genotype	Source
A. niger		
N402	*cspA1*	Bos *et al.* (1988)
AB4.1	$pyrG^{-}$	(Hartingsveldt *et al.*, 1987)
BN30.2	N402, $\Delta atg1$::hyg^{R}	this study
BN29.3	N402, $\Delta atg8$::hyg^{R}	this study
BN32.2	N402, $\Delta atg17$::hyg^{R}	this study
BN38.9	AB4.1, P*gpdA*::*N-citA*::*gfp*, $pyrG^{+}$	this study
BN39.2	BN38.9, $\Delta atg1$::hyg^{R}	this study
BN40.8	BN38.9, $\Delta atg8$::hyg^{R}	this study
AW20.10	BN38.9, $\Delta atg17$::hyg^{R}	this study
30.2 II	BN30.2, P*gpdA*::*gfp*, phl^{R}	this study
29.3 I	BN29.3, P*gpdA*::*gfp*, phl^{R}	this study
32.2 I	BN32.2, P*gpdA*::*gfp*, phl^{R}	this study
AR19#1	AB4.1, P*gpdA*::*gfp*, $pyrG^{+}$	Vinck *et al.* (2005)
A. nidulans		
SRS29	*pyrG*89, *pyroA*4, P*gpdA*::*NcitA*::*gfp*	Suelmann *et al.* (2000)

Construction of strains

The vector for constitutive expression of mitochondrially targeted GFP was constructed as follows. A 1.1 kb *NcitA*::*gfp* fragment was PCR amplified from genomic DNA of the *A. nidulans* strain SRS29 (Suelmann *et al.*, 2000), blunt-end ligated into pJET1.2 (Fermentas) and sequenced. Subsequently, the fragment was excised using *Bgl*II and *BamH*I and ligated into the 3.5 kb *Bgl*II-*BamH*I backbone of pAN52-1N (GenBank: Z32697.1). Next, a 2.2 kb *Bgl*II-*Nco*I *PgdpA* fragment from pAN52-1N was inserted into the *Bgl*II-*Nco*I opened intermediate construct. Finally, a 3.9 kb *Xba*I *pyrG** fragment was isolated from pAB94 (Gorcom *et al.*, 1988) and inserted at the *Xba*I site to give the final construct: *PgpdA-NcitA*::*gfp-TtrpC-pyrG**, which was transformed to *A. niger* strain AB4.1 (Hartingsveldt *et al.*, 1987). Single copy integration at the *pyrG* locus was confirmed by Southern analysis according to the method described by Meyer *et al.* (2010) (data not shown). The strain was named BN38.9.

Constructs for gene replacements with the hygromycin resistance cassette were generated as follows. Approximately 1 kb flanking regions of the *atg*1 (An04g03950), *atg*8 (An07g10020) and *atg*17 (An02g04820) open reading frames were PCR amplified from genomic DNA of the N402 wild-type strain using primer pairs according to Table 5.2, blunt-end ligated into pJET1.2 (Fermentas) and sequenced. Flanks were isolated from the pJET1.2 vectors using enzymes cutting at the outermost restriction sites (Table 5.2) and three-way ligated into a *Not*I-*Kpn*I opened pBluescript II SK(+) (Fermentas). For finalizing the *atg*1 and *atg*17 deletion constructs, the hygromycin resistance cassette was isolated as *Nhe*I-*Xba*I fragement and ligated between the flanking regions within the intermediate pBluescript constructs. For insertion of the hygromycin resistance cassette between the *atg*8 flanks, *Xho*I and *Xba*I were used. Linearized *atg*1, *atg*8 and *atg*17 deletion cassettes were transformed to *A. niger* strain N402 and homologous integration was confirmed by Southern analysis (data not shown) giv-

Table 5.2 – Primers used

Primer pairs (sequence 5' to 3' oriented)	Restriction site	Target
f: ataagaatgcggccgcATTAGTGAGTCGGTTGATGCCATG	*Not*I	5' flank *atg*1 (An04g03950)
r: ctagctagcttaatcctagtctagaGAGCGAAAGACAGGTCGGGA	*Nhe*I, *Xba*I	
f: ctagctagcCAGGCAACTGCATTCCAAGCTCG	*Nhe*I	3' flank *atg*1 (An04g03950)
r: cggggtaccGAATGACAAGCTACGGGTGAAAGA	*Kpn*I	
f: ataagaatgcggccgcGCCAGTAGTGGGTAGGGATTTGG	*Not*I	5' flank *atg*8 (An07g10020)
r: ccgctcgagttaatcctagtctagaGATAAGTAGATGAGGGCGGCTAG	*Xho*I, *Xba*I	
f: ccgctcgagGCGCTGGTCGATCTCCTCGTTTC	*Xho*I	3' flank *atg*8 (An07g10020)
r: cggggtaccGTGCAATCCAGGACCTGGACACAAA	*Kpn*I	
f: ataagaatgcggccgcGTGCTGCCAGTCTCGATTGG	*Not*I	5' flank *atg*17 (An02g04820)
r: ctagctagcttaatcctagtctagaGTCGGCGTAATTGGCGCTGA	*Nhe*I, *Xba*I	
f: ctagctagcTGCTCTGGTATTTCAGAGAGCTCG	*Nhe*I	3' flank *atg*17 (An02g04820)
r: cggggtaccGGTGATAATTGGGCTACTATGGGA	*Kpn*I	
f: ggaagatctcttggtttggtccATGGCTTCCACCTTGAGACTGG	*Bgl*II, *Nco*I	*NcitA* strain SRS29
r: cgcggatccccccaagtctaagcggccgcttacTTGTACAGCTCGTCCATGCCG	*BamH*I, *Not*I	*gfp* strain SRS29

f: forward strand; r: reverse strand; restriction sites are underlined

ing the stains BN30.2, BN29.3 and BN32.2, respectively (Table 5.1). For constitutive expression of cytosolically targeted GFP in atg mutants, the vector pGPDGFP (Lagopodi *et al.*, 2002) was co-transformed with pAN8.1 (Mattern *et al.*, 1988) to *A. niger* strains BN30.2, BN29.3 and BN32.2 (Table 5.1). Positive transformants were isolated by screening for cytosolic fluorescence and named 30.2 II, 29.3 I and 32.2 I, respectively (Table 5.1). Deletion of *atg*1, *atg*8 and *atg*17 in the strain expressing the mitochondria-targeted GFP was performed by transforming linearized *atg*1, *atg*8 and *atg*17 deletion constructs to *A. niger* strain BN38.9. Homologous integration of the constructs at their respective loci was confirmed by Southern analysis (data not shown) and the resulting strains were named BN39.2, BN40.8 and AW20.10, respectively (Table 5.1).

Bioreactor cultivation and sampling

Bioreactor cultivations were performed as previously described by Jørgensen *et al.* (2010). Briefly, autoclaved 6.6 L bioreactor vessels (BioFlo3000, New Brunswick Scientific) holding 5 L sterile synthetic medium were inoculated with $5 \cdot 10^9$ conidia. During cultivation, the temperature was set to 30°C and pH 3 was maintained by addition of titrants (2 M NaOH, 1 M HCl). The supply of sterile air was set to 1 L $\cdot$ min^{-1}. To avoid loss of hydrophobic spores through the exhaust gas, the stirrer speed was set to 250 rpm and air was supplied via the head space during the first six hours of cultivation. After this initial germination phase, the stirrer speed was increased to 750 rpm, air was supplied via the sparger and 0.01% (v/v) polypropylene glycol (PPG) P2000 was added to prevent foaming. O_2 and CO_2 partial pressures of the exhaust gas were analyzed with a Xentra 4100C analyzer (Servomex BV, Netherlands). Dissolved oxygen tension (DOT) and pH were measured electrochemically with autoclavable sensors (Mettler

Toledo). At regular intervals, samples were taken from the cultures. Aliquots for microscopic analysis were either directly analyzed (fluorescence microscopy) or quickly frozen in liquid nitrogen (automated image analysis), the remainder of the samples was vacuum filtrated using glass microfiber filters (Whatmann). Retained biomass and filtrates were directly frozen in liquid nitrogen and stored at -80°C. Biomass concentrations were gravimetrically determined from freeze dried mycelium of a known mass of culture broth.

Microscopic and image analysis

For the analysis of hyphal diameters, microscopic samples were slowly defrosted on ice and subsequently fixed and stained in a single step by mixing them at a 1:1 ratio with Lactophenolblue solution (Fluka). Per sample, a minimum of 40 micrographs were taken using a 40x objective and an ICC50 camera (Leica). The microscope and camera settings were optimized to obtain micrographs with strong contrast. To measure hyphal diameters in an automated manner, a previously developed and described macro (Nitsche *et al.*, 2012a) for the open source program ImageJ (Abràmoff *et al.*, 2004) was used. DIC and fluorescence images were taken with a Zeiss axioplan 2 imaging microscope equipped with DIC optics. For the GFP settings, an epi-fluorescence filter cubeXF 100-2 with excitation 450-500 nm and emission 510-560 nm was used. Confocal images were obtained using a Zeiss Observer microscope coupled to a LSM 5 exciter. Excitation in the GFP settings was achieved with a 488 Argon laser line with emission 505-550 nm.

Results

Autophagy-related genes *atg*1 and *atg*8 but not *atg*17 are essential for efficient autophagy in *A. niger*

To study the phenotypes of autophagy deficient *A. niger* mutants in surface and submerged cultures, we identified and deleted orthologs of three genes known to encode essential components of the autophagic machinery in *S. cerevisae* (Tsukada *et al.*, 1993; Matsuura *et al.*, 1997; Cheong *et al.*, 2005; Kabeya *et al.*, 2005). Two of the target genes encode proteins that are part of the regulatory ATG1 kinase complex, namely the kinase ATG1 itself and the scaffold protein ATG17. The third target gene encodes the ubiquitin-like protein ATG8, which is a structural component required for the formation of autophagosomal membranes. We identified the following ortholog pairs *Scatg*1/An04g03950 ($E = 4e^{-151}$), *Scatg*8/An07g10020 ($E = 4e^{-67}$) and *Scatg*17/An02g04820 ($E = 2e^{-12}$) by reciprocal best BlastP hit analysis and subsequently deleted these target genes in the *A. niger* laboratory wild-type strain N402 by replacement with a

hygromycin resistance cassette. Gene deletions were confirmed by Southern analysis (data not shown).

Previous studies in *A. oryzae* (Kikuma *et al.*, 2006) and *Penicillium chrysogenum* (Bartoszewska *et al.*, 2011a) demonstrated localization of cytosolic fluorescent protein to vacuoles under starvation conditions in wild-type strains, whereas mutants impaired in autophagy did not show vacuolar localization of cytosolic GFP. Therefore we generated Δ*atg*1, Δ*atg*8 and Δ*atg*17 strains in a background with constitutive expression of cytosolic GFP to assess whether deletion of the respective *atg* genes impairs autophagy in *A. niger*. Vacuolar localization of cytosolic GFP was observed for the wild-type strain during nutrient limitation, while both Δ*atg*1 and Δ*atg*8 mutants did not show GFP fluorescence inside vacuoles, indicating deficient autophagy. Interestingly, deletion of *atg17* did not affect vacuolar localization of cytosolic GFP (see Figure 5.1). These results suggest that both *atg*1 and *atg*8 but not *atg*17 are essential for efficient autophagy in *A. niger*.

In order to monitor autophagy dependent turnover of mitochondria (mitophagy) (Kanki *et al.*, 2011) induced by carbon starvation, we generated wild-type and atg mutant strains with constitutive expression of mitochondrially targeted GFP. We used the same approach to vi-

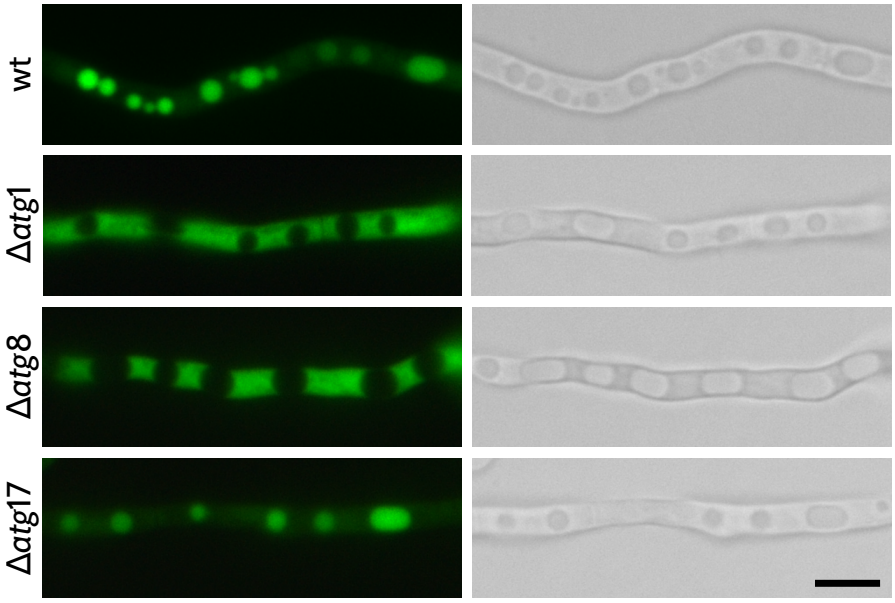

Figure 5.1 – Localization of cytosolically expressed GFP during carbon starvation
The strains were pregrown for 8 hours at 30°C on coverslips in Petri dishes with liquid MM. Subsequently coverslips with adherent hyphae were washed and transferred to MM without carbon source. Micrographs were taken 40 hours after transfer. Wild-type and Δ*atg17* mutant showed vacuolar localization of GFP, whereas both Δ*atg1* and Δ*atg*8 mutants showed cytosolic localization. Scale bar: 5 μm

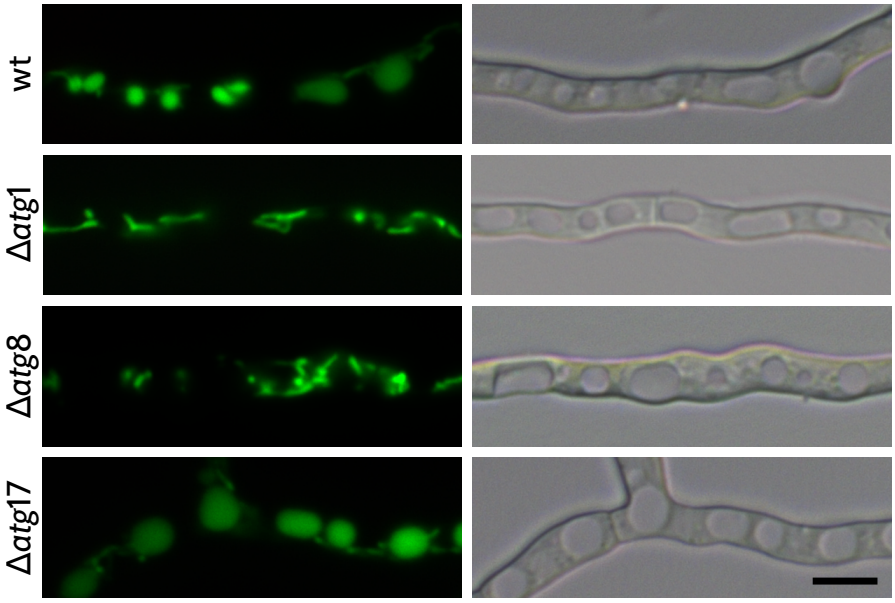

Figure 5.2 – Localization of mitochondrially expressed GFP during carbon starvation
The strains were grown as described in Figure 5.1. Wild-type and Δ*atg*17 mutant showed vacuolar localization of GFP, whereas both Δ*atg*1 and Δ*atg*8 mutants showed mitochondrial localization. Under nutrient-rich conditions, all strains showed fluorescent patterns resembling tubular mitochondrial networks as previously shown by Suelmann *et al.* (2000). Scale bar: 5 μm

sualize mitochondria as described by Suelmann *et al.* (2000), who showed that N-terminal fusion of the mitochondrial targeting sequence from the citrate synthase A to a fluorescent protein efficiently labeled mitochondria. For wild-type and mutant reporter strains, exponentially growing hyphae showed fluorescent tubular structures resembling those described by Suelmann *et al.* (Figure 5.6). During carbon starvation however, microscopic analysis of those mitochondrial reporter strains indicated considerable differences in mitochondrial turnover between wild-type and atg mutants (Figure 5.2). The differences correspond to those observed for the localization of cytosolic GFP (Figure 5.1). The localization of GFP remained mitochondrial in both Δ*atg*1 and Δ*atg*8 mutant strains, whereas wild-type and Δ*atg*17 strains showed vacuolar localization of mitochondrially expressed GFP. Thus suggesting that mitochondrial turnover induced by carbon starvation is mediated by autophagy, which is severely impaired in the Δ*atg*1 and Δ*atg*8 mutants.

Phenotypes of Δ*atg*1, Δ*atg*8 and Δ*atg*17 strains in surface cultures

Depending on which species of filamentous fungi is studied and which *atg* gene is under investigation, defective autophagy results in complete or severe impairment of conidiation during surface growth (Richie *et al.*, 2007; Bartoszewska *et al.*, 2011a; Kikuma *et al.*, 2006). To test whether conidiation in *A. niger* atg mutants is affected as well, we harvested and counted conidia from colonies grown for 7 days on solid MM. Although colonies of the Δ*atg*1 and Δ*atg*8 mutants developed conidiophores and turned dark, the colonies showed slightly attenuated pigmentation (see Figure 5.3A) indicating reduced spore densities and/or differences in melanization of spores. Indeed, the number of spores recovered from the Δ*atg*1 and Δ*atg*8 colonies were significantly reduced (see Figure 5.3C). With a decrease of 70%, conidiation was most affected in the Δ*atg*8 mutant. Interestingly, although the Δ*atg*17 mutant showed vacuolar localization of cytosolic (Figure 5.1) and mitochondrial (Figure 5.2) GFP under carbon starvation and its colony appearance was indistinguishable from that of the wild-type, the number of recovered conidia was reduced by 20%, thus suggesting an intermediate phenotype of the Δ*atg*17 mutant. In agreement to studies in *A. oryzae* (Kikuma *et al.*, 2006) the Δ*atg*8 strain showed slower radial growth on synthetic medium (see Figure 5.3B). However, even considering the differences in colony sizes, conidiation was most reduced for the Δ*atg*8 mutant as shown by the spore densities (see Figure 5.3C). Compared to the *A. oryzae* Δ*atg*8 mutant, which was reported not to develop aerial hyphae and conidia (Kikuma *et al.*, 2006), the conidiation phenotype in *A. niger* is much less pronounced.

In filamentous fungi, autophagy has been suggested to contribute to nutrient recycling along the mycelial network promoting foraging of individual substrate exploring hyphae and conidial development (Richie *et al.*, 2007; Shoji *et al.*, 2006; Shoji *et al.*, 2011). We have investigated the phenotypes of the mutants during nitrogen and carbon limitation on solid MM (see Figure 5.4A). The Δ*atg*1 and Δ*atg*8 mutants were clearly more affected by nutrient limitation than the wild-type as shown by their strong conidiation phenotypes. Whereas the mutants were comparably affected by carbon limitation, the Δ*atg*8 mutant was more sensitive to nitrogen limitation than the Δ*atg*1 mutant. In accordance with results presented in Figures 5.1, 5.2 and 5.3A, the phenotype of the Δ*atg*17 mutant during nitrogen and carbon limitation is indistinguishable from that of the wild-type.

In addition to its role in nutrient recycling, numerous reports have shown that autophagy is closely associated with Programmed Cell Death (PCD) (Pinan-Lucarré *et al.*, 2005; Veneault-Fourrey *et al.*, 2006; Codogno *et al.*, 2005). Major triggers of PCD are reactive oxygen species (ROS) and the damage they can cause to lipids, carbohydrates, DNA and proteins. We were interested in oxidative stress related phenotypes of the autophagy mutants and performed sensitivity assays with H_2O_2 and the superoxide anion generator menadione (see Figure 5.4B-C)

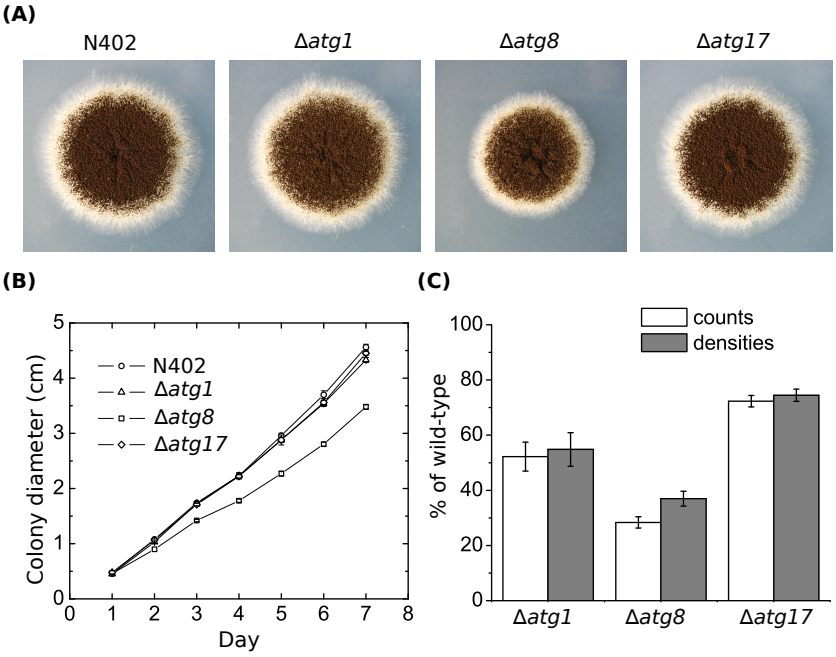

Figure 5.3 — Phenotypes of wild-type and atg mutants.
Strains were grown for seven days on solid MM at 30°C. (A) Colony appearance. (B) Colony diameters (n = 3). (C) Recovered conidia (n = 3).

which were shown to cause distinct oxidative stress responses in yeast and filamentous fungi (Thorpe *et al.*, 2004; Tucker *et al.*, 2004; Jamieson, 1992; Pócsi *et al.*, 2005). In comparison to the wild-type, the mutants displayed differential phenotypes in response to treatment with the two compounds. Interestingly, H_2O_2 and menadione had opposing effects. The mutants were more sensitive to H_2O_2, while their resistance to menadione was increased. The $\Delta atg17$ mutant displayed an intermediate phenotype, which was more comparable to that of the wild-type.

Taken together the phenotypic characterization suggests that autophagy is severely impaired in the $\Delta atg1$ and $\Delta atg8$ mutants. Contrary to this, the $\Delta atg17$ mutant showed little to no phenotypic differences when compared to the wild-type. The subsequent analysis of autophagy impairment during submerged cultivation was therefore restricted to the investigation of $\Delta atg1$ and $\Delta atg8$ mutants.

Phenotypes of Δ*atg*1 and Δ*atg*8 strains during submerged growth

We have previously demonstrated that the majority of the autophagy genes show joint induction after exponential growth in carbon-limited submerged batch cultures of *A. niger*. Concomitantly, old hyphae grown during the exponential phase underwent cell death resulting in an increased fraction of empty hyphal compartments and secondary (cryptic) growth of thin non-branching hyphae (Nitsche *et al.*, 2012a). Although it has been shown for filamentous fungi that autophagy plays an important role in nutrient recycling during surface growth (Richie *et al.*, 2007; Shoji *et al.*, 2006; Shoji *et al.*, 2011), its function in submerged cultures remains obscure. To gain insights into the role of autophagy during submerged carbon star-

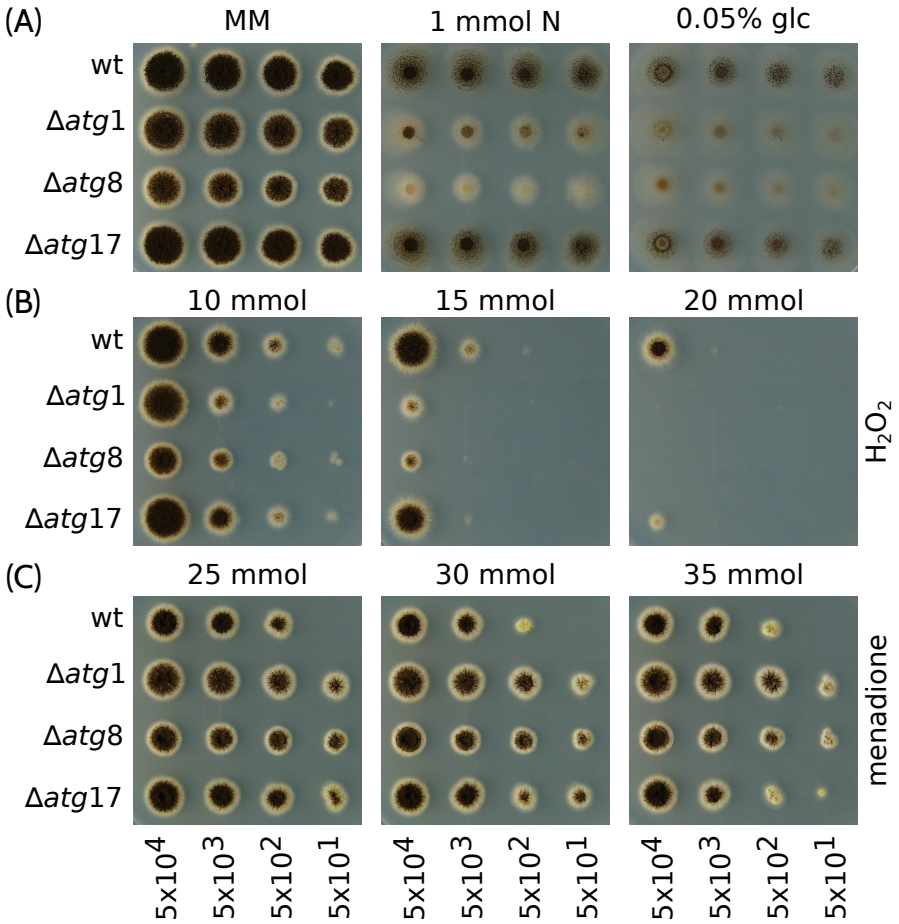

Figure 5.4 – Sensitivity assay of wild-type and atg mutants
10-fold dilutions ($5 \cdot 10^4$ - $5 \cdot 10^1$ conidia) were spotted on plates with (A) MM and MM with N (nitrate) or C (glucose) limitation, MM supplemented with (B) H_2O_2 or (C) menadione. Plates were incubated for 4 days at 30°C.

vation and to investigate how autophagy is related to the phenomena of cell death and secondary growth, we grew the $\Delta atg1$ and $\Delta atg8$ mutants in bioreactors and maintained the cultures starving up to six days after carbon depletion (Figure 5.5). Bioreactor cultivations were reproducible and monitoring of physiological parameters (DOT, off-gas and titrant addition) allowed synchronization of cultures. The described cultivation conditions prevented the formation of mycelial aggregates (pellets) and guaranteed a dispersed macromorphology during all cultivations. Interestingly, in contrast to the colony expansion rate on solid media (Figure 5.3A-B), the maximum specific growth rates for both mutants during exponential growth were affected to the same extend during submerged cultivation. Both mutants grew slower ($\mu_{\max} = 0.22\text{h}^{-1} \pm 0.005$) than the wild-type ($\mu_{\max} = 0.27\text{h}^{-1} \pm 0.021$). Considering the reproducibility of replicate cultures, the biomass profiles did not show any significant differences during the post-exponential phase (see Figure 5.5).

It was shown that autophagy is important for mitochondrial maintenance and degradation of excess mitochondria during the stationary phase of *S. cerevisiae* cultures, which is of outermost importance because mitochondria play a key role in metabolism and cell death

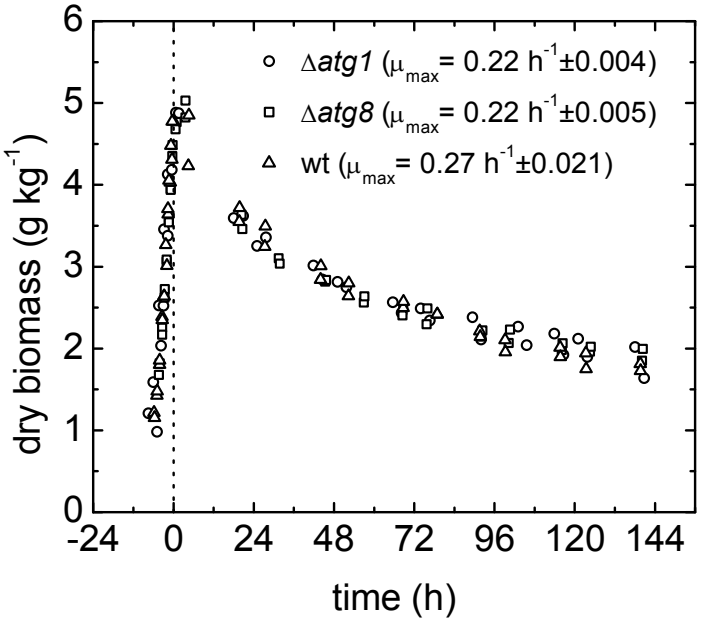

Figure 5.5 – Growth curves of carbon-limited submerged batch cultures
Growth curves for carbon-limited batch cultures of wild-type, $\Delta atg1$ and $\Delta atg8$ mutants. The time point of carbon depletion was set to 0 hours and used to synchronize replicate cultures.

signaling (Zhang *et al.*, 2007). We thus examined the morphology and degradation of mitochondria in *A. niger* wild-type, Δ*atg*1 and Δ*atg*8 strains during carbon starvation in bioreactor batch cultures by fluorescence microscopy of strains which constitutively express mitochondrially targeted GFP. Analysis of hyphae from the exponential growth phase showed fluorescent tubular structures resembling those described by Suelmann *et al.* (2000) and no difference in mitochondrial morphology was observed between the wild-type and the two mutants (Figure 5.6A). However, clear differences became apparent upon depletion of the carbon source. The mitochondrially targeted GFP was located inside the vacuoles in the wild-type background, whereas no vacuolar GFP signal was detected for both Δ*atg*1 and Δ*atg*8 mutants (Figure 5.6B-C). The density of mitochondrial structures decreased in the wild-type hyphae but accumulated in the space between vacuoles in the mutants. There were also considerable differences in the mitochondrial morphology. Remaining mitochondrial structures were largely tubular in the wild-type, while they appeared as fragmented and punctuated structures in the mutants.

In flow chamber experiments with *A. oryzae* Pollack *et al.* (2008) showed that carbon depletion induces outgrowth of hyphae with strongly reduced diameters. We previously observed a similar morphological response during carbon starvation in submerged cultures of *A. niger* (Nitsche *et al.*, 2012a). Hyphal population dynamics for the cytoplasm filled mycelial fraction demonstrated a gradual transition from thick (old) to thin (young) hyphae during the post-exponential phase which reflects cell death resulting in the emergence of empty thick compartments fueling secondary regrowth in the form of elongating thin hyphae. To examine whether autophagy affects this transition dynamic, we analyzed microscopic pictures of wild-type and both Δ*atg*1 and Δ*atg*8 mutant cultures. During exponential growth (day 0) all three strains displayed single populations of thick hype with mean diameters of approximately 2.2 μm. After carbon depletion, populations of thin hyphae with mean diameters of around 1 μm emerged. While this transition was gradual for the wild-type, it was clearly accelerated for the Δ*atg*1 and Δ*atg*8 mutants suggesting enhanced cell death rates for the older (thick) hyphae (Figure 5.7).

Discussion

To our knowledge, this is the first study of autophagy in the industrially important filamentous fungus *A. niger*. Improving our understanding of this catabolic pathway and its role during submerged cultivation is of great interest because autophagy has been shown to be involved in endogenous recycling and the regulation of cell death, both of which can have a direct impact on the yield of bioprocesses (Bartoszewska *et al.*, 2011b; Zustiak *et al.*, 2008). For different fil-

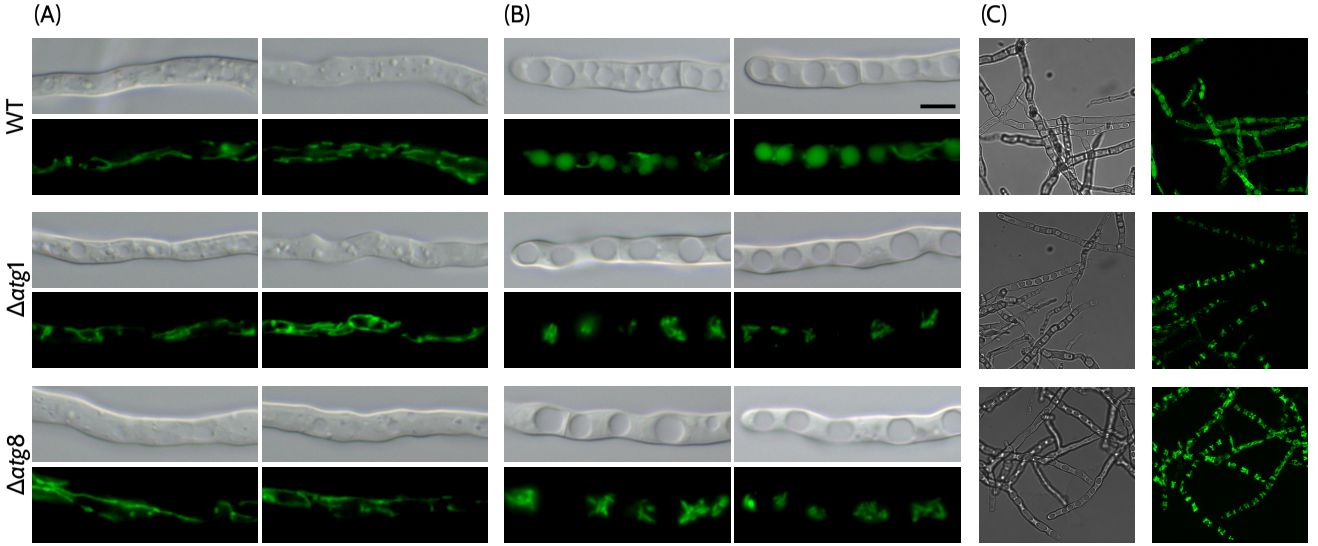

Figure 5.6 – Localization of mitochondrially expressed GFP during batch cultivation
Constitutive expression of mitochondrially targeted GFP in wild-type, Δ*atg*1 and Δ*atg*8 mutants during carbon-limited batch cultures. Differential interference contrast and fluorescence microscopy of hyphae from the exponential growth phase (A) and 7 hours post-carbon depletion (B). Confocal laser scanning microscopy of mycelial biomass at 14 hours post-carbon depletion (C). Scale bar: 5 μm.

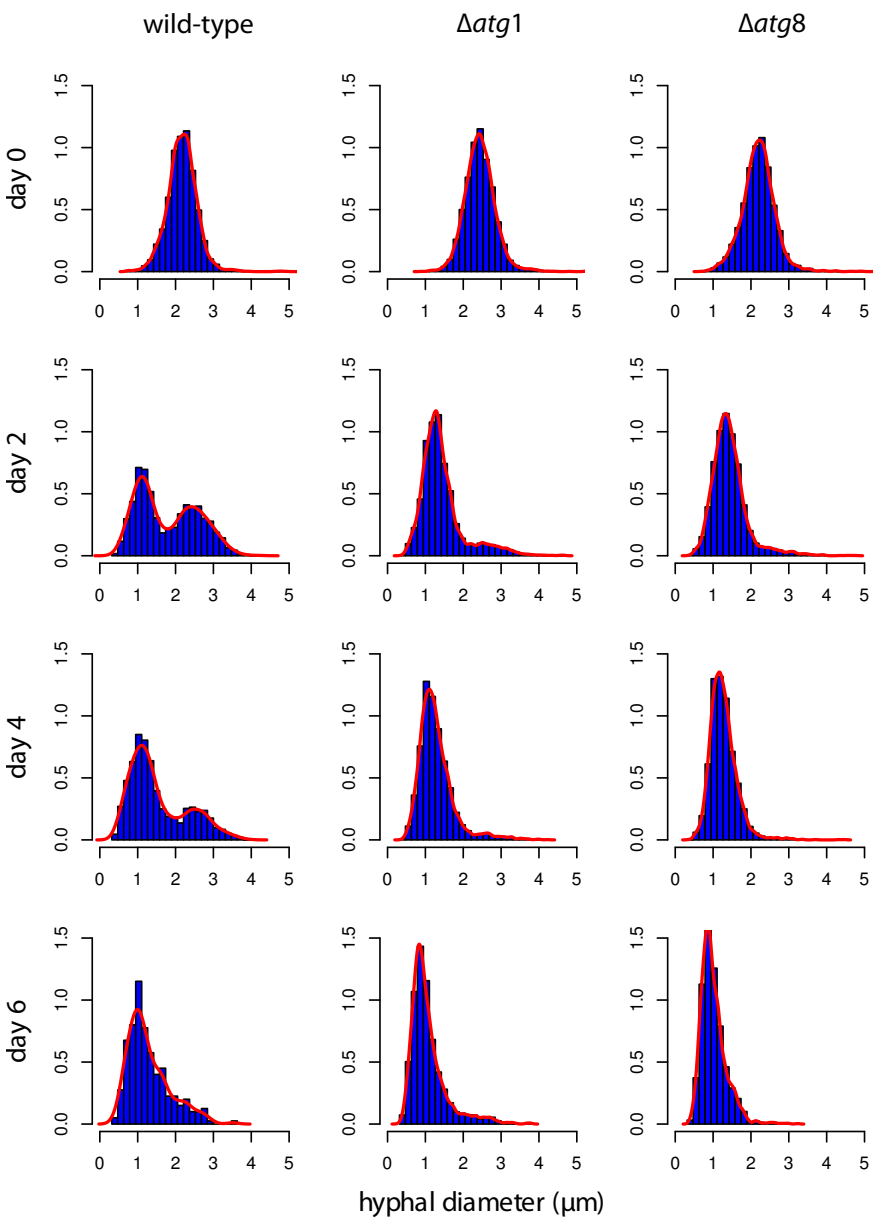

Figure 5.7 — Hyphal diameter populations
Population dynamics of hyphal diameters for wild-type, Δ*atg*1 and Δ*atg*8 mutants. ≥ 40 micrographs of dispersed hyphae were analyzed per strain and time point as described in the materials and methods sections.

amentous fungi, several studies analyzed phenomena of carbon starved submerged cultures (White *et al.*, 2002; Emri *et al.*, 2004; Emri *et al.*, 2005b; Emri *et al.*, 2006). The generic term that has emerged in this context is autolysis. It has been generally used to describe hallmarks of aging cultures including biomass decline, increasing extracellular ammonia concentration, hyphal fragmentation and increasing extracellular hydrolase activities (White *et al.*, 2002). Considerable effort has been made to analyze extracellular hydrolase activities (McNeil *et al.*, 1998; McIntyre *et al.*, 2000; Emri *et al.*, 2005b) as well as developmental mutants differentially affected in aging carbon starved cultures (Emri *et al.*, 2005b). However, the role of autophagy in those cultures has not attained much attention yet. In a recent systems level analysis of the *A. niger* transcriptome during submerged carbon starvation, we identified autophagy as a predominantly induced key process (Nitsche *et al.*, 2012a). In this present study, we thus aimed at elucidating whether autophagy protects from or promotes loss of hyphal integrity, which was mainly observed by the formation of empty hyphal ghosts.

In order to study autophagy deficiency in *A. niger*, we deleted two genes encoding components of the regulatory ATG1 kinase complex, namely the genes highly homologous to the kinase ATG1 itself and the scaffold protein ATG17. In addition, we deleted the *atg*8 gene encoding a membrane protein required for autophagosome formation and extension. In agreement to studies in yeast and other filamentous fungi (Bartoszewska *et al.*, 2011b), our results demonstrate that the deletion of either *atg*1 or *atg*8 is sufficient to severely impair autophagy in *A. niger*. However, conflicting with results obtained in *S. cerevisiae* (Cheong *et al.*, 2005; Kabeya *et al.*, 2005), where the absence of ATG17 severely reduces the level of autophagy, we were not able to demonstrate that autophagy is considerably impaired in the *A. niger* Δ*atg*17 mutant. Similarly, the deletion of *atg*13 in *A. oryzae* encoding another subunit of the ATG1 kinase complex was reported to only gently affect autophagy, whereas deletion of its counterpart in *S. cerevisiae* clearly impaired it (Kikuma *et al.*, 2011). The authors suggested that ATG13 acts as an amplifier resulting in higher autophagic activities in *A. oryzae*. Probably, ATG17 has a similar enhancing role during autophagy induction in *A. niger* leading to the intermediate phenotypes described in this study.

Endogenous recycling of nutrients by autophagy has been supposed to be an important mechanism for nutrient trafficking along the mycelial network promoting foraging of substrate exploring filaments and the formation of aerial hyphae bearing conidiophores (Shoji *et al.*, 2006; Shoji *et al.*, 2011; Richie *et al.*, 2007). Similar to studies in other filamentous fungi (Richie *et al.*, 2007; Bartoszewska *et al.*, 2011a; Kikuma *et al.*, 2006), impairment of autophagy in *A. niger* considerably reduced conidiation (Figure 5.3), a phenotype, which was much enhanced by more severe carbon and nitrogen starvation conditions (Figure 5.4A).

In addition to its role in nutrient recycling, autophagy has been shown to be associated with PCD, which is classically categorized into three types, namely apoptotic (type I), autophagic (type II) and necrotic (type III) cell death. Although autophagy is also referred to as type II programmed cell death, it is not explicitly causative to cell death. Depending on the organism, cell type and stressor, autophagy has been shown to promote both cell death and survival. In filamentous fungi, it has for example been demonstrated to protect against cell death during the heterokaryon incompatibility reaction in *Podospora anserina* (Pinan-Lucarré *et al.*, 2005) or during carbon starvation in *Ustilago maydes* (Nadal *et al.*, 2010). Contrary to this, autophagy induced cell death is for example required for rice plant infection by *Magnaporthe grisea* (Veneault-Fourrey *et al.*, 2006). Loss of cellular integrity and subsequent death induced by damage of organelles, macromolecules and membranes through reactive oxygen species is a major threat for aerobic organisms. Well described enzymatic and non-enzymatic defense systems have evolved that detoxify ROS (Bai *et al.*, 2003). Autophagy is one of the major pathways for turnover of redundant or damaged organelles and proteins. The hypersensitivity of autophagy mutants to H_2O_2 thus fits our expectation and could be explained by an impaired capability of the mutants to sequester and degrade proteins and organelles damaged by H_2O_2. Increased resistance to menadione however, was unexpected but might be related to an adaptive stress response in autophagy deficient mutants. In *S. cerevisiae* it was for example shown that disruption of essential ATG genes results in increased oxidative stress and superoxide dismutase activities (Zhang *et al.*, 2007). Adaptive responses to oxidative stress induced by sublethal concentrations of exogenous oxidants have been demonstrated to protect yeast cells against higher lethal concentrations (Jamieson, 1992; Fernandes *et al.*, 2007). However, future studies will be required to elucidate the adaptive mechanism leading to menadione resistance in autophagy deficient mutants.

Hyphal population dynamics showed that the transition from old (thick) to young (thin) hyphae in response to carbon starvation during submerged cultivation was accelerated for both $\Delta atg1$ and $\Delta atg8$ mutants when compared to the wild-type (Figure 5.7). These results suggest that autophagy delays cell death of old hyphae under carbon starvation. Similar to a study with yeast (Suzuki *et al.*, 2011), fluorescence microscopy of wild-type, $\Delta atg1$ and $\Delta atg8$ reporter strains with GFP-labeled mitochondria revealed that degradation of mitochondria in response to carbon depletion is impaired in autophagy deficient mutants. The degradation of excess mitochondria during the stationary phase constitutes a physiological adaptation to the reduced energy requirement of the cells (Kanki *et al.*, 2011). It is tempting to speculate that autophagy impairment leads to increasing cellular ROS levels caused by the accumulation of excessive and damaged mitochondria, subsequently leading to loss of cellular integrity and finally the emergence of empty hyphal compartments. Taken together, the results indicate that the in-

duction of autophagy is not only required for endogenous recycling but also for physiological adaptation to carbon starvation by turnover of excessive organelles.

Acknowledgments

This work was supported by grants of the SenterNovem IOP Genomics project (IGE07008). Part of this project was carried out within the research programme of the Kluyver Centre for Genomics of Industrial Fermentation, which is part of the Netherlands Genomics Initiative / Netherlands Organization for Scientific Research. This work was (co)financed by the Netherlands Consortium for Systems Biology (NCSB) which is part of the Netherlands Genomics Initiative / Netherlands Organisation for Scientific Research. We thank Reinhard Fischer from the Karlsruhe Institute of Technology in Germany for providing us with the strain SRS29. We thank Crescel Martis and Leonie Schmerfeld for technical assistance.

Summary and discussion

In industrial biotechnology, *Aspergillus niger* is well known as a versatile cell factory with a naturally high secretion capacity (Pel *et al.*, 2007) which is commonly exploited for large scale production of a wide range of organic acids, enzymes and proteins. To optimize production processes, several cellular activities that determine product yields have been intensively studied during the last decades, including, for example, the unfolded protein response and protease secretion (Peberdy, 1994; MacKenzie *et al.*, 2005; Jørgensen *et al.*, 2009; Mattern *et al.*, 1992; Braaksma *et al.*, 2009). Many fungal bioprocesses are operated as fed-batch cultures (Zustiak *et al.*, 2008) preventing catabolite repression by ensuring a nutrient-limited growth regime. Nutrient limitation, however, induces diverse catabolic processes that can negatively affect product yields for example by product hydrolysis or disintegration of hyphal integrity resulting in decreasing active biomass fractions.

As nutrient limitation can be life-threatening, complex responses have evolved that ultimately lead to fungal self-propagation. Endogenous recycling and extracellular hydrolysis are thought to liberate building blocks and energy to fuel asexual development during carbon starvation. Despite the negative effect on product yields, there has been no previous comprehensive investigation of carbon starvation in the industrially important filamentous fungus *A. niger*. We therefore followed an approach to comprehensively study carbon starvation in *A. niger* during submerged cultivation, which is described in this thesis and is discussed as follows: (I) Establishment of computational resources for omics data analysis and interpretation in chapters 2 and 3; (II) Cultivation of *A. niger*, data generation, analysis and interpretation in chapter 4; (III) Investigation of a candidate pathway with strong transcriptional induction during carbon starvation by molecular genetic approaches in chapter 5.

Genome-wide transcriptional analysis has great potential to provide system-level insights into cellular responses, but requires an unbiased, high-throughput statistical approach for data analysis, interpretation and eventually generation of hypothesis. The application of open source and open access computational tools is desirable at universities in particular, and can be considered beneficial as they are freely distributed and actively developed by leading experts from within the scientific community. However, they can be less intuitive and depend on a command-line-interface, as it is the case for R/Bioconductor (R-Team, 2008; Gentleman *et al.*, 2004) used in this thesis for transcriptome data analysis. Therefore, chapter 2 was intended as an introduction to transcriptome data analysis using R/Bioconductor, by providing a step-by-step tutorial analyzing two public transcriptome datasets of *A. niger* (Nitsche *et al.*, 2012b). Experience has shown that this approach is suited to bring biologists into contact with R/Bioconductor, even allowing them to analyze their own datasets.

Following the initial phase of data analysis, including the identification of differentially or co-expressed gene sets, omics data should be biologically interpreted to e.g. drive the generation of new hypotheses. A powerful, high-throughput and unbiased approach is enrichment analysis of functional annotations (B. H. J. v. d. Berg *et al.*, 2009). Amongst the most commonly used functional annotations for enrichment analysis is Gene Ontology (GO) annotation (Ashburner *et al.*, 2000). In chapter 3, this valuable resource for functional analysis of omics data was extended to the genus *Aspergillus* by mapping the *A. nidulans* GO annotation to all Aspergilli with published genome sequences and implementing the web application FetGOat (Fisher's exact test Gene Ontology annotation tool, http://www.broadinstitute.org/fetgoat/index.html) for GO enrichment analysis. Both the annotation and FetGOat were used in two case studies to re-analyze two public datasets, demonstrating their applicability, ease of use and potential to generate new hypotheses (Nitsche *et al.*, 2011).

Having set up the computational tools for omics data analysis, genome-wide transcriptional profiles of carbon starving submerged cultures of *A. niger* were established, analyzed and interpreted in chapter 4. The experimental setup involved submerged batch cultivation in carbon-limited minimal medium applying bioreactor technology which ensured high reproducibility, monitoring and control of physiology and macromorphology. The major morphological responses to carbon starvation were the emergence of empty hyphal compartments (hyphal ghosts), secondary (cryptic) growth of thin non-branching hyphae and subsequently formation of asexual developmental structures. These morphological hallmarks suggest that secondary growth and conidiation are fuelled by recycling of resources derived from emptying hyphal compartments. Importantly, microscopic analysis has shown no indication of hydrolytic weakening and fragmentation of fungal cell walls. Principally, resources from empty compartments could be thought to be directly recycled by neighboring compartments via an endogenous route or first leak into the culture broth where they are subsequently taken up by growing hyphae.

Transcriptomic data analysis showed that throughout the course of carbon starvation, approximately 50% of the transcripts were differentially expressed. The numbers of up- and downregulated genes were easy to compare. In order to identify major transcriptionally induced and repressed cellular processes, GO annotation enrichment analysis was applied for sets of up- and downregulated genes. The repressed processes were primarily related to transcription, translation and respiration which reflect the physiological adaptation to carbon starvation and energy deprivation. On the contrary, the major transcriptionally induced processes included catabolic and reproductive pathways. As such, autophagy and conidiation were most dominantly induced. Furthermore, analysis focusing on carbohydrases and proteases revealed strong transcriptional induction of several secreted and non-secreted hydrolases.

More than 30 autophagy-related genes have been identified to date in yeast and filamentous fungi (Kanki *et al.*, 2011; Xie *et al.*, 2007). For 23 of these genes, ortholog candidates were identified in *A. niger* and all except one were transcriptionally induced during carbon starvation. This concerted induction of the autophagy pathway gave rise to questions about the role of autophagy during carbon starvation. Does autophagy protect against the formation of empty hyphal compartments or does it promote these processes? Is autophagy required for effective elongation of thin hyphae during the secondary (cryptic) growth phase under carbon starvation or not? In looking for these answers, three genes (*atg*1, *atg*8 and *atg*17), that have been predicted to be essential for efficient autophagy in other orgnamisms (Tsukada *et al.*, 1993; Matsuura *et al.*, 1997; Cheong *et al.*, 2005; Kabeya *et al.*, 2005), were deleted in *A. niger* wild-type and fluorescent reporter strains. Phenotypic characterization of the mutant strains indicated that *atg*1 and *atg*8 are essential for efficient autophagy in *A. niger*, whereas deletion of *atg*17 had little to no effect. Analysis of the Δ*atg*1 and Δ*atg*8 mutant strains during submerged growth in carbon-limited batch cultures showed that the morphogenetic adaptation to carbon starvation, including the emergence of empty hyphal compartments and secondary growth of thinner non-branching hyphae, was accelerated when autophagy was impaired. Furthermore, we demonstrated that mitochondrial turnover in response to carbon depletion was severely impaired in both Δ*atg*1 and Δ*atg*8 mutants. This suggests that autophagy thus delays cell death during carbon starvation by organelle turnover which is important for physiological adaptation during carbon starvation. Further investigation will be required to elucidate the effect of impaired autophagy in *A. niger* on product yields. For example, it has been observed in *Penicillium chrysogenum* that the impairment of autophagy delays cell degeneration and results in enhanced production levels (Bartoszewska *et al.*, 2011a).

It has proved difficult to answer how hyphal ghosts are formed. Either hyphal compartments lyse meaning that their content leaks into the culture broth or they are actively evacuated by neighboring compartments which thus resembles endogenous recycling. Although secretome data indicated that there was no considerable accumulation of intracellular proteins in the culture broth during carbon starvation, immediate hydrolysis of leaked cytosolic proteins cannot be excluded. However, an accelerated emergence of empty compartments in the Δ*atg*1 and Δ*atg*8 mutants suggests that endogenous recycling by neighboring compartments does not occur via autophagic processes.

This study is the first systems level investigation of carbon starvation in the filamentous fungus *A. niger*. While we followed a single lead from the transcriptomic data analysis, there are many more processes remaining to be investigated and the dataset obtained forms a comprehensive framework for future investigations of the complex cellular responses.

Samenvatting en discussie

In de industriële biotechnologie staat *Aspergillus niger* bekend als een veelzijdige celfabriek met een van nature hoge secretiecapaciteit (Pel *et al.*, 2007), waarvan vaak gebruik wordt gemaakt voor de productie van een breed spectrum aan organische zuren, enzymen en proteïnen. Om de productie te optimaliseren, zijn in de laatste decennia verschillende cellulaire activiteiten die de productieopbrengsten kunnen bepalen, zoals de ongevouwen eiwit respons en secretie van proteases, intensief bestudeerd (Peberdy, 1994; MacKenzie *et al.*, 2005; Jørgensen *et al.*, 2009; Mattern *et al.*, 1992; Braaksma *et al.*, 2009). Voor veel bioprocessen met schimmels wordt gebruik gemaakt van fed-batch culturen (Zustiak *et al.*, 2008), waarmee catabolische repressie wordt voorkomen door de hoeveelheid voedingsstoffen tijdens het productieproces te beperken. Voedingsstoflimitatie zet echter diverse catabolische processen in gang die een negatieve invloed kunnen hebben op productopbrengsten door bijvoorbeeld hydrolyse van het product of afname van het aandeel actieve biomassa door verlies van de integriteit van hyfen.

Omdat voedingsstoflimitatie levensbedreigend kan zijn, zijn er complexe reacties geëvolueerd die uiteindelijk tot zelfvermeerdering van de schimmel leiden. Door endogene recycling en extracellulaire hydrolyse worden tijdens koolstofhongering bouwstenen en energie als brandstof voor de aseksuele ontwikkeling (sporulatie) vrijgemaakt. Ondanks het negatieve effect op productopbrengsten is er tot nu toe geen omvangrijk onderzoek uitgevoerd om koolstofhongering in de industrieel belangrijke schimmel *A. niger* te bestuderen. Om deze reden hebben wij uitgebreid onderzoek gedaan naar koolstofhongering in *A. niger* tijdens submerse cultivering, volgens de methode zoals die in dit proefschrift wordt beschreven en die kan worden onderverdeeld in de volgende fasen: (I) Instellen van de software voor omics data analyse en interpretatie in hoofdstuk 2 en 3; (II) Cultivering van *A. niger* en generatie, analyse en interpretatie van data in hoofdstuk 4; (III) Onderzoek van een mogelijke route met sterke transcriptionele inductie tijdens koolstofhongering met behulp van moleculair-genetische benaderingen in hoofdstuk 5.

Genoom-brede transcriptionele analyse heeft een groot potentieel om op systeemniveau inzicht te krijgen in cellulaire reacties, maar vereist wel objectieve, high-throughput statistische benaderingen voor data-analyse, interpretatie en uiteindelijk generatie van hypotheses. Vooral op universiteiten is de toepassing van open source software wenselijk en kan het worden beschouwd als voordelig, omdat het vrij verspreid en actief ontwikkeld wordt door deskundigen uit de wetenschappelijke gemeenschap zelf. Het is echter ook mogelijk dat het gebruik ervan minder intuïtief is door afhankelijkheid van een command-line-interface, zoals het geval is bij R/Bioconductor (R-Team, 2008; Gentleman *et al.*, 2004). Deze open source software werd gebruikt in dit proefschrift voor transcriptionele data-analyse. Om deze reden is hoofdstuk

2 bedoeld als een inleiding tot transcriptionele data-analyse met behulp van R/Bioconductor door middel van een stap-voor-stap handleiding. Daarin worden twee openbare transcriptionele datasets van *A. niger* geanalyseerd (Nitsche *et al.*, 2012b). De ervaring heeft geleerd dat deze aanpak geschikt is om biologen in contact te brengen met R/Bioconductor en ze zelfs in staat stelt hun eigen datasets te analyseren.

Na de eerste fase van data-analyse met inbegrip van de identificatie van differentieel tot expressie komende of co-expressie genensets moeten omics data biologisch worden geïnterpreteerd om bijvoorbeeld nieuwe hypothesen te genereren. Verrijkingsanalyse van functionele annotaties is een krachtige, high-throughput en onbevooroordeelde aanpak (B. H. J. v. d. Berg *et al.*, 2009). Tot de meest gebruikte functionele annotaties voor verrijkingsanalyse behoort de Gene Ontology (GO) annotatie (Ashburner *et al.*, 2000). In hoofdstuk 3 werd deze waardevolle bron voor functionele analyse van omics gegevens gegenereerd voor het genus *Aspergillus* door het mappen van de *A. nidulans* GO annotatie op alle Aspergilli met gepubliceerde genoom sequenties en het implementeren van de webapplicatie FetGOat (Fisher's exact test Gene Ontology annotation tool, http://www.broadinstitute.org/fetgoat/index.html) voor GO verrijkingsanalyse. Zowel de annotatie als FetGOat werden gebruikt in twee case studies waarin openbare datasets opnieuw geanalyseerd werden. Hierdoor zijn hun toepasbaarheid, gebruiksgemak en de mogelijkheid om nieuwe hypotheses te genereren gedemonstreerd (Nitsche *et al.*, 2011).

Na het instellen van de software voor omics data analyse zijn in hoofdstuk 4 genoom-brede transcriptionele profielen van submerse culturen met koolstofhongering van *A. niger* bepaald, geanalyseerd en geïnterpreteerd. De experimentele opstelling omvatte submerse batch cultivering in een koolstoflimiterend minimaal medium met toepassing van bioreactortechnologie, waardoor een hoge mate van herhaalbaarheid, bewaking en beheersing van fysiologie en macromorfologie gewaarborgd was. De belangrijkste morfologische reacties op koolstofhongering waren het ontstaan van lege hyfale compartimenten, secundaire (cryptische) groei van dunne, onvertakte hyfen en vervolgens vorming van ongeslachtelijke voortplantingsstructuren. Deze morfologische kenmerken suggereren dat secundaire groei en sporulatie tijdens koolstofhongering mogelijk zijn door hergebruik van voedingsstoffen afkomstig van het legen van hyfale compartimenten. Microscopische analyse gaf geen aanwijzing voor hydrolytische verzwakking en fragmentatie van de celwand van de schimmel. De inhoud van lege compartimenten zou direct gerecycled kunnen zijn door naburige compartimenten via een endogene route of eerst in het cultuur medium zijn gelekt waar het vervolgens door groeiende hyfen opgenomen is.

Transcriptionele data-analyse toonde aan dat in de loop van koolstofhongering circa 50% van de transcripten differentieel tot expressie komt. Het aantal hoog en laag gereguleerde ge-

nen was goed vergelijkbaar. Om belangrijke transcriptioneel geïnduceerde of gerepresseerde cellulaire processen te identificeren, werd GO annotatie verrijkingsanalyse voor hoog en laag gereguleerde genensets toegepast. De onderdrukte processen werden in de eerste plaats gerelateerd aan transcriptie, translatie en respiratie, wat de fysiologische adaptatie aan koolstofhongering en energieverlies weerspiegelt. Aan de andere kant omvatten de belangrijkste transcriptioneel geïnduceerde processen catabolische en reproductieve routes. Als zodanig waren autofagie en sporulatie de twee meest dominant geïnduceerde processen. Daarnaast heeft analyse gericht op carbohydrasen en proteasen sterke transcriptionele inductie van verschillende uitgescheiden en niet-uitgescheiden hydrolasen laten zien.

In gisten en filamenteuze schimmels zijn er tot nu toe meer dan 30 autofagie-gerelateerde genen geïdentificeerd (Kanki *et al.*, 2011; Xie *et al.*, 2007). Voor 23 daarvan zijn orthologe kandidaatgenen in *A. niger* geïdentificeerd en deze werden op één na allemaal transcriptioneel geïnduceerd tijdens de koolstofhongering. Deze gezamenlijke inductie van de autofagie route gaf aanleiding tot vragen over de rol van autofagie tijdens koolstofhongering. Beschermt autofagie tegen de vorming van lege hyfale compartimenten of induceert het dit proces? Is autofagie vereist voor effectieve verlenging van dunne hyfen in de tweede groeifase tijdens koolstofhongering of niet? Op zoek naar antwoorden werden drie genen (*atg*1, *atg*8 en *atg*17), waarvan voorspeld werd dat ze essentieel zijn voor efficiënte autofagie (Tsukada *et al.*, 1993; Matsuura *et al.*, 1997; Cheong *et al.*, 2005; Kabeya *et al.*, 2005), verwijderd in de *A. niger* wild-type en fluorescerende reporterstammen. Fenotypische karakterisering van de gemuteerde stammen toonde aan dat *atg*1 en *atg*8 essentieel zijn voor een efficiënte autofagie in *A. niger*, terwijl de verwijdering van *atg*17 weinig tot geen effect had. Analyse van de Δ*atg*1 en Δ*atg*8 mutanten tijdens submerse groei in koolstofgelimiteerde batch cultures heeft laten zien dat morfogenetische aanpassingen aan koolstofhongering, waaronder het verschijnen van lege hyfale compartimenten en secundaire groei van dunne onvertakte hyfen, worden versneld wanneer autofagie is aangetast. Verder werd aangetoond dat de door koolstofhongering geïnduceerde turnover van mitochondriën zowel in Δ*atg*1 als in Δ*atg*8 mutanten ernstig verstoord is. Dit suggereert dat autofagie door turnover van organellen tot vertraging van celdood tijdens koolstofhongering leidt, wat belangrijk is voor de fysiologische adaptatie. Er is verder onderzoek nodig om het effect van een aangetaste autofagie in *A. niger* op productopbrengsten te verhelderen. In *Penicillium chrysogenum* is bijvoorbeeld opgemerkt dat aantasting van autofagie de celdegeneratie vertraagt en tot verhoogde productie leidt (Bartoszewska *et al.*, 2011a).

Het bleek moeilijk te bepalen of lege hyfen lyseren, wat betekent dat hun inhoud in het cultuur medium lekt, of dat de inhoud van de lege compartimenten actief wordt geëvacueerd door naburige compartimenten en op deze manier endogeen gerecycleerd wordt. Hoewel uit de secretome gegevens bleek dat er tijdens koolstofhongering geen significante accumulatie was van

intracellulaire eiwitten in het cultuur medium, kon niet worden uitgesloten dat onmiddellijke hydrolyse van gelekte cytosolische eiwitten had plaatsgevonden. Desondanks toont het versneld ontstaan van lege compartimenten in de $\Delta atg1$ en $\Delta atg8$ mutanten aan dat endogene recycling van naburige compartimenten niet optreedt via autofagie.

Deze studie is het eerste onderzoek naar koolstofhongering in de schimmel *A. niger* op systeemniveau. Aangezien we slechts een enkele aanwijzing uit de transcriptionele data-analyse zijn gevolgd, bestaan er veel meer processen die nog moeten worden onderzocht. De gegenereerde dataset vormt een omvangrijk kader voor toekomstig onderzoek naar deze complexe cellulaire processen.

Publications

Nitsche B.M., Jørgensen T.R., Akeroyd M. and Ram A.F.J. (2012) The carbon starvation response of *Aspergillus niger* during submerged cultivation: Insights from the transcriptome and secretome. *BMC Genomics.* 13:380

Carvalho N.D.S.P, Jørgensen T.R., Arentshorst M., **Nitsche B.M.**, van den Hondel C.A.M.J.J., Archer D.B. and Ram A.F.J. (2012) Genome-wide expression analysis upon constitutive activation of the HacA bZIP transcription factor in *Aspergillus niger* reveals a coordinated cellular response to counteract ER stress. *BMC Genomics.* 13:350

Nitsche B.M., Ram A.F.J. and Meyer V. (2012) The use of open source bioinformatics tools to dissect transcriptomic data. *Methods Mol Biol.* 835:311-31

Nitsche B.M., Crabtree J., Cerqueira G.C., Meyer V., Ram A.F.J. and Wortman J.R. (2011) New resources for functional analysis of omics data for the genus *Aspergillus*. *BMC Genomics.* 12:486

Jørgensen T.R., **Nitsche B.M.**, Lamers G.E., Arentshorst M., van den Hondel C.A.M.J.J. and Ram A.F.J. (2010) Transcriptomic insights into the physiology of *Aspergillus niger* approaching a specific growth rate of zero. *Appl Environ Microbiol.* 76(16):5344-55

Meyer V., Arentshorst M., Flitter S.J., **Nitsche B.M.**, Kwon M.J., Reynaga-Pena C.G., Bartnicki-Garcia S., van den Hondel C.A.M.J.J. and Ram A.F.J. (2009) Reconstruction of signaling networks regulating fungal morphogenesis by transcriptomics. *Eukaryot Cell.* 8(11):1677-91

Curriculum vitae

Benjamin was born on 29th September 1979 in Berlin, Germany, where he graduated from high school in 2000. After one year of mandatory social service in the German city of Münster, Benjamin enrolled as a student of biotechnology at the Technische Universität Berlin, Germany. In 2006 he went to Japan for a period of six month to conduct his Master's research project in the Computational and Experimental Systems Biology Group at RIKEN Yokohama Institute. In 2007 he graduated from University and went to Leiden, the Netherlands, where he worked for nine month as a contract researcher in the biotech startup Hitexacoat under supervision of Prof. Dr. C.A.M.J.J. van den Hondel and Dr. A.F.J. Ram. In 2008 he started as a PhD student at the Universiteit Leiden in the Molecular Microbiology and Biotechnology group under supervision of Prof. Dr. C.A.M.J.J. van den Hondel and Dr. A.F.J. Ram. Since January 2012 he holds a researcher position at the Technische Universität Berlin in the Applied and Molecular Microbiology department of Prof. Dr. V. Meyer.

Acknowledgments

From my point of view, time proceeded quickly during this PhD project, much quicker than initially expected. This is actually a good sign, I think. It is not because the mission is almost accomplished as I am writing these acknowledgments, on the contrary: it proves that this was an extremely nice period for me. There have been a multitude of reasons, circumstances and people involved and in the following I will try to express my deep gratitude. But, before doing so, let me first apologize in case that I forgot to acknowledge you or others below. I did not intend to do so. Importantly, there is no correlation between the order that people are mentioned here and the importance of their contributions, should they be scientific, social or financial.

So, let's start! Prof. van den Hondel, first of all I would like to thank you for your fantastic achievements in the field of filamentous fungal research and the scientific infrastructure that you have helped to establish in the Netherlands and abroad. I very much appreciate your creativity, friendliness and open-minded character. And, very astonishing for a German student, you remembered my name after our first meeting and greeted me with "Hi Benjamin!" the next day we met on the corridor. Instead of saying "Hello Prof. van den Hondel!", I was invited to just reply "Hi Cees!", marvelous!

Arthur, heel erg bedankt, hoor! You should realize that I am not able to express my gratitude properly here. You have always been my perfect supervisor. I have been learning lots and lots of things from you. I hope that one day I will be as patient with my students as you have always been. It's like you taught me to walk and now I am on my own in the country of science. I hope that our paths will mutually cross.

Vera, you have actually been "the link". I still remember reading your mail mentioning the possibility to do an internship in Leiden; the rest is history. But of course, you are not limited to be the linking person. You have an astonishingly positive attitude and an outstanding capability to help people find their way. I am looking forward to a prosperous period, thank you!

Thomas, we spent approximately half of the time of my PhD project working together in Leiden. This was great because I could learn lots and lots of things from you both as an expert in bioreactor cultivations and as a sharp-thinking and independent scientist, *mange tak*!

My dear colleagues from the IBL and MMB group, let me collectively thank all of you for the nice atmosphere, inspiring working environment and the fantastic *borrels*. Mark, Davy, Ellen, Sandra and Sandra, Gerda, Neuza, Angelique, Tim, Tabea, Gerben, Natascha, Anne-Marie, Min, Joohae, Trish and everybody I forgot. Special thanks go to my students, who did a lot of nice experiments: Tom, Crescel, Negin, Markus and Leonie! I also fondly remember the IOP

project meetings. Thank you Jolanda, Jerre, Marc, Han, Hein, Maurien, Peter, Michiel, Henk and Ruud. Furthermore, I would like to acknowledge all collaborators as well as Senter Novem.

Let me change gears to proceed with some private acknowledgments. I would like to thank all members of the Tendoryu Aikido Dojo in Den Haag for their enthusiasm and hospitality. I enjoyed sharing our experiences and learned many valuable things from all of you. Erwin, I am especially grateful for the nice lessons you gave. I hope that we will have many more opportunities for *ishin denshin*. Please stay just as you are. Peter, I really appreciate your help with all typesetting issues and your support during finalizing this thesis. Roslin, thanks for proof-reading the non-submitted parts of this thesis. Hoi Clarije, Simon, Cato en Siem - ik ben jullie niet vergeten! Bedankt voor de leuke tijd samen! Hopelijk gaat het nog lang zo door! Maarten and Beata, great that we incidentally met as you were among our first contacts in Leiden. Lena did not only take care of Tim, Marlene and Nils, but we could also frequently enjoy your hospitality, thank you.

And now it's Lena's turn. How could I ever be able to thank you for everything on a piece of paper? We have spent more than 1/4 of our lives together by now and you have always supported me, in particular in going abroad. Leiden was great for me although I know it was a hard time for you. It's nice to share our memories of Leiden, a very special period, especially when we think of Amelie and Jannis. And finally I am extremely grateful for all the love and support that I have received from my parents and my brother.

Berlin, Germany
August 26, 2012

References

Abràmoff, M. D., Hospitals, I. and **Magalhães, P. J.** (2004) Image Processing with ImageJ *Medicine*. **11**(7):36–42.

Adams, T. H., Wieser, J. K. and **Yu, J. H.** (1998) Asexual sporulation in Aspergillus nidulans *Microbiol Mol Biol Rev*. **62**(1):35–54.

Adrian, A. and **Rahnenfuhrer, J.** 2010 *topGO: Enrichment analysis for Gene Ontology* 2010.

Agger, T., Spohr, A. B., Carlsen, M. and **Nielsen, J.** (1998) Growth and product formation of Aspergillus oryzae during submerged cultivations: verification of a morphologically structured model using fluorescent probes. *Biotechnology and bioengineering*. **57**(3):321–329.

Alic, M., Bennett, J. W. and **Lasure, L. L.** 1991 More gene manipulations in fungi Academic Press, 1991 ISBN: 9780120886425.

Andersen, M. R., Salazar, M. P., Schaap, P. J., Vondervoort, P. J. I. van der, Culley, D., Thykaer, J., Frisvad, J. C., Nielsen, K. F., Albang, R., Albermann, K., Berka, R. M., Braus, G. H., Braus-stromeyer, S. A., Corrochano, L. M., Dai, Z., Dijck, P. W. M. V., Hofmann, G., Lasure, L. L., Magnuson, J. K., Menke, H., Meijer, M., Meijer, S. L., Nielsen, J. B., Nielsen, M. L., Ooyen, A. J. J. V., Pel, H. J., Poulsen, L., Samson, R. A., Stam, H., Tsang, A., Brink, J. M. V. D., Atkins, A., Aerts, A., Shapiro, H., Pangilinan, J., Salamov, A., Lou, Y., Lindquist, E., Lucas, S., Grimwood, J., Grigoriev, I. V., Kubicek, C. P., Martinez, D., Peij, N. M. E. V., Roubos, J. A., Nielsen, J. and **Baker, S. E.** (2011) Comparative genomics of citric-acid-producing Aspergillus niger ATCC 1015 versus enzyme-producing CBS 513.88 *Genome Research*. **21**(6):885–897.

Archer, D. B. (2000) Filamentous fungi as microbial cell factories for food use. *Current opinion in biotechnology*. **11**(5):478–83.

Arnaud, M. B., Chibucos, M. C., Costanzo, M. C., Crabtree, J., Inglis, D. O., Lotia, A., Orvis, J., Shah, P., Skrzypek, M. S., Binkley, G., Miyasato, S. R., Wortman, J. R. and **Sherlock, G.** (2010) The Aspergillus Genome Database, a curated comparative genomics resource for gene, protein and sequence information for the Aspergillus research community *Nucleic Acids Res*. **38**(Database issue):D420–7.

Ashburner, M., Ball, C. A., Blake, J. A., Botstein, D., Butler, H., Cherry, J. M., Davis, A. P., Dolinski, K., Dwight, S. S., Eppig, J. T., Harris, M. A., Hill, D. P., Issel-Tarver, L., Kasarskis, A., Lewis, S., Matese, J. C., Richardson, J. E., Ringwald, M., Rubin, G. M. and **Sherlock, G.** (2000) Gene ontology: tool for the unification of biology. The Gene Ontology Consortium *Nat Genet*. **25**(1):25–29.

Bader, G. D. and **Hogue, C. W.** (2003) An automated method for finding molecular complexes in large protein interaction networks *BMC Bioinformatics*. **4**:2.

Bainbridge, B. W., Bull, A. T., Pirt, S. J., Rowley, B. I. and **Trinci, A. P. J.** (1971) Biochemical and structural changes in non-growing maintained and autolysing cultures of Aspergillus nidulans *Transactions of the British Mycological Society*. **56**(3):371–85.

Bai, Z., Harvey, L. M. and **McNeil, B.** (2003) Oxidative stress in submerged cultures of fungi *Crit Rev Biotechnol*. **23**(4):267–302.

Barhoom, S. and **Sharon, A.** (2007) Bcl-2 proteins link programmed cell death with growth and morphogenetic adaptations in the fungal plant pathogen Colletotrichum gloeosporioides. *Fungal genetics and biology*. **44**(1):32–43.

Baron, R. M. and **Kenny, D. A.** (1986) The moderator-mediator variable distinction in social psychological research: conceptual, strategic, and statistical considerations. *Journal of personality and social psychology*. **51**(6):1173–82.

Barrett, T., Troup, D. B., Wilhite, S. E., Ledoux, P., Evangelista, C., Kim, I. F., Tomashevsky, M., Marshall, K. a., Phillippy, K. H., Sherman, P. M., Muertter, R. N., Holko, M., Ayanbule, O., Yefanov, A. and **Soboleva, A.** (2011) NCBI GEO: archive for functional genomics data sets--10 years on. *Nucleic acids research*. **39**(Database issue):D1005–10.

Bartoszewska, M., Kiel, J. A. K. W., Bovenberg, R. A. L., Veenhuis, M. and **Klei, I. J. van der** (2011) Autophagy deficiency promotes beta-lactam production in Penicillium chrysogenum. *Applied and environmental microbiology*. **77**(4):1413–22.

Bartoszewska, M. and **Kiel, J. A. K. W.** (2011) The role of macroautophagy in development of filamentous fungi. *Antioxidants and redox signaling*. **14**(11):2271–87.

Bateman, A., Coin, L., Durbin, R., Finn, R. D., Hollich, V., Griffiths-Jones, S., Khanna, A., Marshall, M., Moxon, S., Sonnhammer, E. L. L., Studholme, D. J., Yeats, C. and **Eddy, S. R.** (2004) The Pfam protein families database. *Nucleic acids research*. **32**(Database issue):D138–41.

Beek, C. P. van der and **Roels, J. A.** (1984) Penicillin production: biotechnology at its best *Antonie van Leeuwenhoek*. **50**:625–639.

Benjamini, Y. and **Hochberg, Y.** (1995) Controlling the False Discovery Rate: A Practical and Powerful Approach to Multiple Testing *Journal of the Royal Statistical Society. Series B (Methodological)*. **57**(1):289–300.

Berg, B. H. J. van den, Thanthiriwatte, C., Manda, P. and **Bridges, S. M.** (2009) Comparing gene annotation enrichment tools for functional modeling of agricultural microarray data. *BMC bioinformatics*. **10**(Suppl 11):S9.

Berg, R. A. van den, Hoefsloot, H. C. J., Westerhuis, J. A., Smilde, A. K. and **Werf, M. J. van der** (2006) Centering, scaling, and transformations: improving the biological information content of metabolomics data. *BMC genomics*. **7**:142.

Berg, R. A. van den, Braaksma, M., Veen, D. van der, Werf, M. J. van der, Punt, P. J., Oost, J. van der and **Graaff, L. H. de** (2010) Identification of modules in Aspergillus niger by gene co-expression network analysis *Fungal Genet Biol*. **47**(6):539–50.

Bernales, S., Schuck, S. and **Walter, P.** (2007) ER-phagy: selective autophagy of the endoplasmic reticulum. *Autophagy*. **3**(3):285–7.

Bleichrodt, R.-J. (2012) Intercompartmental streaming in Aspergillus PhD thesis Universiteit Utrecht, 2012, 1–144.

Bluthgen, N., Brand, K., Cajavec, B., Swat, M., Herzel, H. and **Beule, D.** (2005) Biological profiling of gene groups utilizing Gene Ontology *Genome Inform*. **16**(1):106–115.

Bolstad, B. M., Collin, F., Brettschneider, J., Simpson, K., Cope, L., Irizarry, R. A. and **Speed, T. P.** (2005) Quality assessment of affymetrix genechip data. *Bioinformatics and Computational Biology Solutions Using R and Bioconductor* New York: Springer, 2005.

Bos, C. J., Debets, A. J., Swart, K., Huybers, A., Kobus, G. and **Slakhorst, S. M.** (1988) Genetic analysis and the construction of master strains for assignment of genes to six linkage groups in Aspergillus niger. *Current genetics*. **14**(5):437–43.

Bourgon, R., Gentleman, R. C. and **Huber, W.** (2010) Independent filtering increases detection power for high-throughput experiments *Proc Natl Acad Sci U S A*. **107**(21):9546–9551.

Braaksma, M., Smilde, A. K., Werf, M. J. van der and **Punt, P. J.** (2009) The effect of environmental conditions on extracellular protease activity in controlled fermentations of Aspergillus niger. *Microbiology*. **155**(Pt 10):3430–9.

Braaksma, M., Martens-Uzunova, E. S., Punt, P. J. and **Schaap, P. J.** (2010) An inventory of the Aspergillus niger secretome by combining in silico predictions with shotgun proteomics data. *BMC genomics*. **11**(1):584.

Brayton, K. A., Lau, A. O. T., Herndon, D. R., Hannick, L., Kappmeyer, L. S., Berens, S. J., Bidwell, S. L., Brown, W. C., Crabtree, J., Fadrosh, D., Feldblum, T., Forberger, H. A., Haas, B. J., Howell, J. M., Khouri, H., Koo, H., Mann, D. J., Norimine, J., Paulsen, I. T., Radune, D., Ren, Q., Smith, R. K., Suarez, C. E., White, O., Wortman, J. R., Knowles, D. P., McElwain, T. F. and **Nene, V. M.** (2007) Genome sequence of Babesia bovis and comparative analysis of apicomplexan hemoprotozoa. *PLoS pathogens*. **3**(10):1401–13.

Broderick, A. J. and **Greenshields, R. N.** (1981) Sporulation of Aspergillus niger and Aspergillus ochraceus in Continuous Submerged Liquid Culture *Microbiology*. **126**(1):193–202.

Cantarel, B. L., Coutinho, P. M., Rancurel, C., Bernard, T., Lombard, V. and **Henrissat, B.** (2009) The Carbohydrate-Active EnZymes database (CAZy): an expert resource for Glycogenomics. *Nucleic acids research*. **37**(Database issue):D233–8.

Carlton, J. M., Adams, J. H., Silva, J. C., Bidwell, S. L., Lorenzi, H., Caler, E., Crabtree, J., Angiuoli, S. V., Merino, E. F., Amedeo, P., Cheng, Q., Coulson, R. M. R., Crabb, B. S., Del Portillo, H. A., Essien, K., Feldblyum, T. V., Fernandez-Becerra, C., Gilson, P. R., Gueye, A. H., Guo, X., Kang'a, S., Kooij, T. W. A., Korsinczky, M., Meyer, E. V.-S., Nene, V., Paulsen, I., White, O., Ralph, S. A., Ren, Q., Sargeant, T. J., Salzberg, S. L., Stoeckert, C. J., Sullivan, S. A., Yamamoto, M. M., Hoffman, S. L., Wortman, J. R., Gardner, M. J., Galinski, M. R., Barnwell, J. W. and **Fraser-Liggett, C. M.** (2008) Comparative genomics of the neglected human malaria parasite Plasmodium vivax. *Nature*. **455**(7214):757–63.

Cheong, H., Yorimitsu, T., Reggiori, F., Legakis, J. E., Wang, C.-W. and **Klionsky, D. J.** (2005) Atg17 Regulates the Magnitude of the Autophagic Response *Molecular Biology of the Cell*. **16**(7):3438–3453.

Cheong, H., Nair, U., Geng, J. and **Klionsky, D. J.** (2008) The Atg1 Kinase Complex Is Involved in the Regulation of Protein Recruitment to Initiate Sequestering Vesicle Formation for Nonspecific Autophagy in Saccharomyces cerevisiae *Molecular Biology of the Cell*. **19**(2):668–681.

Clarke, P. G. and **Clarke, S.** (1996) Nineteenth century research on naturally occurring cell death and related phenomena. *Anatomy and embryology*. **193**(2):81–99.

Codogno, P. and **Meijer, A. J.** (2005) Autophagy and signaling: their role in cell survival and cell death. *Cell death and differentiation*. **12**:1509–18.

Conesa, A., Gotz, S., Garcia-Gomez, J. M., Terol, J., Talon, M. and **Robles, M.** (2005) Blast2GO: a universal tool for annotation, visualization and analysis in functional genomics research *Bioinformatics*. **21**(18):3674–3676.

Crabtree, J., Angiuoli, S. V., Wortman, J. R. and **White, O. R.** (2007) Sybil: methods and software for multiple genome comparison and visualization. *Methods in molecular biology*. **408**:93–108.

Damveld, R. A., VanKuyk, P. A., Arentshorst, M., Klis, F. M., Hondel, C. A. M. J. J. van den and **Ram, A. F. J.** (2005) Expression of agsA, one of five 1,3-alpha-D-glucan synthase-encoding genes in Aspergillus niger, is induced in response to cell wall stress *Fungal Genet Biol*. **42**(2):165–177.

Damveld, R. a., Arentshorst, M., Franken, A., VanKuyk, P. A., Klis, F. M., Hondel, C. A. M. J. J. van den and **Ram, A. F. J.** (2005) The Aspergillus niger MADS-box transcription factor RlmA is required for cell wall reinforcement in response to cell wall stress *Mol Microbiol*. **58**(1):305–319.

Diamantis, A., Magiorkinis, E., Sakorafas, G. H. and **Androutsos, G.** (2008) A brief history of apoptosis: from ancient to modern times. *Onkologie*. **31**(12):702–6.

Dunning Hotopp, J. C., Lin, M., Madupu, R., Crabtree, J., Angiuoli, S. V., Eisen, J. A., Eisen, J., Seshadri, R., Ren, Q., Wu, M., Utterback, T. R., Smith, S., Lewis, M., Khouri, H., Zhang, C., Niu, H., Lin, Q., Ohashi, N., Zhi, N., Nelson, W., Brinkac, L. M., Dodson, R. J., Rosovitz, M. J., Sundaram, J., Daugherty, S. C., Davidsen, T., Durkin, A. S., Gwinn, M., Haft, D. H., Selengut, J. D., Sullivan, S. A., Zafar, N., Zhou, L., Benahmed, F., Forberger, H., Halpin, R., Mulligan, S., Robinson, J., White, O., Rikihisa, Y. and **Tettelin, H.** (2006) Comparative genomics of emerging human ehrlichiosis agents. *PLoS genetics*. **2**(2):e21.

Du, Z., Li, L., Chen, C.-F., Yu, P. S. and **Wang, J. Z.** (2009) G-SESAME: web tools for GO-term-based gene similarity analysis and knowledge discovery. *Nucleic acids research*. **37**(Web Server issue):W345–9.

Edinger, A. L. and **Thompson, C. B.** (2004) Death by design: apoptosis, necrosis and autophagy *Current Opinion in Cell Biology*. **16**(6):663–669.

Elander, R. P. (2003) Industrial production of beta-lactam antibiotics. *Applied microbiology and biotechnology*. **61**(5-6):385–92.

Emri, T., Molnár, Z., Pusztahelyi, T. and **Pócsi, I.** (2004) Physiological and morphological changes in autolyzing Aspergillus nidulans cultures. *Folia microbiologica*. **49**(3):277–84.

Emri, T., Molnár, Z. and **Pócsi, I.** (2005) The appearances of autolytic and apoptotic markers are concomitant but differently regulated in carbon-starving Aspergillus nidulans cultures. *FEMS microbiology letters*. **251**(2):297–303.

Emri, T., Molnár, Z., Pusztahelyi, T., Varecza, Z. and **Pócsi, I.** (2005) The fluG-BrlA pathway contributes to the initialisation of autolysis in submerged Aspergillus nidulans cultures *Mycol Res*. **109**(Pt 7):757–763.

Emri, T., Molnár, Z., Veres, T., Tünde, P., Dudas, G. and **Pócsi, I.** (2006) Glucose-mediated repression of autolysis and conidiogenesis in Emericella nidulans *Mycol Res*. **110**(Pt 10):1172–1178.

Emri, T., Molnár, Z., Szilágyi, M. and **Pócsi, I.** (2008) Regulation of autolysis in Aspergillus nidulans. *Applied biochemistry and biotechnology*. **151**(2-3):211–20.

Etxebeste, O., Ugalde, U., Espeso, E. A., *et al.* (2010) Adaptative and Developmental Responses to Stress in Aspergillus nidulans *Current Protein and Peptide Science*. **11**(8):704–718.

Fedorova, N. D., Khaldi, N., Joardar, V. S., Maiti, R., Amedeo, P., Anderson, M. J., Crabtree, J., Silva, J. C., Badger, J. H., Albarraq, A., Angiuoli, S., Bussey, H., Bowyer, P., Cotty, P. J., Dyer, P. S., Egan, A., Galens, K., Fraser-Liggett, C. M., Haas, B. J., Inman, J. M., Kent, R., Lemieux, S., Malavazi, I., Orvis, J., Roemer, T., Ronning, C. M., Sundaram, J. P., Sutton, G., Turner, G., Venter, J. C., White, O. R., Whitty, B. R., Youngman, P., Wolfe, K. H., Goldman, G. H., Wortman, J. R., Jiang, B., Denning, D. W. and **Nierman, W. C.** (2008) Genomic islands in the pathogenic filamentous fungus Aspergillus fumigatus. *PLoS genetics*. **4**(4):e1000046.

Fedorova, N. D., Badger, J. H., Robson, G. D., Wortman, J. R. and **Nierman, W. C.** (2005) Comparative analysis of programmed cell death pathways in filamentous fungi *BMC Genomics*. **6**:177.

Fernandes, P., Mannarino, S., Silva, C., Pereira, M., Panek, A. and **Eleutherio, E.** (2007) Oxidative stress response in eukaryotes: effect of glutathione, superoxide dismutase and catalase on adaptation to peroxide and menadione stresses in Saccharomyces cerevisiae *Redox Report*. **12**(5):236–244.

Fischer, R. (2002) Conidiation in Aspergillus nidulans *Molecular Biology of Fungal Development* ed. by **H. D. Osiewacz** New York: Marcel Dekker, 2002, 59–86.

Fisher, R. A. (1922) On the Interpretation of $\chi 2$ from Contingency Tables, and the Calculation of P *Journal of the Royal Statistical Society. Series B (Methodological)*. **85**(1):87–94.

Fogarty, W. (1994) Enzymes of the Genus Aspergillus *Aspergillus (Biotechnology Handbooks)* ed. by **J. Smith** New York: Plenum Press, 1994 chap. 7, 177–205 ISBN: 0-306-445-45-X.

Galagan, J. E., Calvo, S. E., Cuomo, C., Ma, L. J., Wortman, J. R., Batzoglou, S., Lee, S. I., Basturkmen, M., Spevak, C. C., Clutterbuck, J., Kapitonov, V., Jurka, J., Scazzocchio, C., Farman, M., Butler, J., Purcell, S., Harris, S., Braus, G. H., Draht, O., Busch, S., D'Enfert, C., Bouchier, C., Goldman, G. H., Bell-Pedersen, D., Griffiths-Jones, S., Doonan, J. H., Yu, J., Vienken, K., Pain, A., Freitag, M., Selker, E. U., Archer, D. B., Penalva, M. A., Oakley, B. R., Momany, M., Tanaka, T., Kumagai, T., Asai, K., Machida, M., Nierman, W. C., Denning, D. W., Caddick, M. X., Hynes, M., Paoletti, M., Fischer, R., Miller, B., Dyer, P., Sachs, M. S., Osmani, S. A. and **Birren, B. W.** (2005) Sequencing of Aspergillus nidulans and comparative analysis with A. fumigatus and A. oryzae *Nature*. **438**(7071):1105–1115.

Galluzzi, L. and **Kroemer, G.** (2008) Necroptosis: a specialized pathway of programmed necrosis. *Cell*. **135**(7):1161–3.

Gardner, M. J., Bishop, R., Shah, T., Villiers, E. P. de, Carlton, J. M., Hall, N., Ren, Q., Paulsen, I. T., Pain, A., Berriman, M., Wilson, R. J. M., Sato, S., Ralph, S. A., Mann, D. J., Xiong, Z., Shallom, S. J., Weidman, J., Jiang, L., Lynn, J., Weaver, B., Shoaibi, A., Domingo, A. R., Wasawo, D., Crabtree, J., Wortman, J. R., Haas, B., Angiuoli, S. V., Creasy, T. H., Lu, C., Suh, B., Silva, J. C., Utterback, T. R., Feldblyum, T. V., Pertea, M., Allen, J., Nierman, W. C., Taracha, E. L. N., Salzberg, S. L., White, O. R., Fitzhugh, H. A., Morzaria, S., Venter, J. C., Fraser, C. M. and **Nene, V.** (2005) Genome sequence of Theileria parva, a bovine pathogen that transforms lymphocytes. *Science*. **309**(5731):134–7.

Gaudet, P. (2009) The Gene Ontology's Reference Genome Project: a unified framework for functional annotation across species *PLoS Comput Biol*. **5**(7):e1000431.

Gautier, L., Cope, L., Bolstad, B. M. and **Irizarry, R. A.** (2004) affy-analysis of Affymetrix GeneChip data at the probe level *Bioinformatics*. **20**(3):307–315.

Gentleman, R. C., Carey, V. J., Bates, D. M., Bolstad, B., Dettling, M., Dudoit, S., Ellis, B., Gautier, L., Ge, Y., Gentry, J., Hornik, K., Hothorn, T., Huber, W., Iacus, S., Irizarry, R. A., Leisch, F., Li, C., Maechler, M., Rossini, A. J., Sawitzki, G., Smith, C., Smyth, G., Tierney, L., Yang, J. Y. and **Zhang, J.** (2004) Bioconductor: open software development for computational biology and bioinformatics *Genome Biol*. **5**(10):R80.

Gentleman, R. C., Carey, V., Huber, W. and **Hahne, F.** 2006 genefilter: methods for filtering genes from microarray experiments 2006.

Ghedin, E., Wang, S., Spiro, D., Caler, E., Zhao, Q., Crabtree, J., Allen, J. E., Delcher, A. L., Guiliano, D. B., Miranda-Saavedra, D., Angiuoli, S. V., Creasy, T., Amedeo, P., Haas, B., El-Sayed, N. M., Wortman, J. R., Feldblyum, T., Tallon, L., Schatz, M., Shumway, M., Koo, H., Salzberg, S. L., Schobel, S., Pertea, M., Pop, M., White, O., Barton, G. J., Carlow, C. K. S., Crawford, M. J., Daub, J., Dimmic, M. W., Estes, C. F., Foster, J. M., Ganatra, M., Gregory, W. F., Johnson, N. M., Jin, J., Komuniecki, R., Korf, I., Kumar, S., Laney, S., Li, B.-W., Li, W., Lindblom, T. H., Lustigman, S., Ma, D., Maina, C. V., Martin, D. M. A., McCarter, J. P., McReynolds, L., Mitreva, M., Nutman, T. B., Parkinson, J., Peregrín-Alvarez, J. M., Poole, C., Ren, Q., Saunders, L., Sluder, A. E., Smith, K., Stanke, M., Unnasch, T. R., Ware, J., Wei, A. D., Weil, G., Williams, D. J., Zhang, Y., Williams, S. A., Fraser-Liggett, C., Slatko, B., Blaxter, M. L. and **Scott, A. L.** (2007) Draft genome of the filarial nematode parasite Brugia malayi. *Science*. **317**(5845):1756–60.

Giansanti, V., Torriglia, A. and **Scovassi, A. I.** (2011) Conversation between apoptosis and autophagy: "Is it your turn or mine?". *Apoptosis : an international journal on programmed cell death*. **16**(4):321–33.

Gorcom, R. F. van and **Hondel, C. A. M. J. J. van den** (1988) Expression analysis vectors for Aspergillus niger. *Nucleic acids research*. **16**(18):9052.

Grün, C. (2003) Structure and biosynthesis of fungal alpha-glucans PhD thesis University of Utrecht, 2003, 1–144.

Hagen, **J. B.** (2012) Five Kingdoms, More or Less: Robert Whittaker and the Broad Classification of Organisms *BioScience*. **62**(1):67–74.

Hahne, **F.**, **Huber**, **W.**, **Gentleman**, **R. C.** and **Falcon**, **S.** 2008 Bioconductor case studies Springer Verlag, 2008 ISBN: 978-0387772394.

Hamann, **A.**, **Brust**, **D.** and **Osiewacz**, **H. D.** (2008) Apoptosis pathways in fungal growth, development and ageing *Trends Microbiol.* **16**(6):276–283.

Harr, **B.** and **Schlotterer**, **C.** (2006) Comparison of algorithms for the analysis of Affymetrix microarray data as evaluated by co-expression of genes in known operons *Nucleic Acids Res.* **34**(2):e8.

Hartingsveldt, **W. van**, **Mattern**, **I. E.**, **Zeijl**, **C. M. van**, **Pouwels**, **P. H.** and **Hondel**, **C. A. M. J. J. van den** (1987) Development of a homologous transformation system for Aspergillus niger based on the pyrG gene. *Molecular and general genetics*. **206**(1):71–5.

Hollander, **M.** and **Wolfe**, **D. A.** 1999 Nonparametric Statistical Methods Wiley-Interscience, 1999 ISBN: 0471190454.

Horner, **W. E.**, **Helbling**, **a.**, **Salvaggio**, **J. E.** and **Lehrer**, **S. B.** (1995) Fungal allergens. *Clinical microbiology reviews*. **8**(2):161–79.

Hrdlicka, **P. J.**, **Sørensen**, **A. B.**, **Poulsen**, **B. R.**, **Ruijter**, **G. J. G.**, **Visser**, **J.** and **Iversen**, **J. J. L.** (2004) Characterization of nerolidol biotransformation based on indirect on-line estimation of biomass concentration and physiological state in batch cultures of Aspergillus niger. *Biotechnology progress*. **20**(1):368–76.

Hu, **L.**, **Bao**, **J.** and **Reecy**, **J. M.** (2008) CateGOrizer: A Web-Based Program to Batch Analyze Gene Ontology Classification Categories *Online Journal of Bioinformatics*. **9**(2):108–112.

Hulsen, **T.**, **Vlieg**, **J. de** and **Alkema**, **W.** (2008) BioVenn - a web application for the comparison and visualization of biological lists using area-proportional Venn diagrams *BMC Genomics*. **9**:488.

Inoue, **Y.** and **Klionsky**, **D. J.** (2010) Regulation of macroautophagy in Saccharomyces cerevisiae *Seminars in cell developmental biology*. **21**(7):664–670.

Irizarry, **R. A.**, **Bolstad**, **B. M.**, **Collin**, **F.**, **Cope**, **L. M.**, **Hobbs**, **B.** and **Speed**, **T. P.** (2003) Summaries of Affymetrix GeneChip probe level data *Nucleic Acids Res.* **31**(4):e15.

Irizarry, **R. A.**, **Gautier**, **L.**, **Huber**, **W.** and **Bolstad**, **B.** 2006 *makecdfenv: CDF Environment Maker* 2006.

Jaccard, **P.** (1908) Nouvelles recherches sur la distribution florale *Bulletin de la Sociète Vaudense des Sciences Naturelles*. **44**:223–270.

Jamieson, **D. J.** (1992) Saccharomyces cerevisiae has distinct adaptive responses to both hydrogen peroxide and menadione. *Journal of bacteriology*. **174**(20):6678–81.

Jaques, **A. K.** (2003) Disruption of the gene encoding the ChiB1 chitinase of Aspergillus fumigatus and characterization of a recombinant gene product *Microbiology*. **149**(10):2931–2939.

Joardar, **V.**, **Lindeberg**, **M.**, **Jackson**, **R. W.**, **Selengut**, **J.**, **Dodson**, **R.**, **Brinkac**, **L. M.**, **Daugherty**, **S. C.**, **Deboy**, **R.**, **Durkin**, **A. S.**, **Giglio**, **M. G.**, **Madupu**, **R.**, **Nelson**, **W. C.**, **Rosovitz**,

M. J., **Sullivan**, **S.**, **Crabtree**, **J.**, **Creasy**, **T.**, **Davidsen**, **T.**, **Haft**, **D. H.**, **Zafar**, **N.**, **Zhou**, **L.**, **Halpin**, **R.**, **Holley**, **T.**, **Khouri**, **H.**, **Feldblyum**, **T.**, **White**, **O.**, **Fraser**, **C. M.**, **Chatterjee**, **A. K.**, **Cartinhour**, **S.**, **Schneider**, **D. J.**, **Mansfield**, **J.**, **Collmer**, **A.** and **Buell**, **C. R.** (2005) Whole-genome sequence analysis of Pseudomonas syringae pv. phaseolicola 1448A reveals divergence among pathovars in genes involved in virulence and transposition. *Journal of bacteriology*. **187**(18):6488–98.

Jones, **M. G.** (2007) The first filamentous fungal genome sequences: Aspergillus leads the way for essential everyday resources or dusty museum specimens? *Microbiology*. **153**(1):1–6.

Jørgensen, **T. R.**, **Goosen**, **T.**, **Hondel**, **C. A. M. J. J. van den**, **Ram**, **A. F. J.** and **Iversen**, **J. J. L.** (2009) Transcriptomic comparison of Aspergillus niger growing on two different sugars reveals coordinated regulation of the secretory pathway. *BMC genomics*. **10**:44.

Jørgensen, **T. R.**, **Nitsche**, **B. M.**, **Lamers**, **G. E. M.**, **Arentshorst**, **M.**, **Hondel**, **C. A. M. J. J. van den** and **Ram**, **A. F. J.** (2010) Transcriptomic insights into the physiology of Aspergillus niger approaching a specific growth rate of zero *Appl Environ Microbiol*. **76**(16):5344–5355.

Jørgensen, **T. R.**, **Nielsen**, **K. F.**, **Arentshorst**, **M.**, **Park**, **J.**, **Hondel**, **C. A. M. J. J. van den**, **Frisvad**, **J. C.** and **Ram**, **A. F. J.** (2011) Submerged Conidiation and Product Formation by Aspergillus niger at Low Specific Growth Rates Are Affected in Aerial Developmental Mutants. *Applied and environmental microbiology*. **77**(15):5270–7.

Kabeya, **Y.**, **Kamada**, **Y.**, **Baba**, **M.**, **Takikawa**, **H.**, **Sasaki**, **M.** and **Ohsumi**, **Y.** (2005) Atg17 Functions in Cooperation with Atg1 and Atg13 in Yeast Autophagy *Molecular Biology of the Cell*. **16**(5):2544–53.

Kanehisa, **M.**, **Goto**, **S.**, **Furumichi**, **M.**, **Tanabe**, **M.** and **Hirakawa**, **M.** (2010) KEGG for representation and analysis of molecular networks involving diseases and drugs. *Nucleic acids research*. **38**(Database issue):D355–60.

Kanki, **T.**, **Klionsky**, **D. J.** and **Okamoto**, **K.** (2011) Mitochondria autophagy in yeast. *Antioxidants and redox signaling*. **14**(10):1989–2001.

Kanki, **T.** and **Klionsky**, **D. J.** (2008) Mitophagy in yeast occurs through a selective mechanism *J Biol Chem*. **283**(47):32386–32393.

Kardos, **N.** and **Demain**, **A. L.** (2011) Penicillin: the medicine with the greatest impact on therapeutic outcomes. *Applied microbiology and biotechnology*. **92**(4):677–87.

Kelly, **D. E.**, **Krasevec**, **N.**, **Mullins**, **J.** and **Nelson**, **D. R.** (2009) The CYPome (Cytochrome P450 complement) of Aspergillus nidulans. *Fungal genetics and biology*. **46 Suppl 1**(1):S53–61.

Kerr, **J.**, **Wyllie**, **A.** and **Currie**, **A.** (1972) Apoptosis: a basic biological phenomenon with wide-ranging implications in tissue kinetics *Apoptosis*. **26**:239–257.

Kikuma, **T.**, **Arioka**, **M.** and **Kitamoto**, **K.** (2007) Autophagy during conidiation and conidial germination in filamentous fungi. *Autophagy*. **3**(2):128–9.

Kikuma, **T.** and **Kitamoto**, **K.** (2011) Analysis of autophagy in Aspergillus oryzae by disruption of Aoatg13, Aoatg4, and Aoatg15 genes. *FEMS microbiology letters*. **316**(1):61–9.

Kikuma, T., Ohneda, M., Arioka, M. and **Kitamoto, K.** (2006) Functional analysis of the ATG8 homologue Aoatg8 and role of autophagy in differentiation and germination in Aspergillus oryzae *Eukaryot Cell*. **5**(8):1328–1336.

Kim, S., Matsuo, I., Ajisaka, K., Nakajima, H. and **Kitamoto, K.** (2002) Cloning and characterization of the nagA gene that encodes beta-n-acetylglucosaminidase from Aspergillus nidulans and its expression in Aspergillus oryzae. *Bioscience, biotechnology, and biochemistry*. **66**(10):2168–75.

Kimura, S., Maruyama, J.-I., Kikuma, T., Arioka, M. and **Kitamoto, K.** (2011) Autophagy delivers misfolded secretory proteins accumulated in endoplasmic reticulum to vacuoles in the filamentous fungus Aspergillus oryzae. *Biochemical and biophysical research communications*. **406**(3):464–70.

Klionsky, D. J. and **Ohsumi, Y.** (1999) Vacuolar import of proteins and organelles from the cytoplasm *Annual review of cell and developmental biology*. **15**(1):1–32.

Klis, F. M., Boorsma, A. and **De Groot, P. W. J.** (2006) Cell wall construction in Saccharomyces cerevisiae *Yeast (Chichester, England)*. **23**(3):185–202.

Kroemer, G., Galluzzi, L. and **Vandenabeele, P.** (2008) Classification of cell death: recommendations of the Nomenclature Committee on Cell Death 2009 *Cell Death and Differentiation*. **16**(1):3–11.

Kuyk, P. A. V. A. N., Diderich, J. A., Cabe, A. P. M. A. C., Hererro, O., Ruijter, G. J. G. and **Visser, J.** (2004) Aspergillus niger mstA encodes a high-affinity sugar/H+ symporter which is regulated in response to extracellular pH *Biochem J*. **379**(Pt 2):375–383.

Lagopodi, A. L., Ram, A. F. J., Lamers, G. E. M., Punt, P. J., Hondel, C. A. M. J. J. van den, Lugtenberg, B. J. J. and **Bloemberg, G. V.** (2002) Novel aspects of tomato root colonization and infection by Fusarium oxysporum f. sp. radicis-lycopersici revealed by confocal laser scanning microscopic analysis using the green fluorescent protein as a marker. *Molecular plant-microbe interactions : MPMI*. **15**(2):172–9.

Lahoz, R., Reyes, F. and **Cribeiro, L.** (1986) Behaviour of the cell walls of Aspergillus niger during the autolytic phase of growth *FEMS Microbiology Letters*. **36**:265–268.

Latge, J. (1999) Aspergillus fumigatus and aspergillosis *Clinical microbiology reviews*. **12**(2):310–50.

Li, C. and **Wong, W. H.** (2001) Model-based analysis of oligonucleotide arrays: expression index computation and outlier detection *Proc Natl Acad Sci U S A*. **98**(1):31–36.

Lim, W. K., Wang, K., Lefebvre, C. and **Califano, A.** (2007) Comparative analysis of microarray normalization procedures: effects on reverse engineering gene networks *Bioinformatics*. **23**(13):i282–8.

Lin, M.-K., Lee, Y.-J., Lough, T. J., Phinney, B. S. and **Lucas, W. J.** (2009) Analysis of the pumpkin phloem proteome provides insights into angiosperm sieve tube function. *Molecular and cellular proteomics*. **8**(2):343–56.

Lockshin, R. A. and **Williams, C.** (1964) Programmed cell death-II. Endocrine potentiation of the breakdown of the intersegmental muscles of silkmoths *Journal of Insect Physiology*. **10**:643–649.

Lockshin, R. A. and **Zakeri, Z.** (2004) Apoptosis, autophagy, and more. *The international journal of biochemistry and cell biology*. **36**(12):2405–19.

Lu, P., Vogel, C., Wang, R., Yao, X. and **Marcotte, E. M.** (2007) Absolute protein expression profiling estimates the relative contributions of transcriptional and translational regulation. *Nature biotechnology*. **25**(1):117–24.

Mabey, J. E., Anderson, M. J., Giles, P. F., Miller, C. J., Attwood, T. K., Paton, N. W., Bornberg-Bauer, E., Robson, G. D., Oliver, S. G. and **Denning, D. W.** (2004) CADRE: the Central Aspergillus Data REpository *Nucleic Acids Res*. **32**(Database issue):D401–5.

MacDonald, J. W. 2008 *affycoretools: Functions useful for those doing repetitive analyses with Affymetrix GeneChips* 2008.

MacKenzie, D. A., Guillemette, T., Al-Sheikh, H., Watson, A. J., Jeenes, D. J., Wongwathanarat, P., Dunn-Coleman, N. S., Peij, N. van and **Archer, D. B.** (2005) UPR-independent dithiothreitol stress-induced genes in Aspergillus niger *Mol Genet Genomics*. **274**(4):410–418.

Maere, S., Heymans, K. and **Kuiper, M.** (2005) BiNGO: a Cytoscape plugin to assess overrepresentation of gene ontology categories in biological networks *Bioinformatics*. **21**(16):3448–3449.

Mao, K., Wang, K., Zhao, M., Xu, T. and **Klionsky, D. J.** (2011) Two MAPK-signaling pathways are required for mitophagy in Saccharomyces cerevisiae. *The Journal of cell biology*. **193**(4):755–67.

Markham, P. and **Collinge, A.** (1987) Woronin bodies of filamentous fungi *FEMS microbiology letters*. **46**(1):1–11.

Martens-Uzunova, E. S., Zandleven, J. S., Benen, J. A., Awad, H., Kools, H. J., Beldman, G., Voragen, A. G., Berg, J. A. van den and **Schaap, P. J.** (2006) A new group of exo-acting family 28 glycoside hydrolases of Aspergillus niger that are involved in pectin degradation *Biochem J*. **400**(1):43–52.

Martinez, B. and **Ibarreta, D. E.** (1969) Stability of the Cell Walls of Neurospora crassa during Autolysis *Cell*. (1954).

Matsuura, A., Tsukada, M., Wada, Y. and **Ohsumi, Y.** (1997) Apg1p, a novel protein kinase required for the autophagic process in Saccharomyces cerevisiae. *Gene*. **192**(2):245–50.

Mattern, I. E., Punt, P. J. and **Hondel, C. A. M. J. J. van den** (1988) A vector of Aspergillus transfromation conferring phleomycin resistance *Fungal Genet. Newsl.* **35**:25–30.

Mattern, I. E., Noort, J. M. van, Berg, P. van den, Archer, D. B., Roberts, I. N. and **Hondel, C. A. M. J. J. van den** (1992) Isolation and characterization of mutants of Aspergillus niger deficient in extracellular proteases. *Molecular and general genetics : MGG*. **234**(2):332–6.

McDonagh, A., Fedorova, N. D., Crabtree, J., Yu, Y., Kim, S., Chen, D., Loss, O., Cairns, T., Goldman, G. H., Armstrong-James, D., Haynes, K., Haas, H., Schrettl, M., May, G., Nierman, W. C. and **Bignell, E.** (2008) Sub-telomere directed gene expression during initiation of invasive aspergillosis. *PLoS pathogens*. **4**(9):e1000154.

McIntyre, M., Berry, D. R. and **McNeil, B.** (2000) Role of proteases in autolysis of Penicillium chrysogenum chemostat cultures in response to nutrient depletion *Appl Microbiol Biotechnol*. **53**(2):235–242.

McNeil, B., Berry, D. R., Harvey, L. M., Grant, A. and **White, S.** (1998) Measurement of autolysis in submerged batch cultures of Penicillium chrysogenum *Biotechnol Bioeng*. **57**(3):297–305.

Meijer, W. H., Klei, I. J. van der, Veenhuis, M. and **Kiel, J. A. K. W.** (2007) ATG genes involved in non-selective autophagy are conserved from yeast to man, but the selective Cvt and pexophagy pathways also require organism-specific genes. *Autophagy*. **3**(2):106–16.

Meškauskas, A., Fricker, M. D. and **Moore, D.** (2004) Simulating colonial growth of fungi with the Neighbour-Sensing model of hyphal growth *Mycological Research*. **108**(11):1241–1256.

Meyer, V., Ram, A. F. J. and **Punt, P. J.** (2010) Genetics, genetic manipulation and approaches to strain improvement of filamentous fungi *Manual of Industrial Microbiology and Biotechnology* ed. by **D. J. AL** and **Demain** New York, Wiley, 2010, 318–329.

Miller, K. Y., Toennis, T. M., Adams, T. H. and **Miller, B. L.** (1991) Isolation and transcriptional characterization of a morphological modifier: the Aspergillus nidulans stunted (stuA) gene. *Molecular and general genetics*. **227**(2):285–92.

Mims, C. and **Richardson, E.** (1988) Ultrastructural analysis of conidiophore development in the fungus Aspergillus nidulans using freeze-substitution *Protoplasma*. **144**:132–141.

Mogensen, J. M., Frisvad, J. C., Thrane, U. and **Nielsen, K. F.** (2010) Production of Fumonisin B2 and B4 by Aspergillus niger on grapes and raisins. *Journal of agricultural and food chemistry*. **58**(2):954–8.

Molnár, Z., Meszaros, E., Szilagyi, Z., Rosen, S., Emri, T. and **Pócsi, I.** (2004) Influence of fadAG203R and deltaflbA mutations on morphology and physiology of submerged Aspergillus nidulans cultures *Appl Biochem Biotechnol*. **118**(1-3):349–360.

Mootha, V. K., Lindgren, C. M., Eriksson, K.-F., Subramanian, A., Sihag, S., Lehar, J., Puigserver, P., Carlsson, E., Ridderstråle, M., Laurila, E., Houstis, N., Daly, M. J., Patterson, N., Mesirov, J. P., Golub, T. R., Tamayo, P., Spiegelman, B., Lander, E. S., Hirschhorn, J. N., Altshuler, D. and **Groop, L. C.** (2003) PGC-1alpha-responsive genes involved in oxidative phosphorylation are coordinately downregulated in human diabetes. *Nature genetics*. **34**(3):267–73.

Müller, C., Spohr, A. B. and **Nielsen, J.** (2000) Role of substrate concentration in mitosis and hyphal extension of Aspergillus. *Biotechnology and bioengineering*. **67**(4):390–7.

Murooka, Y. and **Yamshita, M.** (2008) Traditional healthful fermented products of Japan. *Journal of industrial microbiology and biotechnology*. **35**(8):791–8.

Nadal, M. and **Gold, S. E.** (2010) The autophagy genes atg8 and atg1 affect morphogenesis and pathogenicity in Ustilago maydis *Molecular Plant Pathology*. **11**:463–478.

Naef, F., Lim, D. A., Patil, N. and **Magnasco, M.** (2002) DNA hybridization to mismatched templates: a chip study *Phys Rev E Stat Nonlin Soft Matter Phys*. **65**(4 Pt 1):40902.

Nitsche, B. M., Crabtree, J., Cerqueira, G. C., Meyer, V., Ram, A. F. J. and **Wortman, J. R.** (2011) New resources for functional analysis of omics data for the genus Aspergillus. *BMC genomics*. **12**:486.

Nitsche, B. M., Jørgensen, T. R., Akeroyd, M., Meyer, V. and **Ram, A. F. J.** (2012) The carbon starvation response of Aspergillus niger during submerged cultivation: Insights from the transcriptome and secretome. *BMC genomics*. **13**:380.

Nitsche, B. M., Ram, A. F. J. and **Meyer, V.** (2012) The use of open source bioinformatics tools to dissect transcriptomic data. *Methods in molecular biology (Clifton, N.J.)* **835**:311–31.

Nobel, H. D., Ende, H. V. D. and **Klis, F. M.** (2000) Cell wall maintenance in fungi *Trends in Microbiology*. **8**(8):344–345.

Owsianowski, E., Walter, D. and **Fahrenkrog, B.** (2008) Negative regulation of apoptosis in yeast *Biochim Biophys Acta*. **1783**(7):1303–1310.

Peberdy, J. F. (1994) Protein secretion in filamentous fungi-trying to understand a highly productive black box *Trends Biotechnol*. **12**(2):50–57.

Peer, A. F. van, Müller, W. H., Boekhout, T., Lugones, L. G., Wösten, H. A. B., Muller, W. H. and **Wosten, H. A.** (2009) Cytoplasmic continuity revisited: closure of septa of the filamentous fungus Schizophyllum commune in response to environmental conditions. *PloS one*. **4**(6):e5977.

Pel, H. J., Winde, J. H. de, Archer, D. B., Dyer, P. S., Hofmann, G., Schaap, P. J., Turner, G., Vries, R. P. de, Albang, R., Albermann, K., Andersen, M. R., Bendtsen, J. D., Benen, J. A., Berg, M. A. van den, Breestraat, S., Caddick, M. X., Contreras, R., Cornell, M., Coutinho, P. M., Danchin, E. G., Debets, A. J., Dekker, P., Dijck, P. W. van, Dijk, A. van, Dijkhuizen, L., Driessen, A. J., D'Enfert, C., Geysens, S., Goosen, C., Groot, G. S., Groot, P. W. de, Guillemette, T., Henrissat, B., Herweijer, M., Hombergh, J. P. van den, Hondel, C. A. M. J. J. van den, Heijden, R. T. van der, Kaaij, R. M. van der, Klis, F. M., Kools, H. J., Kubicek, C. P., VanKuyk, P. A., Lauber, J., Lu, X., Maarel, M. J. E. C. van der, Meulenberg, R., Menke, H., Mortimer, M. A., Nielsen, J., Oliver, S. G., Olsthoorn, M., Pal, K., Peij, N. N. van, Ram, A. F. J., Rinas, U., Roubos, J. A., Sagt, C. M., Schmoll, M., Sun, J., Ussery, D., Varga, J., Vervecken, W., Vondervoort, P. J. van de, Wedler, H., Wosten, H. A., Zeng, A. P., Ooyen, A. J. van, Visser, J. and **Stam, H.** (2007) Genome sequencing and analysis of the versatile cell factory Aspergillus niger CBS 513.88 *Nat Biotechnol*. **25**(2):221–231.

Person, a. K., Chudgar, S. M., Norton, B. L., Tong, B. C. and **Stout, J. E.** (2010) Aspergillus niger: an unusual cause of invasive pulmonary aspergillosis. *Journal of medical microbiology*. **59**(Pt 7):834–8.

Pinan-Lucarré, B., Balguerie, A. and **Clavé, C.** (2005) Accelerated cell death in Podospora autophagy mutants *Eukaryotic cell*. **4**(11):1765–1774.

Pitt, J. I. and **Hocking, A. D.** 1997 Fungi and Food Spoilage London: Blackie Academic and Professional, 1997 ISBN: 0412554607.

Pócsi, I., Miskei, M., Karányi, Z., Emri, T., Ayoubi, P., Pusztahelyi, T., Balla, G. and **Prade, R. A.** (2005) Comparison of gene expression signatures of diamide, H2O2 and menadione

exposed Aspergillus nidulans cultures-linking genome-wide transcriptional changes to cellular physiology. *BMC genomics*. **6**:182.

Pollack, J. K., Li, Z. J. and **Marten, M. R.** (2008) Fungal mycelia show lag time before re-growth on endogenous carbon. *Biotechnology and bioengineering*. **100**(3):458–65.

Punt, P. J., Biezen, N. van, Conesa, A., Albers, A., Mangnus, J. and **Hondel, C. van den** (2002) Filamentous fungi as cell factories for heterologous protein production. *Trends in biotechnology*. **20**(5):200–6.

Punt, P. J., Schuren, F. H. J., Lehmbeck, J., Christensen, T., Hjort, C. and **Hondel, C. A. M. J. J. van den** (2008) Characterization of the Aspergillus niger prtT, a unique regulator of extracellular protease encoding genes. *Fungal genetics and biology*. **45**(12):1591–9.

Pusztahelyi, T., Molnár, Z., Emri, T., Klement, E., Miskei, M., Kerékgyárto, J., Balla, J. and **Pócsi, I.** (2006) Comparative studies of differential expression of chitinolytic enzymes encoded by chiA, chiB, chiC and nagA genes in Aspergillus nidulans. *Folia microbiologica*. **51**(6):547–54.

Reggiori, F. and **Klionsky, D. J.** (2002) Autophagy in the eukaryotic cell *Eukaryotic Cell*. **1**(1):11–21.

Richie, D. L., Fuller, K. K., Fortwendel, J. and **Miley, M. D.** (2007) Unexpected link between metal ion deficiency and autophagy in Aspergillus fumigatus *Eukaryotic cell*. **6**(12):2437–2447.

R-Team 2008 R: A Language and Environment for Statistical Computing Vienna, Austria: R Foundation for Statistical Computing, 2008 ISBN: 3-900051-07-0.

Ruijter, G. J. G., Kubicek, C. P. and **Visser, J.** (2002) Production of organic acids by fungi *The Mycota X Industrial Applications* ed. by **H. Osiewacz** Berlin Heidelberg: Springer, 2002, 213–230.

Rumbold, K., Buijsen, H. J. J. van, Overkamp, K. M., Groenestijn, J. W. van, Punt, P. J. and **Werf, M. J. van der** (2009) Microbial production host selection for converting second-generation feedstocks into bioproducts. *Microbial cell factories*. **8**:64.

Rumbold, K., Buijsen, H. J. J. van, Gray, V. M., Groenestijn, J. W. van, Overkamp, K. M., Slomp, R. S., Werf, M. J. van der and **Punt, P. J.** (2010) Microbial renewable feedstock utilization: a substrate-oriented approach. *Bioengineered bugs*. **1**(5):359–66.

Ryan, J. C., Morey, J. S., Bottein, M.-Y. D., Ramsdell, J. S. and **Van Dolah, F. M.** (2010) Gene expression profiling in brain of mice exposed to the marine neurotoxin ciguatoxin reveals an acute anti-inflammatory, neuroprotective response. *BMC neuroscience*. **11**:107.

Salazar, M., Vongsangnak, W., Panagiotou, G., Andersen, M. R. and **Nielsen, J.** (2009) Uncovering transcriptional regulation of glycerol metabolism in Aspergilli through genome-wide gene expression data analysis *Mol Genet Genomics*. **282**(6):571–586.

Sambrook, J. and **Russell, D. W.** 2001 Molecular cloning: a laboratory manual New York: Cold Spring Harbor Press, 2001.

El-Sayed, N. M., Myler, P. J., Blandin, G., Berriman, M., Crabtree, J., Aggarwal, G., Caler, E., Renauld, H., Worthey, E. A., Hertz-Fowler, C., Ghedin, E., Peacock, C., Bartholomeu,

D. C., Haas, B. J., Tran, A.-N., Wortman, J. R., Alsmark, U. C. M., Angiuoli, S., Anupama, A., Badger, J., Bringaud, F., Cadag, E., Carlton, J. M., Cerqueira, G. C., Creasy, T., Delcher, A. L., Djikeng, A., Embley, T. M., Hauser, C., Ivens, A. C., Kummerfeld, S. K., Pereira-Leal, J. B., Nilsson, D., Peterson, J., Salzberg, S. L., Shallom, J., Silva, J. C., Sundaram, J., Westenberger, S., White, O., Melville, S. E., Donelson, J. E., Andersson, B., Stuart, K. D. and **Hall, N.** (2005) Comparative genomics of trypanosomatid parasitic protozoa. *Science*. **309**(5733):404–9.

El-Sayed, N. M., Myler, P. J., Bartholomeu, D. C., Nilsson, D., Aggarwal, G., Tran, A.-N., Ghedin, E., Worthey, E. A., Delcher, A. L., Blandin, G., Westenberger, S. J., Caler, E., Cerqueira, G. C., Branche, C., Haas, B., Anupama, A., Arner, E., Aslund, L., Attipoe, P., Bontempi, E., Bringaud, F., Burton, P., Cadag, E., Campbell, D. A., Carrington, M., Crabtree, J., Darban, H., Silveira, J. F. da, Jong, P. de, Edwards, K., Englund, P. T., Fazelina, G., Feldblyum, T., Ferella, M., Frasch, A. C., Gull, K., Horn, D., Hou, L., Huang, Y., Kindlund, E., Klingbeil, M., Kluge, S., Koo, H., Lacerda, D., Levin, M. J., Lorenzi, H., Louie, T., Machado, C. R., McCulloch, R., McKenna, A., Mizuno, Y., Mottram, J. C., Nelson, S., Ochaya, S., Osoegawa, K., Pai, G., Parsons, M., Pentony, M., Pettersson, U., Pop, M., Ramirez, J. L., Rinta, J., Robertson, L., Salzberg, S. L., Sanchez, D. O., Seyler, A., Sharma, R., Shetty, J., Simpson, A. J., Sisk, E., Tammi, M. T., Tarleton, R., Teixeira, S., Van Aken, S., Vogt, C., Ward, P. N., Wickstead, B., Wortman, J., White, O., Fraser, C. M., Stuart, K. D. and **Andersson, B.** (2005) The genome sequence of Trypanosoma cruzi, etiologic agent of Chagas disease. *Science*. **309**(5733):409–15.

Schrickx, J. M., Krave, A. S., Verdoes, J. C., Hondel, C. A. M. J. J. van den, Stouthamer, A. H. and **Verseveld, H. W. van** (1993) Growth and product formation in chemostat and recycling cultures by Aspergillus niger N402 and a glucoamylase overproducing transformant, provided with multiple copies of the glaA gene. *Journal of general microbiology*. **139**(11):2801–10.

Schuster, E., Dunn-Coleman, N., Frisvad, J. C. and **Van Dijck, P. W. M.** (2002) On the safety of Aspergillus niger-a review. *Applied microbiology and biotechnology*. **59**(4-5):426–35.

Shannon, P., Markiel, A., Ozier, O., Baliga, N. S., Wang, J. T., Ramage, D., Amin, N., Schwikowski, B. and **Ideker, T.** (2003) Cytoscape: a software environment for integrated models of biomolecular interaction networks *Genome Res.* **13**(11):2498–2504.

Shoji, J.-Y., Arioka, M. and **Kitamoto, K.** (2006) Possible involvement of pleiomorphic vacuolar networks in nutrient recycling in filamentous fungi. *Autophagy*. **2**(3):226–7.

Shoji, J.-Y., Kikuma, T., Arioka, M. and **Kitamoto, K.** (2010) Macroautophagy-mediated degradation of whole nuclei in the filamentous fungus Aspergillus oryzae. *PloS one*. **5**(12):e15650.

Shoji, J.-Y. and **Craven, K. D.** (2011) Autophagy in basal hyphal compartments: A green strategy of great recyclers *Fungal Biology Reviews*. **25**(2):79–83.

Smyth, G. K. (2004) Linear models and empirical bayes methods for assessing differential expression in microarray experiments *Stat Appl Genet Mol Biol.* **3**:Article3.

Subramanian, A., Tamayo, P., Mootha, V. K., Mukherjee, S., Ebert, B. L., Gillette, M. A., Paulovich, A., Pomeroy, S. L., Golub, T. R., Lander, E. S. and **Mesirov, J. P.** (2005) Gene

set enrichment analysis: a knowledge-based approach for interpreting genome-wide expression profiles *Proc Natl Acad Sci U S A*. **102**(43):15545–15550.

Suelmann, R. and **Fischer, R.** (2000) Mitochondrial Movement and Morphology Depend on an Intact Actin Cytoskeleton in Aspergillus nidulans *Trends in Cell Biology*. **45**(1):42–50.

Suzuki, S., Onodera, J. and **Ohsumi, Y.** (2011) Starvation induced cell death in autophagy-defective yeast mutants is caused by mitochondria dysfunction *PloS one*. **6**(2):e17412.

Thakur, S. S., Geiger, T., Chatterjee, B., Bandilla, P., Fröhlich, F., Cox, J. and **Mann, M.** (2011) Deep and Highly Sensitive Proteome Coverage by LC-MS/MS Without Prefractionation. *Molecular and cellular proteomics : MCP*. **10**(8):M110.003699.

Thorpe, G. W., Fong, C. S., Alic, N., Higgins, V. J. and **Dawes, I. W.** (2004) Cells have distinct mechanisms to maintain protection against different reactive oxygen species: oxidative-stress-response genes. *Proceedings of the National Academy of Sciences of the United States of America*. **101**(17):6564–9.

Trinci, A. and **Righelato, R.** (1969) Changes in Constituents and Ultrastructure of Hyphal Compartments during Autolysis *Journal of general microbiology*. **60**(2):239–249.

Tsukada, M. and **Ohsumi, Y.** (1993) Isolation and characterization of autophagy-defective mutants of Saccharomyces cerevisiae *FEBS Lett.* **333**(1):169–174.

Tucker, C. L. and **Fields, S.** (2004) Quantitative genome-wide analysis of yeast deletion strain sensitivities to oxidative and chemical stress. *Comparative and functional genomics*. **5**(3):216–24.

Twine, N. A., Janitz, K., Wilkins, M. R. and **Janitz, M.** (2011) Whole transcriptome sequencing reveals gene expression and splicing differences in brain regions affected by Alzheimer's disease. *PloS one*. **6**(1):e16266.

Usadel, B., Obayashi, T., Mutwil, M., Giorgi, F. M., Bassel, G. W., Tanimoto, M., Chow, A., Steinhauser, D., Persson, S. and **Provart, N. J.** (2009) Co-expression tools for plant biology: opportunities for hypothesis generation and caveats *Plant Cell Environ*. **32**(12):1633–1651.

Veneault-Fourrey, C., Barooah, M., Egan, M., Wakley, G. and **Talbot, N. J.** (2006) Autophagic fungal cell death is necessary for infection by the rice blast fungus. *Science*. **312**(5773):580–3.

Vinck, A., Terlou, M., Pestman, W. R., Martens, E. P., Ram, Hondel, C. A. M. J. J. van den and **Wösten, H. A. B.** (2005) Hyphal differentiation in the exploring mycelium of Aspergillus niger. *Molecular microbiology*. **58**(3):693–9.

Vishniac, W. and **Santer, M.** (1957) The thiobacilli *Bacteriological reviews*. **21**(3):195–213.

White, S., McIntyre, M., Berry, D. R. and **McNeil, B.** (2002) The autolysis of industrial filamentous fungi *Crit Rev Biotechnol*. **22**(1):1–14.

Whittaker, R. H. (1959) On the broad classification of organisms. *The Quarterly review of biology*. **34**:210–26.

Wortman, J. R., Gilsenan, J. M., Joardar, V., Deegan, J., Clutterbuck, J., Andersen, M. R., Archer, D. B., Bencina, M., Braus, G. H., Coutinho, P., Dohren, H. von, Doonan, J., Driessen, A. J., Durek, P., Espeso, E. A., Fekete, E., Flipphi, M., Estrada, C. G., Geysens,

S., Goldman, G. H., Groot, P. W. de, Hansen, K., Harris, S. D., Heinekamp, T., Helmstaedt, K., Henrissat, B., Hofmann, G., Homan, T., Horio, T., Horiuchi, H., James, S., Jones, M., Karaffa, L., Karanyi, Z., Kato, M., Keller, N., Kelly, D. E., Kiel, J. A., Kim, J. M., Klei, I. J. van der, Klis, F. M., Kovalchuk, A., Krasevec, N., Kubicek, C. P., Liu, B., Maccabe, A., Meyer, V., Mirabito, P., Miskei, M., Mos, M., Mullins, J., Nelson, D. R., Nielsen, J., Oakley, B. R., Osmani, S. A., Pakula, T., Paszewski, A., Paulsen, I., Pilsyk, S., Pócsi, I., Punt, P. J., Ram, A. F. J., Ren, Q., Robellet, X., Robson, G., Seiboth, B., Solingen, P. van, Specht, T., Sun, J., Taheri-Talesh, N., Takeshita, N., Ussery, D., VanKuyk, P. A., Visser, H., Vondervoort, P. J. van de, Vries, R. P. de, Walton, J., Xiang, X., Xiong, Y., Zeng, A. P., Brandt, B. W., Cornell, M. J., Hondel, C. A. M. J. J. van den, Visser, J., Oliver, S. G. and **Turner, G.** (2009) The 2008 update of the Aspergillus nidulans genome annotation: a community effort *Fungal Genet Biol*. **46**(Suppl 1):S2–13.

Xie, Z., Nair, U. and **Klionsky, D. J.** (2008) Atg8 Controls Phagophore Expansion during Autophagosome Formation *Molecular Biology of the Cell*. **19**(August):3290 –3298.

Xie, Z. and **Klionsky, D. J.** (2007) Autophagosome formation: core machinery and adaptations *Nat Cell Biol*. **9**(10):1102–1109.

Yamazaki, H., Yamazaki, D., Takaya, N., Takagi, M., Ohta, A. and **Horiuchi, H.** (2007) A chitinase gene, chiB, involved in the autolytic process of Aspergillus nidulans. *Current genetics*. **51**(2):89–98.

Yang, Z. and **Klionsky, D. J.** (2010) Eaten alive: a history of macroautophagy. *Nature cell biology*. **12**(9):814–22.

Zhang, Y., Qi, H., Taylor, R., Xu, W., Liu, L. F. and **Jin, S.** (2007) The role of autophagy in mitochondria maintenance: characterization of mitochondrial functions in autophagy-deficient S. cerevisiae strains *Autophagy*. **3**(4):337–346.

Zustiak, M. P., Pollack, J. K., Marten, M. R. and **Betenbaugh, M. J.** (2008) Feast or famine: autophagy control and engineering in eukaryotic cell culture *Current Opinion in Biotechnology*. **19**(5):518–526.